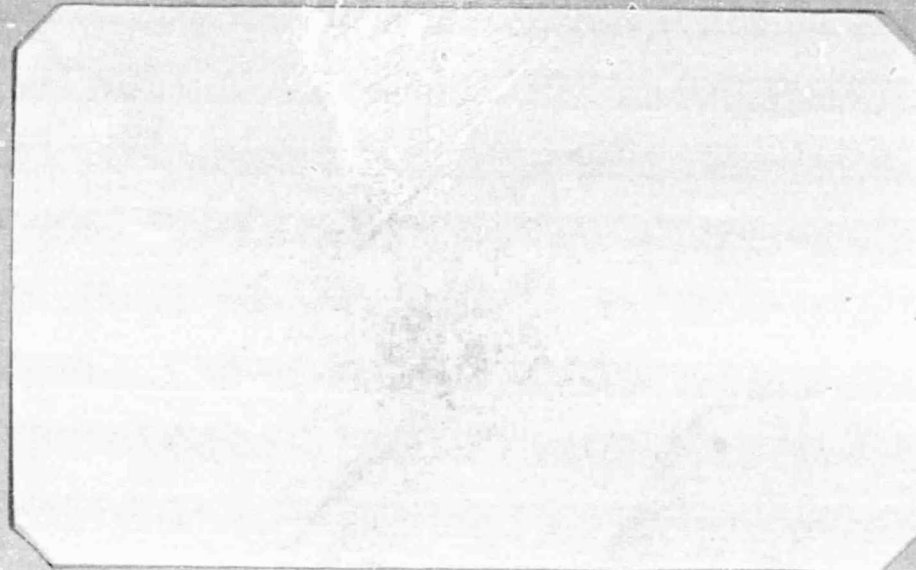


N O T I C E

THIS DOCUMENT HAS BEEN REPRODUCED FROM
MICROFICHE. ALTHOUGH IT IS RECOGNIZED THAT
CERTAIN PORTIONS ARE ILLEGIBLE, IT IS BEING RELEASED
IN THE INTEREST OF MAKING AVAILABLE AS MUCH
INFORMATION AS POSSIBLE

9950-413



(NASA-CR-163584) A STUDY OF THE
APPLICABILITY/COMPATIBILITY OF INERTIAL
ENERGY STORAGE SYSTEMS TO FUTURE SPACE
MISSIONS Final Report (Texas Univ.) 139 p
HC A07/MF A01

N80-32856

Unclas
CSCL 10C G3/44 28885

CENTER FOR ELECTROMECHANICS



THE UNIVERSITY OF TEXAS
COLLEGE OF ENGINEERING
TAYLOR HALL 167
AUSTIN, TEXAS, 78712
512/471-4496



Final Report
for
A Study of the Applicability/Compatibility
of Inertial Energy Storage Systems
to Future Space Missions

Jet Propulsion Laboratory
Contract No. 955679

This work was performed for the Jet Propulsion
Laboratory, California Institute of Technology
Sponsored by The National Aeronautics and Space
Administration under Contract NAS7-100

by
William F. Weldon
Technical Director
Center for Electromechanics
The University of Texas at Austin
Taylor Hall 167
Austin, Texas 78712
(512) 471-4496

August, 1980

This document contains information prepared by the Center for Electromechanics of The University of Texas at Austin under JPL sub-contract. Its content is not necessarily endorsed by the Jet Propulsion Laboratory, California Institute of Technology, or its sponsors.

ABSTRACT

The applicability/compatibility of inertial energy storage systems, i.e. the Homopolar Generator (HPG) and the Compensated Pulsed Alternator (CPA) to future space missions is explored. Areas of CPA and HPG design requiring development for space applications are identified. The manner in which acceptance parameters (kg/J , m^3/J , $\$/\text{J}$) of the CPA and HPG scale with operating parameters of the machines are explored and the types of electrical loads which are compatible with the CPA and HPG are examined. Potential applications including the magnetoplasmadynamic (MPD) thruster, pulsed data transmission, laser ranging, welding and electromagnetic space launch are discussed briefly.

TABLE OF CONTENTS

	<u>Page No.</u>
I. INTRODUCTION	1
II. TECHNICAL DISCUSSION	5
a. Pulsed Homopolar Generator	5
1. Principles of Operation	5
2. Areas Requiring Development for Space Applications	19
3. Scaling of Acceptance Parameters	21
4. Compatibility with Electrical Loads	23
b. Compensated Pulsed Alternator	30
1. Principles of Operation	30
2. Effect of Load Characteristics	32
3. Limitations to Peak Output Power	34
4. Limitations to Minimum Pulse Width	36
5. Areas Requiring Development for Space Applications	37
6. Scaling and Acceptance Parameters	38
c. Potential Applications	40
III. CONCLUSIONS	48
IV. RECOMMENDATIONS	49
V. NEW TECHNOLOGY	50
VI. BIBLIOGRAPHY	51
APPENDICES	
a. Homopolar Generator Rotor Stresses	
b. Homopolar Resistance Welding Process	
c. Analysis of Electromagnetic Launchers	

SECTION I INTRODUCTION

Since several potential space applications of electrical power operate more efficiently at higher input power levels than may be available from the space craft's prime power source, the use of energy storage devices capable of supplying high peak output power is attractive. Table I compares the energy densities which have been achieved in large earth based systems, clarifying the attractiveness of the inertial energy storage systems. Furthermore, the inertial systems of interest, homopolar generators (HPG) and compensated pulsed alternators (CPA), possess the low impedance necessary for interfacing with high powered systems such as the magnetoplasmadynamic (MPD) thrusters. At least one of the generators (the CPA) is capable of producing rapidly repetitive pulses with minimum switching requirements.

TABLE I
ACHIEVED ENERGY DENSITIES
IN LARGE EARTH-BASED ENERGY STORAGE INSTALLATIONS

<u>Type of Storage</u>	<u>Achieved Energy Density (Joules/m³)</u>
<u>CAPACITIVE</u>	
High Inductance	8×10^3
Low Inductance	3×10^3
<u>INDUCTIVE</u>	
Normal	$\sim 10^7$
Superconducting **	2×10^6
<u>INERTIAL</u>	
HPG - Slow	5×10^6
HPG - Fast	3×10^6
HPG - New A-I-R*	$1.3-3.0 \times 10^7$
CPA	4×10^5
<u>CHEMICAL</u>	
Battery	5×10^8
Explosive	$\sim 10^{10}$

**Neglects Refrigeration

*New Design Not Built

One difficulty in evaluating the potential of such generators for space-based applications is that virtually all development to date has been done for fixed land-based systems in which minimum cost rather than minimum weight or volume was the primary criterion. A new program to design a field portable HPG system now underway at CEM sponsored by DARPA and ARRADCOM has resulted in the All-Iron-Rotating (A-I-R) design listed in Table I. Note the substantial improvement made in energy density without incorporating exotic materials into the design.

Table II indicates the potential for improvements in the area of energy density. In each column the first number represents a modified constant stress disc operating at 80% of yield strength and the second number represents operation at 80% of the endurance limit (~infinite life). Filament reinforced epoxy composite rotors can extend these values even farther, but the construction is unsuitable for HPG construction and has not been demonstrated for CPA rotors. Furthermore, any non-ferromagnetic rotor material carries with it the penalty of greatly increased excitation power requirements.

TABLE II
ENERGY DENSITIES FOR VARIOUS ROTOR MATERIALS

Material	Energy Density	
	<u>KJ/kg</u>	<u>MJ/m³</u>
Aluminum (7075)	46.4 (14.3)	130 (40)
Beryllium Copper (1.9%)	10.9 (3.6)	90 (30)
Steel (4340)	16.6 (7.7)	130 (60)
Titanium (Ti-6Al-4v) Composites	38.4 (15.8)	170 (70)

Other factors limit HPG rotor speed: Brush wear considerations, rotor/bearing dynamic response, and bearing/lubricant seal rubbing speeds. Generally, brush wear is the most severe, limiting rotor surface speeds to 200-225 m/sec for long brush life. Significant improvements are possible in this area. For the CPA, the rotor speed is limited by the presence of active windings on the rotor surface. Although advances in filament-reinforced epoxy composite technology promise improvements in this area, present practical limits are on the order of 150 m/sec.

There are other factors associated with rotating machine applications that are peculiar to operation in space. These include performance of bearings, brushes, and seals in the hard vacuum of space, a thorough analysis of gyroscopic and discharge force reactions and an examination of appropriate motoring schemes utilizing power from solar panels or other candidate power supplies.

Five potential applications are discussed. The MPD thruster is of primary interest. Also of interest is the concept of using a pulsed energy source such as an HPG to transmit accumulated data back to earth in brief, high-intensity bursts. Another area of interest is the use of pulsed power sources to power various sensors, such as laser ranging devices. A fourth area of interest involves the possibility of using HPG welding techniques developed by UT-CEM to assemble structures in space. Most of the particulars in this area have already been addressed except for the specific machine design and actually accomplishing a weld under hard vacuum and zero gravity conditions. The vacuum should enhance weld quality by eliminating surface oxides. The zero gravity condition should not prove to be a problem since the weld is accomplished when the metal is in the hot-plastic condition rather than molten.

The fifth area involves the use of an earth, moon, or asteroid based electromagnetic launcher for space launching of materials and supplies.*

*See Appendix B

Also Reference: J.P. Barber, "Electric Rail Gun Application to Space Propulsion," Princeton/AIAA/DGLR 14th International Electric Propulsion Conference, Princeton, NJ, Oct 30-Nov 1, 1979.

SECTION II TECHNICAL DISCUSSION

A. THE PULSED HOMOPOLAR GENERATOR

1. Principles of Operation

The pulsed HPG utilizes the principles of inertial energy storage in a monolithic, metallic flywheel and direct conversion of that stored energy to a pulse of electrical energy through homopolar (acyclic) electro-mechanical conversion as first demonstrated by Michael Faraday in 1831.¹ (See Figure 1.) We have already seen that inertial energy storage offers attractive energy storage densities by comparison with alternate energy storage techniques.

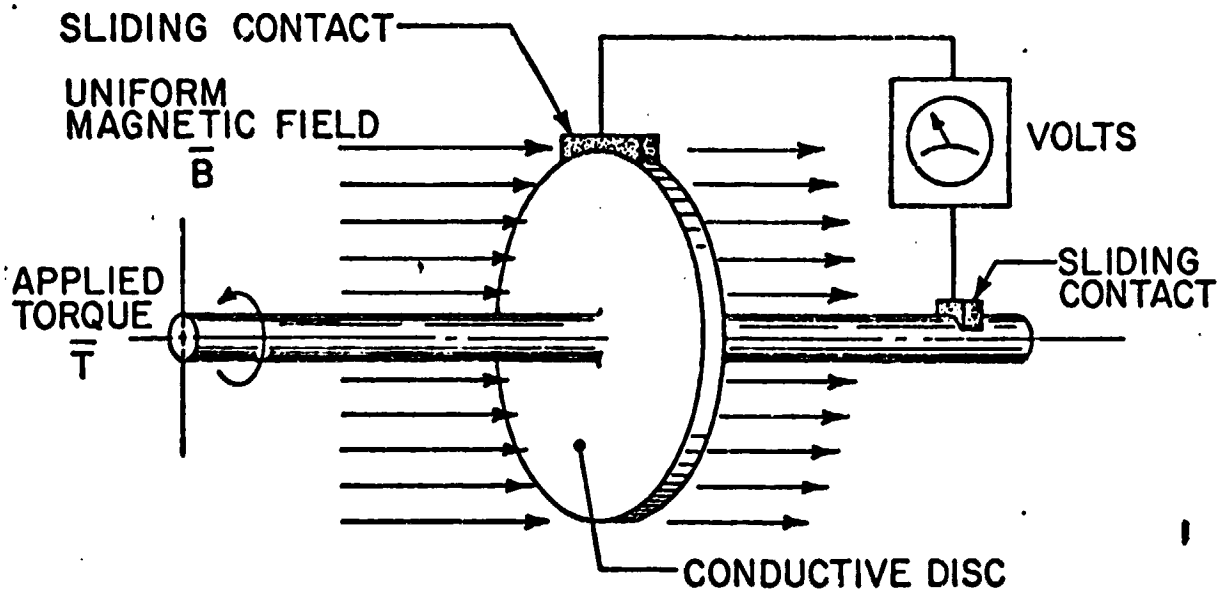
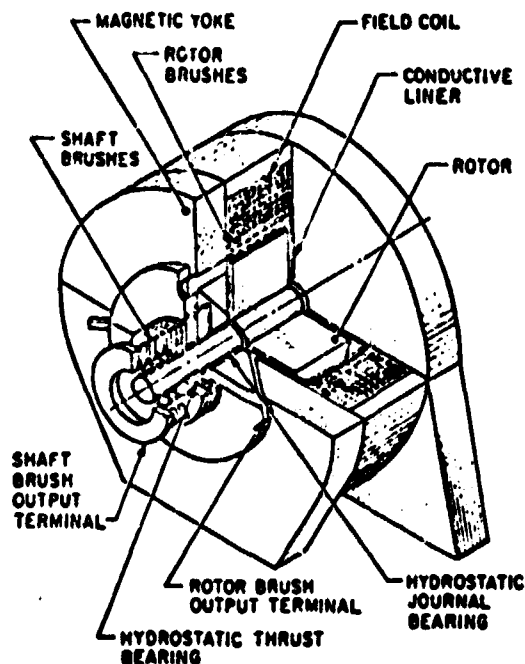


Figure 1. Faraday disc

ORIGINAL PAGE IS
OF POOR QUALITY

Michael Faraday discovered that a thin copper disc rotated in an axial magnetic field, \vec{B} , would develop a voltage between its inner and outer radii. Thus, a resistance placed between the inner and outer radii by means of sliding contacts would allow a current to flow, creating an electromagnetic force which would retard the rotor. This experiment, along with others performed about the same time, led to the formulation of Faraday's Law which states that the electromotive force in any closed circuit is equal to the time rate of change of the magnetic flux coupled by that circuit. This is the familiar principle upon which almost all rotating electromechanical energy convertors operate. The Faraday disc is different from the conventional wound-rotor electrical machines, however, in several important respects. First, the rotor material experiences a unidirectional unchanging magnetic flux and thus does not have to be laminated to minimize eddy current losses as does a rotor in a heteropolar magnetic field. Second, the discharge current passes through the rotor material itself rather than through separate conductors. This means that the armature circuit has extremely low impedance compared to a wound armature. Also, the $\vec{J} \times \vec{B}$ forces (vector cross product of discharge current \vec{J} and applied magnetic field \vec{B}) which retard the rotor during discharge, converting the stored inertial energy directly to an electrical pulse, act directly on the rotor material rather than on a conductor wound on the rotor. These two factors allow extremely large currents to be extracted from such a device, converting the stored energy to electrical energy in a very short time. Unfortunately, this same simple geometry allows the current to make only one pass through the magnetic field in each rotor (there are limited exceptions to this as we will see later) severely limiting the voltage which can be generated by an HPG.

We see then that homopolar conversion allows direct conversion of the energy stored in a monolithic circular, electrically conductive flywheel to a pulse of electrical energy without requiring auxiliary generators, windings, slots, or laminations. This inherent simplicity is perhaps the greatest single attraction of the HPG. We will now examine what is necessary to convert the idealized Faraday disc in Fig. 1 to an operational HPG such as is shown in Fig. 2.



ORIGINAL PAGE IS
OF POOR QUALITY

Figure 2. The 5MJ CEM Homopolar Generator

We must first have a rotor capable of storing energy inertially and of conducting electricity radially. We must have some means of generating a magnetic field for the rotor to operate in and of collecting large currents from the inner and outer radii of the rotor and delivering them to a load during discharge. We require bearings capable of locating the rotor both axially and radially as it is brought up to speed, spins at speed, and is decelerated electromagnetically. We must have some structure to provide support for the bearings and a means of accelerating the rotor up to design speed before discharging.

The HPG Magnetic Circuit

Although in principle the required magnetic field for an HPG can be generated in several ways, in practice this results in some of the most severe limitations to HPG acceptance parameters. Basically, the required magnetic field can be provided by a permanent or electric magnet. However, although they do not require excitation power, permanent magnet materials are expensive, bulky, and operate at low field levels. Since HPG's are usually voltage limited and voltage is directly proportional to the operating magnetic field level, magnetic field cannot usually be sacrificed for the convenience of permanent magnet materials. Electromagnets are of two general types; air cored and iron cored. Air cored magnets are by far

the lightest consisting only of a simple solenoid of copper or aluminum wire whereas iron cored magnets direct the generated flux through a ferromagnetic path (iron or steel). Since the copper conductor is typically 5-10% of the weight of the ferromagnetic magnet for HPG the weight difference between iron and air cored magnets can be a factor of 10-20. However, since the relative magnetic permeability of iron is from a few hundred to a few thousand times that of air the excitation requirements for iron cored magnets are proportionally lower than for air cored magnets. Since excitation power can become an overwhelming consideration in air cored magnets, most HPG's are built of ferromagnetic materials to minimize the excitation requirements. The basic magnetic circuit for a ferromagnetic (iron cored) HPG can be thought of as a simple solenoid of insulated copper or aluminum conductor imbedded in an iron or steel cylinder as shown in Fig. 3. In order to use the magnetic material most efficiently, it is

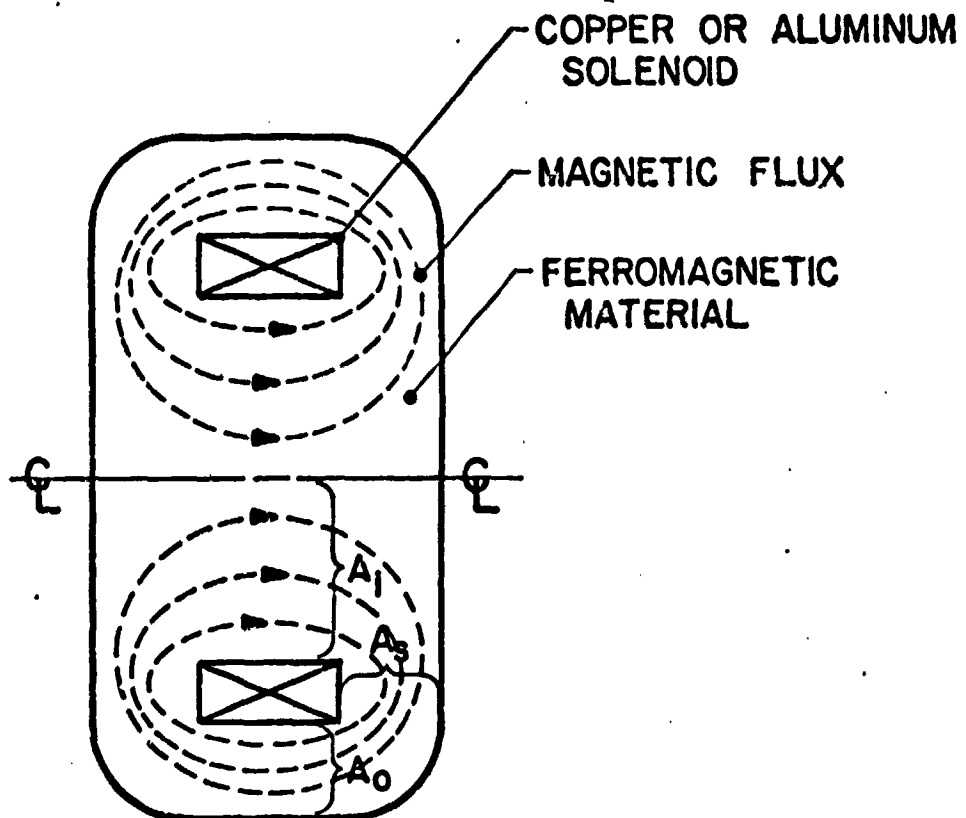


Figure 3. Basic Magnetic Circuit for Homopolar Generator

generally constructed in a "constant flux density" configuration such that the area in the base of the solenoid, A_1 , is the same as the cross-sectional

area of one side plate A_s and also the same as the area of material on the outside of the solenoid, A_o . This basic magnetic circuit may now be divided as shown in Fig. 4 into a disc type rotor and a larger stator or "back iron" whose function is to return the magnetic flux from one side of the rotor to the other. This is the disc type HPG which is typified

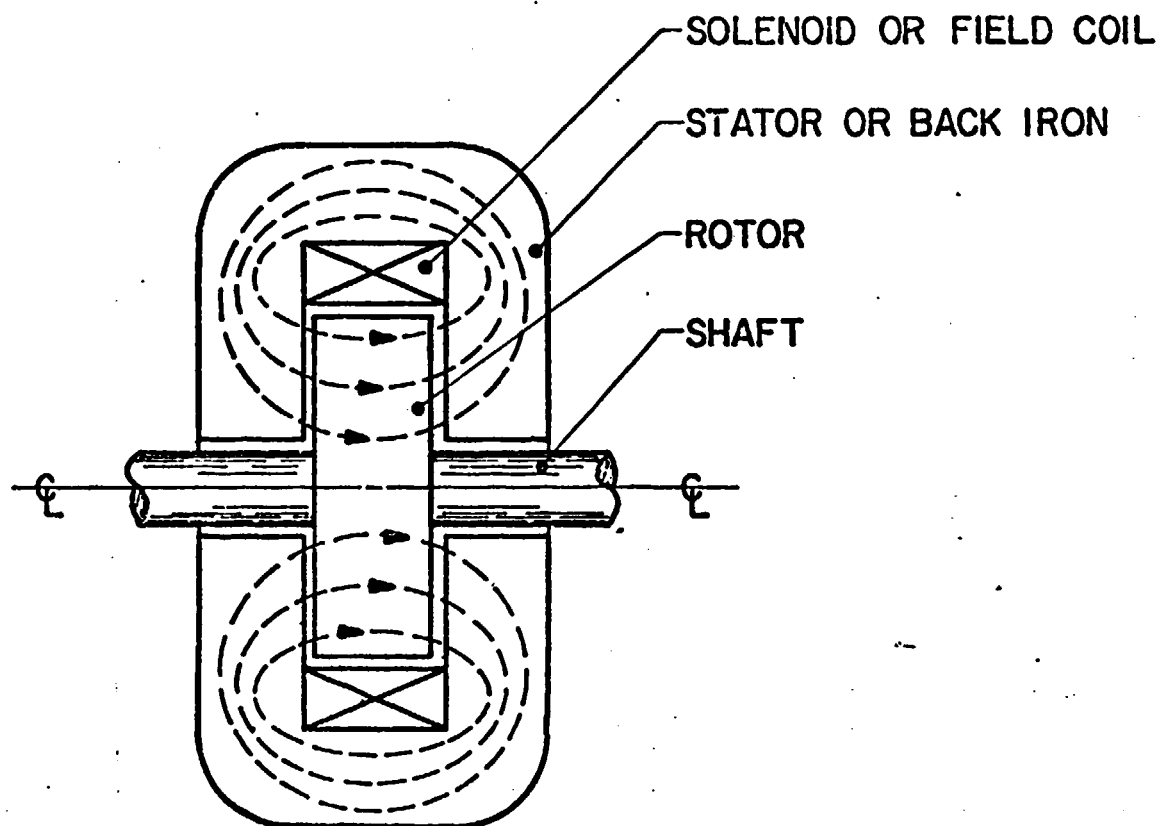


Figure 4. Magnetic Circuit for Disc Type Homopolar Generator

by the 5MJ HPG built by CEM-UT. It can be readily seen that this configuration uses relatively little of the ferromagnetic material to store energy inertially. In fact, although the CEM-UT 5MJ HPG stores approximately 60 MJ/m^3 in its rotor, its overall energy density including field coil, stator, bearings and brushes is only about 6 MJ/m^3 ! However, as will be seen later this disc configuration does have the advantage of having the lowest effective capacitance which gives it the advantage of offering the fastest discharge time of any HPG rotor configuration.

Figure 5 shows how the basic HPG magnetic circuit may be divided to generate the "drum" configuration which utilizes a larger percentage of the ferromagnetic material in which to store energy. The drum type HPG

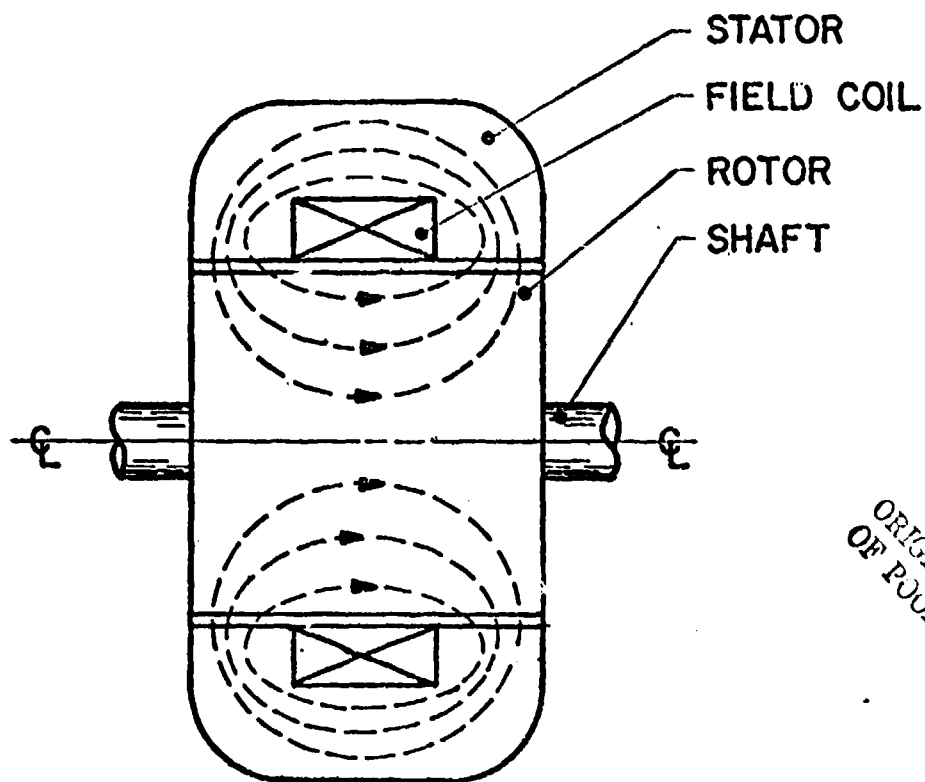


Figure 5. Magnetic Circuit for Drum Type Homopolar Generator

offers higher overall energy density and efficiency at the expense of increased discharge time. This configuration has been used in the past for steady state HPG's as opposed to those intended for pulsed duty.

More recently, a new configuration has been explored by CEM-UT, which offers substantial increases in stored energy density at the expense of certain other performance parameters. This All-Iron-Rotating (A-I-R) configuration shown schematically in Fig. 6 is the configuration for which the improved acceptance parameters have been claimed in the previous progress reports. It can be seen from Fig. 6 that virtually all of the ferromagnetic material is used to store energy inertially in this configuration. The field coil in the A-I-R configuration may either be stationary or may be split and rotate with the two rotors.

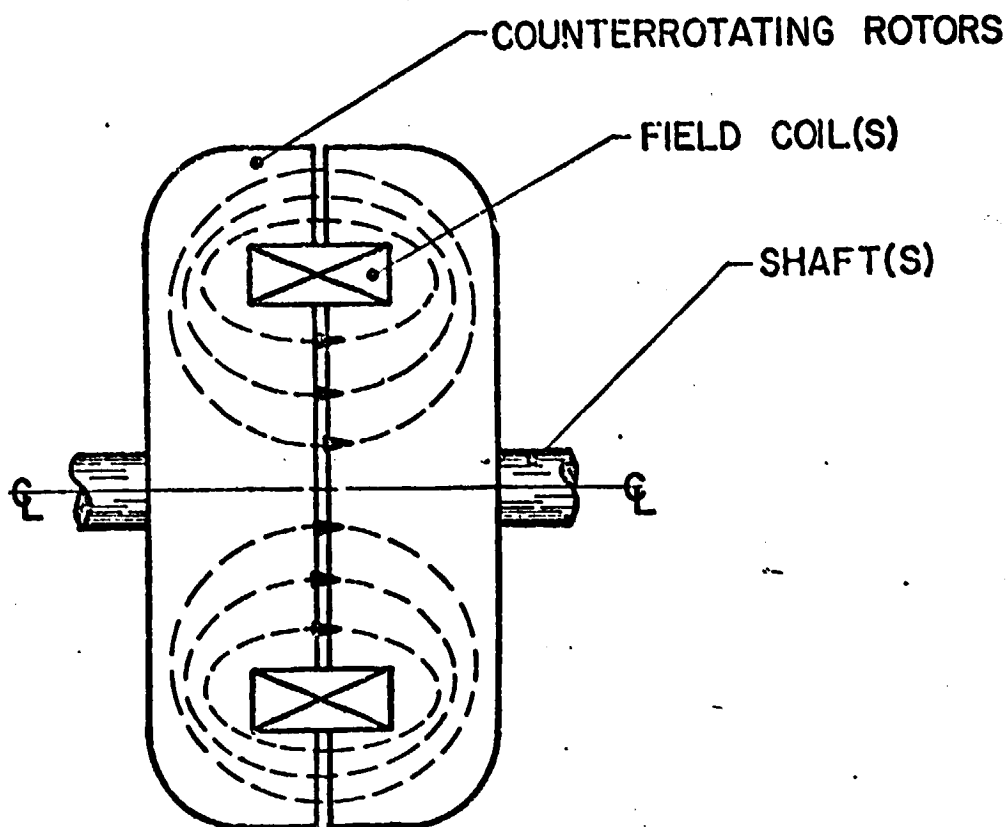


Figure 6. Magnetic Circuit for All-Iron-Rotating Homopolar Generator

HPG Rotor

The rotor is of course the heart of the HPG since it both stores the energy inertially and converts it to electrical energy upon demand. The limitations to rotor speed (and thus to energy density) are covered in depth in Appendix A and are treated only briefly here. For a right circular cylinder the maximum stress due to rotation, σ_{\max} , is related to the following parameters:

$$\sigma_{\max} \propto \rho_m \omega^2 r^2 \quad (1)$$

where

- σ_{\max} = maximum rotational stress
- ρ_m = mass density of rotor material
- ω = rotor angular velocity
- r = rotor radius.

Once the rotor material has been selected, σ_{\max} is fixed. The kinetic energy stored in the rotor is given by equation (2).

$$\text{K.E.} = \frac{J_m \omega^2}{2} = \frac{\pi r^4 t \rho_m \omega^2}{4} \quad (2)$$

where

K.E. = kinetic energy
 J_m = rotor moment of inertia
 t = rotor thickness .

But from equation (1) we have seen that $\rho_m \omega^2 r^2$ is fixed by the choice of rotor material so that we find that the kinetic energy stored in a rotor is only a function of r and t . (equation 2a).

$$\text{K.E.} \propto r^2 t \quad (2a)$$

Recalling Faraday's Law, the voltage generated by any HPG is the time rate of change of the magnetic flux linkage (equation 3).

$$V = \frac{\phi \omega}{2\pi} \quad (3)$$

where

V = HPG voltage
 ϕ = total magnetic flux linked by rotor .

For a constant flux density ferromagnetic disk type HPG

$$\phi = B(\pi r^2) \quad (3a)$$

where B = average magnetic flux density, thus equation (3) becomes

$$V = \frac{B r^2 \omega}{2} \quad (3b)$$

Recall that $r\omega$ the surface speed of the rotor is fixed by the allowable operating stress in the rotor (equation 1) and we find

$$V \propto Br \quad (3c)$$

Recalling equations (2a) and (3c) we find one of the basic limitations of scaling up HPG's. As we increase the rotor size, the stored energy increases much more rapidly than the generated voltage. In order to minimize this effect we see that we should maximize r at the expense of t . Unfortunately as the rotors become larger in radius and thinner they experience "flutter", a dynamic instability of thin disks. Although specific detailed analysis of a rotor configuration is required to determine flutter mode instability, an acceptable "rule of thumb" is given in equation 4.

$$t \geq 0.2 r \quad \text{for rotor stability} \quad (4)$$

Inserting this relationship into equation 2a gives

$$K.E. \propto r^3 \quad (5)$$

and

$$V \propto Br \quad (3c)$$

These two equations govern the voltage and energy scaling for disc type HPG's.

The HPG Brushes

The brushes in an HPG are subjected to extraordinarily difficult duty. They must contact the rotor at its full diameter and thus at maximum surface speed. They must conduct extremely high currents (for high power operation at low voltage) at low voltage drops for maximum efficiency and minimum brush heating. They must operate in a relatively high magnetic field, and thus are subjected to high $\vec{J} \times \vec{B}$ forces. Finally, they must minimize and reject heating due to friction, interface voltage drop, and joule heating in order to minimize brush wear. This last factor is especially important in space applications where service at regular intervals may not be practical and for this same reason the brushes are usually retracted from the rotor surface between discharges. In Figure 7, we observe the limitations imposed upon HPG rotor surface velocity by brush wear considerations. In summary, velocities in the range of 150-200 m/sec are probably of most interest for extended service at present although work is underway which may extend this range. This range of velocity corresponds to brush wear of less than 0.0025 mm per pulse. Table III presents a summary of HPG brush related state-of-the-art.

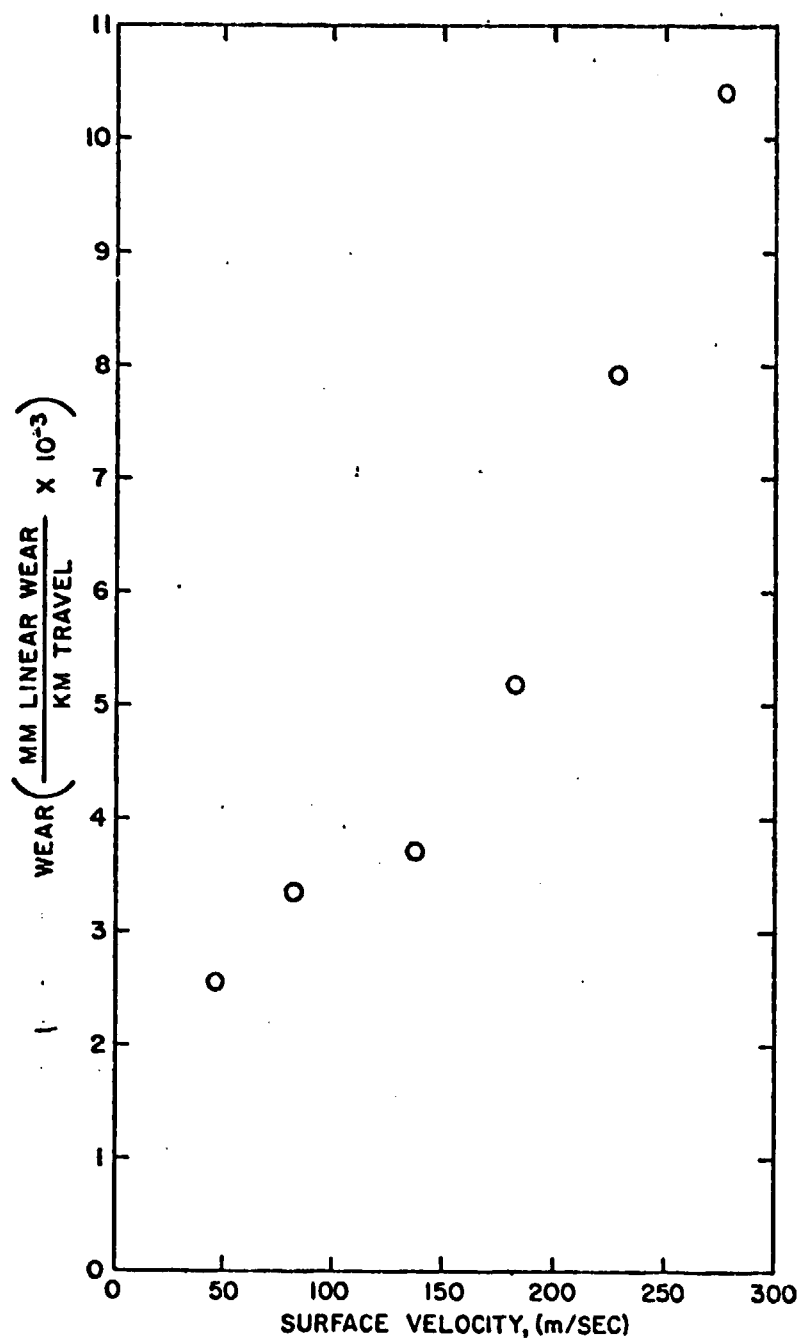


Figure 7. Normalized Brush Wear Rate versus Rotor Surface Speed

Table III. State of the Art for Homopolar Generator Related Technology

SYSTEM (LOCATION)	MAX. ENERGY STORAGE (MJ)	MAX. VOLTAGE (VOLTS)	MAX. CURRENT (KILOAMPS)	PEAK POWER ACHIEVED (MW)	MIN. DISCHARGE TIME (SEC)	PULSE RISE TIME (SEC)	MAX. SURFACE SPEED (m/SEC)	MAX. BRUSH CURRENT DENSITY (KA/CM ²)	MAX. CURRENT PER BRUSH (KA)	BRUSH PACKING FACTOR	SLIP RING CURRENT DENSITY KA/CM ²	OVERALL POWER DENSITY (MW/M ³ ; KJ/KG)	ENERGY DENSITY IN ROTOR (MJ/M ³ KJ/KG)	OVERALL ENERGY DENSITY (MJ/M ³ KJ/KG)
5 MJ Homopolar Generator (CEN-Univ. of Texas)	5	42	560	12	0.7	5×10^{-2}	178	2.41	15.5	0.13 (0.43)*	0.54	14 (.34)	60 (7)	6 (.7)
FDX Homopolar Generator (CEN-Univ. of Texas)	0.365	28 (100)*	280 (1800)*	8 (200)*	5×10^{-3} (10^{-3})*	4×10^{-4}	207 (447)*	1.34	15.5	0.95	1.15	71 (18)	98 (44)	3 (.8)
Cont. Atmos. Brush Tester (CEN-Univ. of Texas)	-	-	5	-	6×10^{-2}	3×10^{-3}	350	3.25	5.0	0.01	0.02	-	-	-
500 MJ Homopolar Gener- ator (Australian Nat'l. Univ.)	500	800	1600	320	>1.	0.6	170	1.9	1.9	0.3	0.057	1.2 (0.2)	50 (6)	1.9 (.4)
Marshall Rail Gun (Australian Nat'l. Univ.)	-	-	100	-	-	5×10^{-5}	1000	60	12.5	-	-	-	-	-
Advanced Sliding Contact Work (CEN-Univ. of Texas)	-	42	220	-	1.0	5×10^{-2}	5	31	0.4	0.1	7.7	-	-	-

*Potential

**On Shaft

Table III. State of the Art for Homopolar Generator Related Technology

SYSTEM (LOCATION)	MAX. ENERGY STORAGE (MJ)	MAX. VOLTAGE (VOLTS)	MAX. CURRENT (KILOAMPS)	PEAK POWER ACHIEVED (MW)	MIN. DISCHARGE TIME (SEC)	PULSE RISE TIME (SEC)	MAX. SURFACE SPEED (m/SEC)	MAX. BRUSH CURRENT DENSITY (KA/CM ²)	MAX. CURRENT PER BRUSH (KA)	BRUSH PACKING FACTOR	SLIP RING CURRENT DENSITY KA/CM ²	OVERALL POWER DENSITY (MW/M ³ ; KW/KG)	ENERGY DENSITY IN ROTOR (MJ/M ³ KJ/KG)	OVERALL ENERGY DENSITY (MJ/M ³ KJ/KG)
5 MJ Homopolar Generator (CEM-Univ. of Texas)	5	42	560	12	0.7	5×10^{-2}	178	2.41	15.5	0.13 (0.43)*	0.54	14 (.34)	60 (7)	6 (.7)
FDX Homopolar Generator (CEM-Univ. of Texas)	0.365	28 (100)*	280 (1800)*	8 (200)*	5×10^{-3} (10^{-3})*	4×10^{-4}	207 (447)*	1.34	15.5	0.95	1.15	71 (18)	98 (44)	3 (.8)
Cont. Atmos. Brush Tester (CEM-Univ. of Texas)	-	-	5	-	5×10^{-2}	3×10^{-3}	350	3.25	5.0	0.01	0.02	-	-	-
500 MJ Homopolar Generator (Australian Nat'l. Univ.)	500	800	1600	320	>1.	0.6	170	1.9	1.9	0.3	0.057	1.2 (0.2)	50 (6)	1.9 (.4)
Marshall Rail Gun (Australian Nat'l. Univ.)	-	-	100	-	-	5×10^{-5}	1000	60	12.5	-	-	-	-	-
Advanced Sliding Contact Work (CEM-Univ. of Texas)	-	42	220	-	1.0	5×10^{-2}	5	31	0.4	0.1	7.7	-	-	-

*Potential

**On Shaft

The current density range of 1-1.5 kA/cm² is probably of the most interest for extended operation in space with today's state of the art sintered copper graphite brushes.

The HPG Bearings

Bearings for rotating machinery are traditionally one of three types; rolling element, hydrodynamic or hydrostatic. Since hydrodynamic bearings have stiffness proportional to shaft speed, they are not suitable for use with HPG rotors which are subjected to high forces during discharge as they slow to a stop. Hydrostatic bearings are capable of higher stiffness and lower shaft losses than rolling element bearings, although their overall losses (including pumping) may be higher. Metallic rolling element bearings often experience operating difficulties in the stray magnetic fields of an HPG since they act as small HPG's themselves! However, rolling element bearings may be preferable for space service and some work presently underway on ceramic rolling element bearings may eliminate their sensitivity to magnetic fields. In any event the bearings will require forced lubrication and heat rejection from the lubricant. Some work has been done on magnetic bearings for HPG's at CEM-UT, but there has not been sufficient support to date to fully explore this option. In the 5 MJ HPG at CEM (Fig. 2) the bearings are supported by the magnetic yoke which is quite stiff. The A-I-R HPG concept requires an external bearing support frame as shown in Figure 7.

Motoring the HPG

Since the HPG, like any rotating electromechanical energy convertor, is reversible; it can be self motored using an external dc power supply. However this mode is less than 50% efficient and increases brush wear and rotor heating. Since the HPG rotor is simply a flywheel it can be brought up to speed by any variable speed prime mover. These include synchronous motor with variable frequency drive, variable speed dc motor drive, and the use of a constant speed motor with hydrostatic drive. For space applications, the synchronous motor with variable frequency drive would probably be most expensive and give the most satisfactory long term service; the dc motor drive would be the most compact and would interface easily with a solar panel power supply and the hydrostatic drive might be incorporated with

The current density range of 1-1.5 kA/cm² is probably of the most interest for extended operation in space with today's state of the art sintered copper graphite brushes.

The HPG Bearings

Bearings for rotating machinery are traditionally one of three types; rolling element, hydrodynamic or hydrostatic. Since hydrodynamic bearings have stiffness proportional to shaft speed, they are not suitable for use with HPG rotors which are subjected to high forces during discharge as they slow to a stop. Hydrostatic bearings are capable of higher stiffness and lower shaft losses than rolling element bearings, although their overall losses (including pumping) may be higher. Metallic rolling element bearings often experience operating difficulties in the stray magnetic fields of an HPG since they act as small HPG's themselves! However, rolling element bearings may be preferable for space service and some work presently underway on ceramic rolling element bearings may eliminate their sensitivity to magnetic fields. In any event the bearings will require forced lubrication and heat rejection from the lubricant. Some work has been done on magnetic bearings for HPG's at CEM-UT, but there has not been sufficient support to date to fully explore this option. In the 5 MJ HPG at CEM (Fig. 2) the bearings are supported by the magnetic yoke which is quite stiff. The A-I-R HPG concept requires an external bearing support frame as shown in Figure 7.

Motoring the HPG

Since the HPG, like any rotating electromechanical energy convertor, is reversible; it can be self motored using an external dc power supply. However this mode is less than 50% efficient and increases brush wear and rotor heating. Since the HPG rotor is simply a flywheel it can be brought up to speed by any variable speed prime mover. These include synchronous motor with variable frequency drive, variable speed dc motor drive, and the use of a constant speed motor with hydrostatic drive. For space applications, the synchronous motor with variable frequency drive would probably be most expensive and give the most satisfactory long term service; the dc motor drive would be the most compact and would interface easily with a solar panel power supply and the hydrostatic drive might be incorporated with

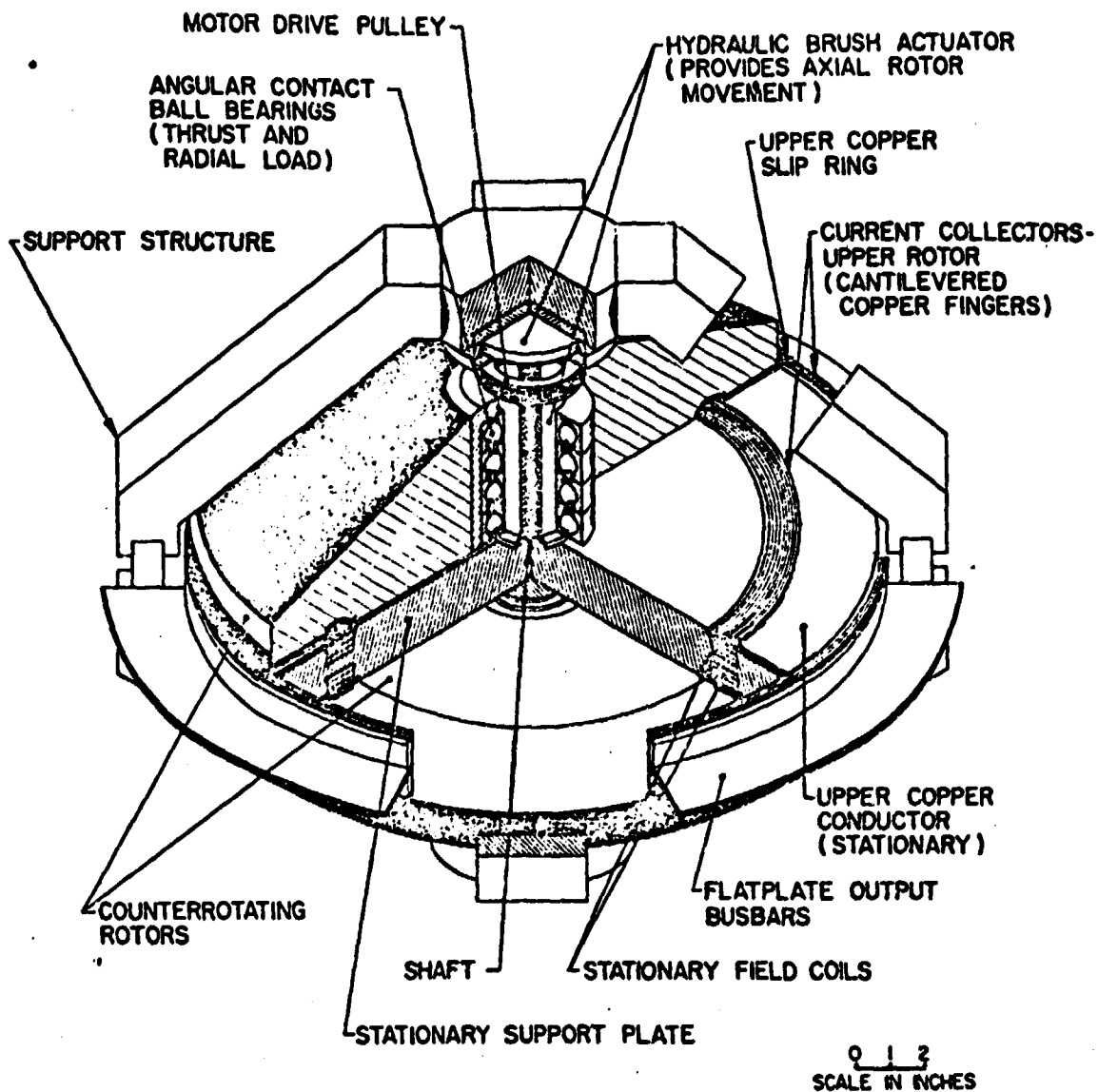


Figure 8. A-I-R HOMOPOLAR
COUNTERROTATING ROTORS

the bearing oil supply system. The selection of the most appropriate system is dependent upon the exact requirements of the mission under consideration.

2. Areas Requiring Development For Space Applications

Although earth based HPG technology may be considered fairly mature, there are certain aspects of the generator design that must be examined closely or changed for space-based operation. In particular these include the operation of bearings, seals, and brushes in the hard vacuum and hostile temperatures of space.

As previously discussed, hydrostatic bearings are desirable for HPG applications because of their high, speed independent, stiffness and low effective coefficient of friction. Also, since there is no metal-to-metal contact in such bearings, they are suitable for long life, low maintenance operation. However, they do require high pressure lubricant (~1000 psi) at relatively high flow rates (~10's gpm) and so require extra space for pumps and reservoirs. Also, the high lubricant flow rates put extra demands on the lubricant seals at the ends of the bearings and these are usually rubbing seals which are subject to wear. CEM does not have experience with extremely long life seals or with the operation of such seals in a hard vacuum, but such experience should be available within NASA.

Rolling element bearings are attractive in that they require fewer auxiliaries and are thus more compact. Also, their lubrication and sealing requirements are less severe, especially if they can be gas cooled and/or bi-phase lubricated. Unfortunately, such bearings do involve metal-to-metal contact and are subject to wear and fatigue. They are also subject to arcing and pitting damage and increased coefficient of friction due to circulating currents induced by stray magnetic fields which are common in HPG's. However, stray fields can be minimized by careful design (in ferromagnetic machines, but not in air cored machines) and it is likely that rolling element bearings are the best choice for space based HPG designs.

Although CEM has extensive operating experience with pulsed high current sliding electrical contacts (see bibliography), how such contacts might operate during extended exposure to the hard vacuum of outer space is not well understood. However, the worst case implication of this problem simply involves the inclusion of a controlled atmosphere within the generator housing to provide an acceptable operating environment for the brushes. The greatest payoff in new brush developments would appear to result from demonstration of acceptable (low) brush wear rates at higher rotor surface speeds. This is especially true of the HPG where rotor speed is not limited by other considerations as is the case with the wound rotor CPA. Present technology allows approximately 10^4 discharges per cm of brush material. Even this wear rate is high for extended space missions.

Liquid metal current collectors eliminate the brush wear problem, but have traditionally proven very troublesome and have virtually been abandoned for rotating machine use. The ready availability of a hard vacuum, however, may well alleviate some of the contamination problems and perhaps liquid metal current collectors should be re-examined in this light.

The final area that needs to be addressed for space based applications of the HPG is unique in that it can be addressed analytically rather than experimentally. This involves the degree to which the discharge reaction torque of pulsed electrical generators can be compensated. At high power levels, the reaction torque of the HPG and CPA rotors is extremely high. This reaction torque can be compensated to a great extent by simply employing counterrotating rotors as in the A-I-R HPG. The moment of inertia of the motors can be closely matched and since the rotors can be run electrically in series and positioned symmetrically about the field coils, they should experience the same $\vec{J} \times \vec{B}$ deceleration. However, due to geometric limitations, the counterrotating rotors cannot be made co-planar, and manufacturing and assembly tolerances may also cause them to be non-co-axial. These imperfections in the torque compensation will produce second and third order effects which may well be significant for space based applications.

3. Scaling of Acceptance Parameters for HPG

For the acceptance parameter MJ/m³ we have seen that the energy density in a HPG rotor is proportional to the cube of the radius for a given material (fixed surface speed). Of course, the rotor volume is also proportional to the cube of the radius for rotors of fixed aspect ratio (comparing similar HPG) so that the MJ/m³ for an HPG rotor is constant. However, we have also seen that the rotor comprises only a fraction of the entire HPG so that

$$(MJ/m^3)_{HPG} = f_1 (MJ/m^3)_{rotor} \quad (6)$$

where

$$f_1 = 0.1 \text{ for disc type}$$

$$f_1 = 0.3 \text{ for drum type}$$

$$f_1 = 0.7 \text{ for A-I-R type}$$

or returning to equation 2 for a complete expression for HPG rotor energy density, we find:

$$K.E. = \frac{\pi r^4 t \rho_m \omega^2}{4}$$

and the rotor volume

$$(Vol)_{rotor} = \pi r^2 t \quad (7)$$

Substituting these relationships into equation 6 gives

$$(MJ/m^3)_{HPG} = \frac{f_1 r^2 \rho_m \omega^2}{4 \times 10^6} \quad (8)$$

Since the majority of the HPG is steel and the copper in the field coil and other conductors is slightly heavier than steel, somewhat offsetting the voids, a good first approximation is to consider the entire volume of the HPG comprised of steel (7833 kg/m³). Using this value the second acceptance parameter is given by

$$(\text{kg/kJ})_{\text{HPG}} = \frac{7833 \text{ kg/m}^3}{(\text{MJ/m}^3)_{\text{HPG}} (10^3 \frac{\text{kJ}}{\text{MJ}})} \quad (9a)$$

$$(\text{kg/kJ})_{\text{HPG}} = \frac{3.13 \times 10^7}{f_1 r^2 \rho_m \omega^2} \quad (9b)$$

Recalling that $r\omega = v$ the surface velocity of the rotor equations 8 and 9 can be rewritten as

$$(\text{MJ/m}^3)_{\text{HPG}} = \frac{f_1 \rho_m v^2}{4 \times 10^6} \quad (8b)$$

$$(\text{kg/kJ})_{\text{HPG}} = \frac{3.13 \times 10^7}{f_1 \rho_m v^2} \quad (9c)$$

Unfortunately the cost per joule is much more dependent upon the configuration and details incorporated into the HPG design than on the size of the device. The CEM 5MJ HPG was built for ~\$50,000 exclusive of engineering in 1974. It is anticipated that once the design and development costs are met, the 5MJ A-I-R HPG being developed by CEM will cost between \$20,000 and \$30,000. These figures are the basis of the relationship in equation 10.

$$(\$/\text{joule})_{\text{HPG}} = 0.01 \quad (10)$$

For the CEM A-I-R HPG, these reduce to:

MJ/m^3	=	30 - 40
kg/kJ	=	0.2 - 0.25
$\$/\text{J}$	=	0.01

4. Compatibility with Electrical Loads

Since the voltage of an HPG is proportional to rotor speed and the kinetic energy stored in the rotor is proportional to the square of the rotor speed, the HPG may be modeled electrically as a capacitor with an effective capacitance given by equation 11a

$$C_{\text{eff}} = \frac{2 \text{ KE}}{V^2} \quad (11a)$$

where

C_{eff} = EFFECTIVE CAPACITANCE (F)

K.E. = ROTOR KINETIC ENERGY (J)

$$\propto r^3 \quad (\text{equation 5})$$

V = HPG Voltage

$$\propto Br \quad (\text{equation 3c})$$

$$\therefore C_{\text{eff}} \propto \frac{r}{B^2} \quad (11b)$$

This being the case, the HPG is suited for driving the same loads as a capacitor (i.e. inductors and resistors) and not well suited for driving other capacitors. This means it is well matched to pulsed magnets and such resistive loads as resistance heaters and arcs. Unfortunately, the relatively low output voltage of the HPG makes it unsuitable for charging inductors too rapidly (due to $L \frac{dI}{dt}$ voltage drop) but its low internal impedance ($\sim 10^{-5}$ ohms) allows it to efficiently deliver extremely high currents ($\sim 10^6$ amps).

The relationship for the discharge of an HPG into an ideal (zero resistance) inductor given by equation 12 is useful for approximating the performance of an HPG with real inductors.

$$\Delta t = \frac{\pi (K.E.)}{I_{\max} V_{\max}} \quad (12)$$

where

Δt = time interval from initiation of discharge to peak current (sec)

K.E. = energy stored in HPG rotor to be transferred to inductor (J)

I_{\max} = peak current

V_{\max} = peak voltage

N.B. - I_{\max} and V_{\max} do not occur at the same time.

A more exact solution for HPG circuit performance can be obtained by modeling the HPG as capacitance in a simple series RLC circuit. In most cases the homopolar machine makes little other contribution to the circuit, the resistance (R) and the inductance (L) being determined primarily by the load and transmission line. The behavior of the circuit may be characterized using the parameter

$$\lambda = \frac{\pi R_m}{\alpha \phi} \sqrt{\frac{J_m}{L_m}} = \frac{\lambda_{sh}}{\alpha} \quad (13)$$

where R_m , L_m , and J_m are the internal resistance, inductance and rotor inertia of the homopolar machine, ϕ is the total magnetic flux cut by the rotor,

$$\alpha = \frac{\sqrt{1 + \frac{L_{load}}{L_m}}}{1 + \frac{R_{load}}{R_m}} \quad (14)$$

and λ_{sh} is the parameter for the short circuited machine. Using λ_{sh} and α one can match a load to a homopolar machine to obtain precisely the desired discharge characteristics.

The family of RLC circuits can be characterized as either under-damped, critically damped, or over-damped as determined by the value of λ . For most cases it is desired to transfer the maximum magnetic energy ($1/2 L_{load} I_{max}^2$) to the load at a specified time (t_{max}). This energy may be determined by calculating I_{max} , the maximum current in the inductor, as follows.

The Under-damped Circuit $0 \leq \lambda < 1$

$$I_{max} = \omega_{max} \sqrt{\frac{J}{L_m + L_{load}}} \exp. \left[-\frac{\lambda}{1-\lambda^2} \sin^{-1} \frac{2}{1-\lambda} \right] \quad (15)$$

$$t_{max} = \frac{\pi^2}{\phi} \sqrt{J (L_m + L_{load})} \frac{1}{\sqrt{1-\lambda^2}} \sin^{-1} \sqrt{1-\lambda^2} \quad (16)$$

The Critically Damped Circuit $\lambda = 1$

$$I_{max} = \frac{\omega_{max}}{e} \sqrt{\frac{J}{L_m + L_{load}}} \quad (17)$$

$$t_{max} = \frac{\pi^2}{\phi} \sqrt{J (L_m + L_{load})} \quad (18)$$

The Over-damped Circuit $1 < \lambda < \infty$

$$I_{max} = \omega_{max} \sqrt{\frac{J}{L_m + L_{load}}} [\lambda + \sqrt{\lambda^2 - 1}] \exp. \left[\frac{\lambda}{\sqrt{\lambda^2 - 1}} \right] \quad (19)$$

$$t_{max} = \frac{\pi^2}{\phi} \sqrt{J (L_m + L_{load})} \cdot \frac{\ln(\lambda + \sqrt{\lambda^2 - 1})}{\sqrt{\lambda^2 - 1}} \quad (20)$$

Where J is the rotor inertia and $\omega_{\max} < (500 \text{ m/sec})/D$.

In order to further characterize the performance of homopolar machines, it is necessary to divide them into slow discharge ($\tau_d > 0.5 \text{ sec}$) and fast discharge ($\tau_d < 0.1 \text{ sec}$) machines. The primary difference between the two is that the skin effect or electromagnetic diffusion time is significant in calculating the effective internal machine resistance for fast discharge machines but not for the slow discharge machines. This difference further manifests itself in the design of the machine in that slow discharge machines can use magnetically unsaturated, ferromagnetic rotors and room temperature field coils to achieve satisfactory performance and operating efficiency, while fast discharge machines require non-ferromagnetic rotors and usually cryogenic or super-conducting field coils. There exists an intermediate range ($0.1 \text{ sec} < \tau_d < 0.5 \text{ sec}$) which may be explored using specially configured ferromagnetic rotors or possibly non magnetic rotors in room temperature or possibly cryogenic field coils.

Internal Machine Resistance

Experimental brush voltage drop data collection from the University of Texas 5 MJ homopolar machine and brush testing facility combined with brush packing factors and conductor geometries evolved from the design studies allow the internal machine resistance (R_m) to be characterized by the following equation

$$R_m = \left[\frac{8.4 \times 10^{-8} W}{D^2} + \frac{2.025 \times 10^{-6} + 3.84 \times 10^{-8} W}{D} \right] \quad (21)$$

where D is rotor diameter and W is the ratio of D to rotor thickness. Equation (21), (22) and (23) assume the use of a steel rotor and aluminum return conductors. Although machine equivalent capacitance (C) is proportional to rotor thickness, the rotor thickness generally should not be allowed to drop below $D/10$ for reasons of dynamic stability. Figure 9 shows R_m as a function of rotor diameter for typical values of W .

Internal Machine Inductance

The same geometric assumptions used in the derivation of equation (21) lead to the following relationship for the internal inductance (L_m) of the homopolar machine.

$$L_m = \left[42.6 \times 10^{-9} + \left(6.6 + \frac{167}{W} \right) \times 10^{-10} D \right] \quad (22)$$

Values for L_m are given in figure 10.

λ_{sh} For Slow Discharge

Equations (21) and (22) can now be substituted into equation (13) to yield the following relationship, assuming an average magnetic field intensity of 1.6 Telsa which is a practical value for steady state, room temperature coils and ferromagnetic rotor and stator.

$$\lambda_{sh} = \frac{0.074 + \frac{0.053}{W}}{D^{3/2}} + \frac{0.504 + \frac{2.23}{W}}{D^{1/2}} \quad (23)$$

For special cases the magnetic field may be pulsed to 1.9 Telsa for the discharge. The resulting λ_{sh} may be determined from equation (23) by multiplying the right side of the equation by 1.9/1.6 (=1.1875). Values for both cases are plotted in figure 11.

Using figures 9, 10, and 11 for a given rotor diameter (D) and thickness (D/W), determine R_m , L_m , and λ_{sh} respectively, find α using equation (14) and the load resistance (R_{load}) for your specific load.

λ may then be calculated using equation (13). Using the value of λ thus obtained determine which of equations (15) through (20) should be used to calculate I_{max} and t_{max} . Figures 9, 10, 11 indicate the appropriate range of values for D.

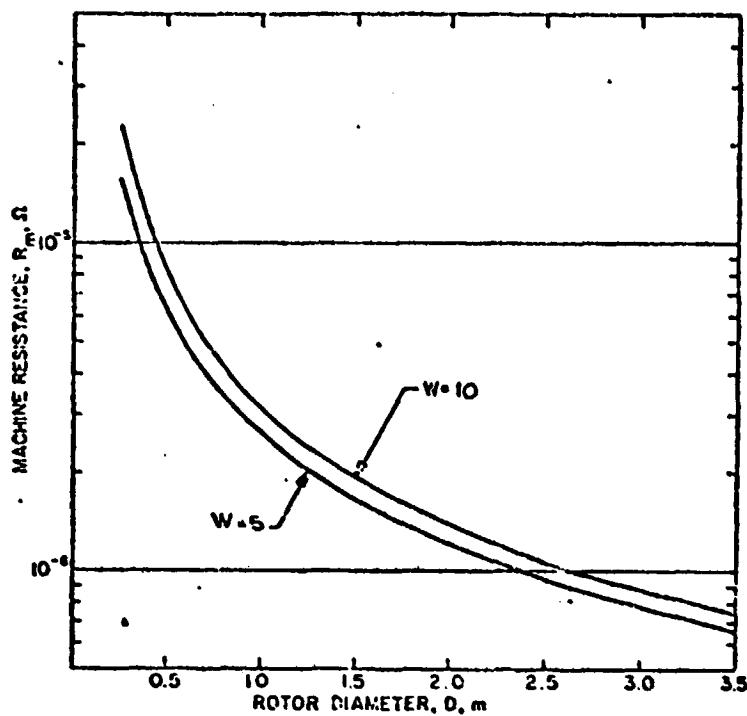


Fig. 9. - Homopolar Machine Resistance (R_m)
as a Function of Rotor Diameter (D)
for Various Rotor Width (D/W) for
Slow Discharge Applications ($\tau_d \geq 0.5$ sec)

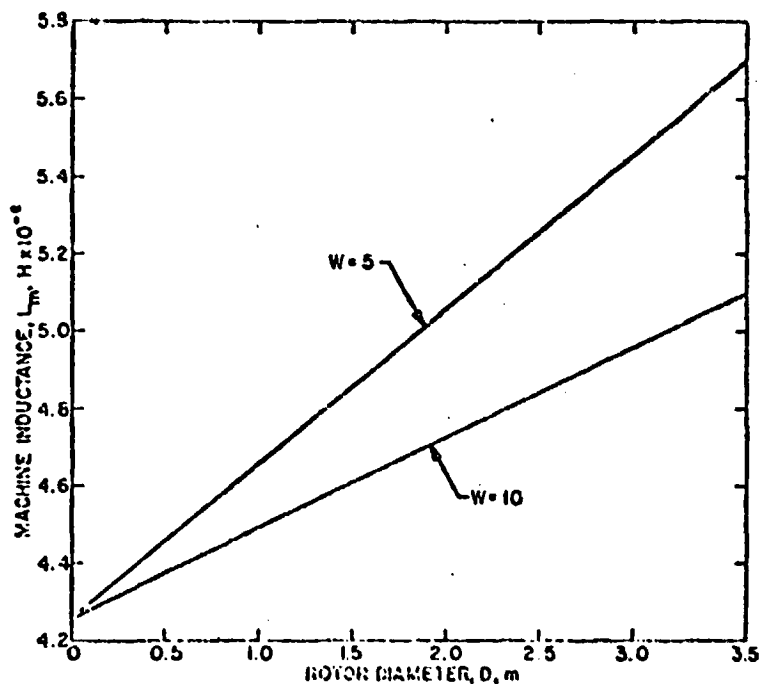


Fig. 10- Homopolar Machine Inductance (L_m)
as a Function of Rotor Diameter (D)
for Various Rotor Widths (D/W) for
Slow Discharge Application ($\tau_d > 0.5$ sec)

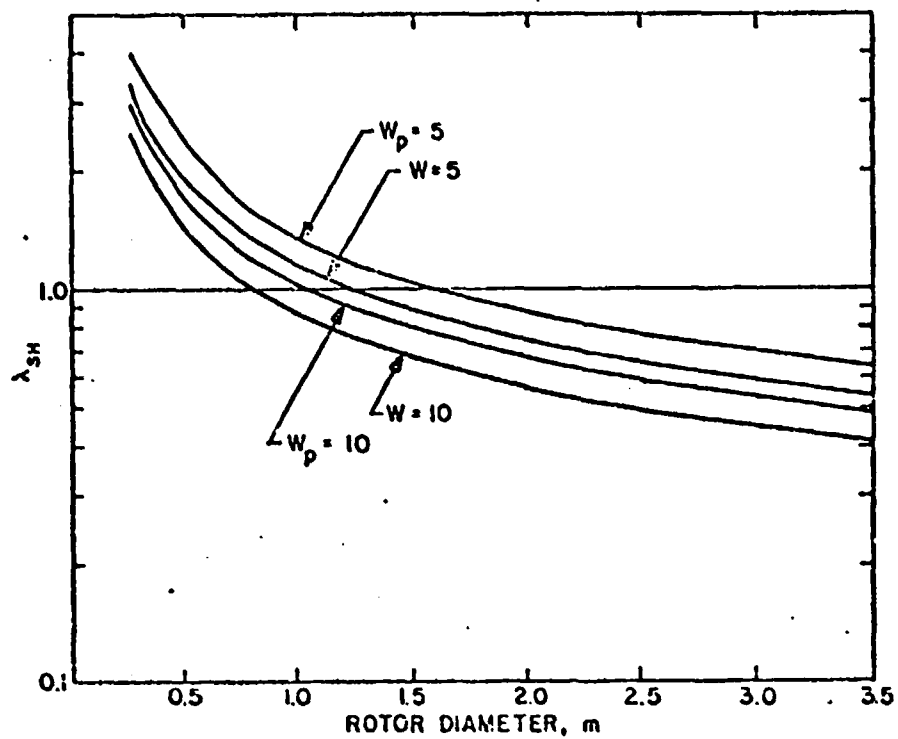


Fig. 11 - λ_{SH} as a Function of Rotor Diameter (D) for Various Rotor Widths (D/W) for Slow Discharge Homopolar Machines ($\tau_d \geq 0.5$ sec)
Subscript "p" indicates pulsed field (see text)

B. THE COMPENSATED PULSED ALTERNATOR

1. Principles of Operation

Recently interest in pulsed power for a variety of applications including magnetic and inertial confinement fusion experiments, advanced weapons systems and industrial manufacturing processes has resulted in many developments in pulsed power supply technology. In several areas inertial energy storage has emerged as an attractive alternative to magnetic or electrostatic energy storage because of the very high energy densities available at relatively low cost. The problem of converting the stored inertial energy to electrical energy, however, has not been satisfactorily resolved in most cases. Conventional alternators are limited in power output by their own internal impedance and although pulsed homopolar generators, having low internal impedance, are capable of very high power outputs, they accomplish this at low voltages which are not always desirable.

In essence, pulse rise times are limited by inductive voltage drop ($L \frac{di}{dt}$). In its simplest form an alternator consists of a single turn coil of wire spun in a magnetic field (Figure 12). Increasing the output voltage of such a machine (to produce faster $\frac{di}{dt}$) requires increasing the magnetic flux density, increasing the surface speed of the rotating coil, or increasing the number of turns in the coil. Ultimately, the magnetic flux density and surface speed of the coil are limited by material properties. The alternator voltage increases linearly with number of turns in the coil, but unfortunately the inductance, which limits pulse rise time, rises with the square of the number of turns resulting in no gain in output power.

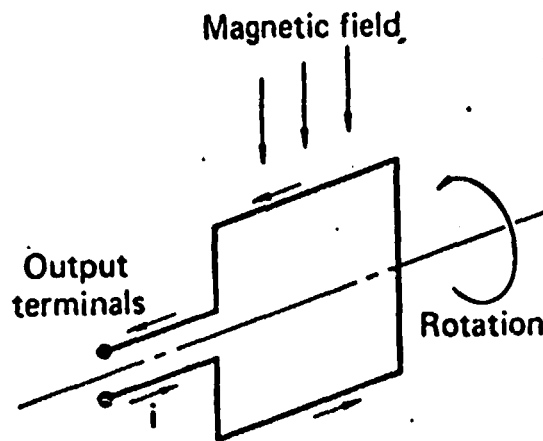


Figure 12. Simple Alternator

The compensated pulsed alternator or compulsator (Figure 13) uses a stationary coil almost identical to the rotating one and connected in series with it to increase output power by flux compression. As the two coils approach one another, the magnetic field generated by the output current is trapped between them and compressed and the effective inductance is therefore reduced. When the two coil axes coincide the inductance is minimized, but the alternator voltage can be at its maximum value. This results in the generation of a very large magnitude current pulse from the machine. In addition the compulsator output voltage during the inductance change can be considerably higher than the open circuit voltage due to $i \frac{dL}{dt}$ effects. As the rotating coil passes the stationary one the inductance again rises to its normal (higher) value, commutating the pulse off.

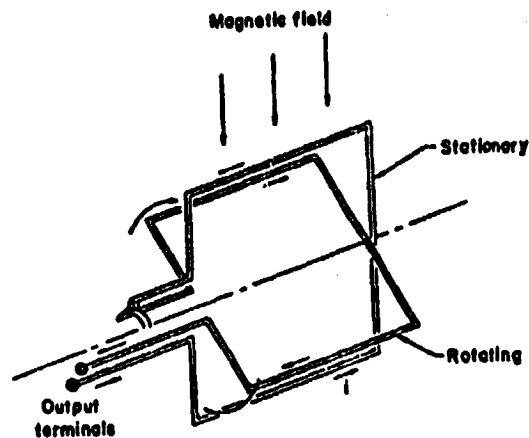


Figure 13. Compensated Pulsed Alternator.

Since the compulsator is essentially a variable inductor in series with a conventional alternator, and depends upon minimizing circuit inductance to generate an output pulse, it is not well suited for driving inductive loads. It is well suited, however, to both capacitive and resistive loads. For convenience the fundamental limitations to compulsator performance can be divided into three groups; those dealing with the effect of load characteristics, those limiting output power, and those limiting minimum pulse width.

2. Effect of Load Characteristics

A simplified (lumped parameter) circuit for a compulsator connected to a resistive load (such as a flashlamp) is shown in Figure 14.

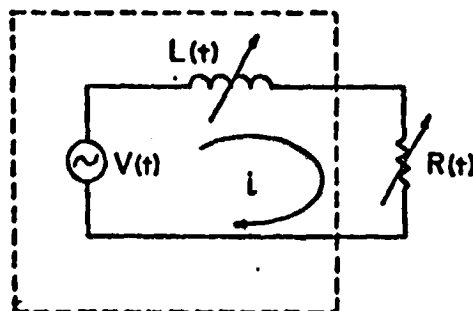


Figure 14. Simplified Circuit Compulsator Driving Resistive Load

The differential equation for this circuit can be written as:

$$\frac{d}{dt}(Li) + Ri = V(t) \quad (24)$$

where L and R are the total instantaneous circuit inductance and resistance, $V(t)$ is the "alternator" voltage (open circuit voltage) due to the armature coil rotating in the applied magnetic field, and i is the instantaneous current. The solution to equation (1) is:

$$i = \frac{1}{L} \left[(L_0 i_0) + \int_0^t V(t) e^{\int_0^t \frac{R}{L} dt} dt \right] e^{-\int_0^t \frac{R}{L} dt} \quad (25)$$

where L_0 and i_0 are initial values of inductance and current at the beginning of the pulse (when the circuit is closed). The first term within the brackets of equation (25) represents the contribution to total output current made by the flux compression aspect of the compulsator while the second term represents the current due to the volt-seconds supplied by the alternator. The first term primarily affects the shape of the output pulse while the second term determines the energy delivered to the load.

For a capacitive load such as a transfer capacitor, the basic circuit is shown in Figure 15 and the differential equation for the circuit is:

$$\frac{d}{dt}(Li) + Ri + \frac{1}{C} \int i dt = V(t) \quad (26)$$

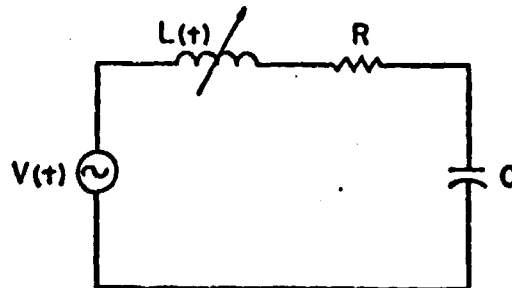


Figure 15. Simplified Circuit Compulsator Driving Capacitive Load

Although the analytical solution of this second order differential equation is quite cumbersome it can be solved numerically and the energy delivered

to a capacitive load by a compulsator has been shown to be

$$E = \eta \frac{\left(\int_0^t v(t) dt \right)^2}{2L_{\min}} \quad (27)$$

where L_{\min} is the minimum total circuit inductance and η is a numerically determined constant which has been found to be around 0.5 for most cases of interest.

3. Limitations to Peak Output Power

It is apparent from equations (25) and (27) that the compulsator's primary advantage, in terms of high output power, over the conventional alternator comes from flux compression, or more specifically, from the interaction of the discharge current with the inductance variation. This in turn implies that the inductance variation must be maximized and since the maximum inductance in the uncompensated position is relatively insensitive to machine variables, really requires that the minimum inductance in the compensated position be reduced as much as possible. This requirement suggests the use of radially thin air gap windings distributed uniformly over the rotor surface rather than salient pole windings or even distributed windings in slots since the slot teeth increase the winding inductance. A significant limitation to peak output power comes then from the conflict between the requirement for minimum radial air gap between the rotor and stator windings in order to minimize L_{\min} and the dielectric strength of the air gap insulation on the windings. The inductance variation is given by $\left(\frac{\tau}{g}\right)^2$ for an iron cored machine (unsaturated), where τ is the conductor width per pole and g is the radial air gap between conductors, so that the sensitivity of machine performance to this air gap limitation is readily apparent.

A second limitation on output power imposed by this air gap winding concerns the shear strength of the insulation system used to bond the stator and rotor windings to the stator and rotor structures. The interaction between the compulsator discharge current and the radial component of the magnetic field in the air gap due to that current causes a tangential force on the conductors which slows the rotor, converting stored inertial energy to electrical energy. This force results in a tangential shear stress

Finally, the requirement that the rotor and stator conductors be radially thin in order to generate minimum inductance is in conflict with the extremely high current densities achievable in the compulsator in that thermal heating of the conductors may become a limiting factor especially in the case of repetitive pulses. This thermal limit can become even more restrictive in that skin effects can confine the fast rising current pulses to the surfaces of the conductors resulting in even more severe heating. This skin effect can be overcome by using stranded and transposed conductors but these increase the minimum inductance somewhat as well as complicating the construction of the machine.

4. Limitations to Minimum Pulse Width

As faster pulses are required the base electrical frequency of the alternator must be increased. The electrical frequency ω_e of the alternator is given by:

$$\omega_e = \frac{P}{2} \omega_m \quad (28)$$

where P is the number of field poles and ω_m is the mechanical rotor speed in radians/sec. The mechanical rotor speed is limited by the stiffness of the rotor and its dynamic behavior in the bearings and by eddy current generation due to the alternating magnetic field experienced by the rotor turning in the heteropolar excitation field. This eddy current limit can be extended by laminating the rotor, but there is a practical limit to the minimum lamination thickness which can be used; and as the rotor laminations are made thinner, rotor construction becomes more difficult and rotor mechanical stiffness suffers.

Increasing the mechanical speed of the rotor has another limitation as well. Increasing rotor speed increases centrifugal loading on the rotor air gap winding. This in turn requires additional banding material in the air gap to restrain the rotor conductors and this leads to increasing the radial air gap spacing which again increases the crucial minimum machine inductance.

This leaves only the option of increasing the number of poles to increase the alternator frequency, but here too we find a limit. As the number of poles increases for a given machine the spacing between poles

must decrease. As this pole-to-pole spacing approaches the air gap distance, the applied field leakage exceeds the useful flux cut by the rotor conductors. This point of diminishing returns makes the addition of more poles futile.

5. Areas Requiring Development for Space Applications

Since the CPA does not stop during the pulse, but only slows down fractionally, the bearing stiffness requirements are not nearly so severe as those of the HPG. For this reason hydrodynamic or rolling element bearings are suitable choices and for space based applications, rolling element bearings would seem the ideal choice for most of the same reasons as given for the HPG.

Magnetic bearings would seem an attractive choice for both the CPA and HPG since they are non-contacting, low loss, and offer adjustable stiffness. They would undoubtedly be suitable for motoring these machines and for sustained speed without discharging, but it is not presently well understood how the magnetic fields required by such bearings might interact with the main fields of these generators. Also, magnetic bearings with sufficient stiffness to sustain discharge forces due to imperfect alignment of electrical axes of rotating and stationary machine conductors have not yet been demonstrated.

The CPA fares somewhat better in terms of brush wear in that (1) the laminated rotor construction and presence of windings on the rotors limit the allowable surface speed to a lower value and (2) the brushes do not operate at the maximum rotor diameter, but rather operate on a reduced diameter slip ring. However, the general comments on brush developments made under the HPG section apply here also. For long term, unattended operation there may also be some problems with the build-up of brush wear debris affecting the high voltage stand-off capability of the brush/slip ring area, but it is anticipated that this problem can be addressed by careful attention to design details. Finally, the brushless rotary flux compressor (BRFC), an outgrowth of the CPA program, requires no brushes at all and is most attractive from the standpoint of machine life.

For the CPA advances are expected to come from (1) improved shear strength of the ground plane insulation, (2) improved hoop strength of the rotor banding, and (3) further refinements in the CPA configuration. It seems reasonable that the ground plane shear strength can be extended from 20 MPa to 40 MPa which would double the allowable peak discharge torque per unit of rotor surface area. Furthermore, rotor banding strength and rotor construction details should be improved to allow extension of peak rotor speed from the current 150 m/sec to 200-250 m/sec. This would result in the following improvements in acceptance parameters for the CPA.

TABLE IV
ACCEPTANCE PARAMETERS
FOR ADVANCED COMPENSATED PULSED ALTERNATORS

	<u>Present</u>	<u>Advanced</u>
MJ/m ³	0.5 - 1	1.5 - 3.0
kg/kJ	7 - 14	2.1 - 4.2
\$/J	0.068 - 0.68	?

6. Scaling and Acceptance Parameters

From this presentation it should have become clear that the design and thus the scaling relationships for a Compulsator involving two electromagnetic generation principles (induction and flux compression) and a much more complicated geometry is much less simple than the HPG case. The magnitude of the problem is such that the LLNL sponsored program for development of Compulsators for solid state lasers has employed a full time engineer and two graduate students at CEM for the last year, plus two programmers at LLNL for the last four months just to develop a computer code for the optimization of a compulsator design to drive xenon flash lamps for solid state lasers. A simple scaling relationship for compulsators does not exist and probably never will. For example, since the output of compulsator is so dependent upon the load characteristics, energy density

figures on a per pulse basis are meaningless without specifying the exact load characteristics. However some generalized observations can be made. In terms of weight, volume, and performance, the CPA components can be divided into three categories: (1) the rotor which stores energy inertially, (2) the magnetic circuit which provides excitation, and (3) the stationary and rotating conductors which accomplish the energy conversion. For space applications, air cored machines may at first seem attractive since they offer potential weight reductions of a few orders of magnitude. Unfortunately, they also exhibit increased excitation power requirements in about the same ratio, and it is anticipated that the high stray magnetic fields associated with such machines would not be acceptable in a space craft. Therefore, only ferromagnetic machines have been considered in this comparison. Since the CPA rotor must be laminated steel and has windings bonded to its surface, surface velocity is usually limited to approximately 150 m/sec although this is not an absolute value. This limits energy density in the rotor to a value of 180 kg/MJ or 44 MJ/m³. Constant flux density considerations dictate that the stator have at least the same radial thickness as the rotor so that even without allowing space for the field coils, these figures are reduced to 720 kg/MJ or 11 MJ/m³. Furthermore, the CPA can only deliver 5-10% of its stored energy per pulse so that on a per pulse basis these values are further reduced to 14.4-7.2 kg/kJ and 0.55-1.1 MJ/m³.

The CEM/LLL Engineering Prototype CPA was constructed for a labor and materials cost of ~\$136,000 exclusive of engineering; and is capable of delivering 200 kJ per pulse at a peak power of 200 MW for an effective cost of \$0.68/joule for \$0.00068/watt. The cost per joule figures are certainly subject to question since only a single, hand-built prototype has been fabricated and the compulsator uses several unorthodox construction techniques. It is anticipated that these costs will be reduced by an order of magnitude for larger machines, but not for smaller ones. The apparent difference in cost is offset by the fact that the CPA is capable of higher voltages, is self-switching, is rep-ratable, and operates at almost constant speed. Furthermore, for space applications extra windings can be incorporated to allow the CPA to operate as a synchronous motor during its spin up phase.

In summary then:

Present MJ/m ³ for CPA	0.5-1
Present kg/kJ for CPA	7-14
Present \$/joule for CPA	0.068-0.68

C. POTENTIAL APPLICATIONS

MPD Thruster

Previous work at Princeton University has demonstrated that the MPD arc jet operates more efficiently at higher power levels than are available from current prime source power supplies. Pulsed energy storage devices are, therefore, necessary to provide power conditioning to allow the MPD arc jet to operate in the high efficiency regime.

The time varying nature of the MPD load can be divided into three parts; the initial breakdown across the gap, the growth of the initial breakdown streamers(s) to fill the annular space, the transport phase during which most of the energy is transferred to the gas. Although little energy is transferred during the first two phases, they are nevertheless quite important, especially for operation with the CPA which seems best suited for this type of load. The two initial or "start-up" phases are the time when the initial current is established in the CPA windings which provides the flux which will be compressed during the main part of the pulse (transport phase). Thus small variations in load impedance during start-up can result in substantial changes in full load performance of the CPA. Unfortunately, without an MPD thruster impedance model, we cannot accurately determine the voltage and current requirements for the CPA.

A suitable model for the time varying electrical impedance of the MPD thruster is not available, especially during the first two phases, so we were not able to calculate the predicted performance of a homopolar generator (HPG) or compensated pulsed alternator (CPA) driving such a load. The development of such a model is within the capabilities of the Center for Electromechanics since we have developed similar models for Tokamak Plasmas and Xenon flash lamps, but it is well beyond the scope of this contract. However, the

similarity of the MPD thruster load to a Xenon flashlamp suggests that the CPA will be suitable for driving such a load.

Welding in Space

The space environment has several features which affect the application of terrestrial joining processes. The most obvious of these are the zero-gravity and vacuum conditions that exist in space. Several joining processes have been considered for use in space, and some experiments have been carried out during the U.S. and U.S.S.R. manned space flight programs. Each of the possible processes has its area of application, and each has its own set of technical problems. Homopolar pulse resistance welding (HPRW), a solid-state welding process which uses a homopolar generator to supply a current pulse for heating, is a new welding process presently under development, at CEM - UT and has not as yet been considered for welding in space.

The HPRW process has several unique characteristics which are attractive for welding in space. Among these are:

1. With modern advancements in homopolar generator technology, the physical size of a generator capable of welding the relatively light-gage metals used in space structures should be significantly smaller than for those processes that require transformer-type power supplies. A moment-free, counterrotating, sealed homopolar generator might occupy a volume of a few cubic feet, for example.
2. If necessary, the energy to power-up the homopolar generator can be obtained directly from the sun by means of a photovoltaic solar panel array. It would appear that in the space welding application it will not be necessary to make large numbers of welds per unit time, so it should be feasible to bring the generator up to speed over a time period of perhaps several hours at very modest power levels. If necessary, several generators can be operated independently to provide the desired welding rate.
3. Unlike the directed-energy welding processes (arc, electron beam, and laser welding), the HPRW process is capable of making a complete seam weld, such as a pipe girth weld, in a single pulse which is typically about one second in duration.
4. No melting occurs in a properly made HPR weld, obviating the need to control the behavior and composition of a molten metal pool.

5. The HPRW process is entirely under automatic control once the welding current pulse has been initiated, which would appear to be almost a requirement for welding in space.

The HPRW process falls into the general category of upset resistance welding processes, although it can be operated in a spot welding mode. When used in the upset mode, the following process requirements must be recognized and provided for:

1. The fit-up between the faying surfaces must result in their being in solid contact prior to welding.
2. A welding fixture must be provided which not only holds the parts in alignment and conducts the current to and from the weld but also applies upsetting force across the weld at the proper point in the weld cycle. The magnitude of the applied force will depend on the joint area, but the stress across the weld interface must be of the order of the yield strength of the metal at its forging temperature.
3. Upset displacement of the metal is necessary to the formation of a satisfactory weld. The magnitude of the upset is typically about 0.5 cm when making a pipe girth weld or a butt weld in 2.5 cm diameter bar. This decrease in length must be allowed for when using the HPRW process to fabricate a structure.

The HPRW process is described in detail in App. B. As configured for welding in space, the following components will be required:

1. Motoring Power Supply - A source of continuous dc, with provision for applying it across the terminals of the homopolar generator.
2. Homopolar Generator - An inertial energy storage device consisting of two counter-rotating discs, a field coil, appropriately arranged sliding electrical contacts, a closing switch, the field power supply, and controls. The counterrotating discs are necessary for welding in space to eliminate unbalanced reaction torques. Sliding electrical contacts may require presence of an

atmosphere for their operation, so the generator enclosure may likely have to be sealed.

3. Welding Fixture - A mechanism that is specific to the size and configuration of the joint and which provides means for connecting the output terminals of the generator solidly to each side of the weld interface. The fixture must also incorporate a subsystem for applying a small initial mechanical force and switching to the larger upset force during the weld cycle.

For comparison, the candidate processes for making permanent joints in space are listed in Table V, and salient features and points of difference from the HPRW process are briefly noted below.

Resistance Spot Welding (RSW) - Requires a power supply of either the transformer, capacitor bank, or battery type. Welds contain a molten and solidified zone, or nugget. If used to make seam welds, can be done only as a series of overlapping spot welds made in sequence, thus requiring complex and precise tooling.

Friction Welding (FW) - Requires substantial mechanical rotation and upset forces, and it would appear that achievement of moment-free operation would be difficult. Unless a three-piece joint is used, one of the parts must have an axis of symmetry and must be free to rotate about that axis.

Diffusion Welding (DW) - Requires the application of substantial compressive force for times of at least minutes while maintaining weld temperatures typically above 1000°F. Benefit of any prior materials processing is usually lost. Best adapted to making area joints.

Explosive Welding (EW) - Probably best adapted to the formation of welds in tubular slip fit joints. Fastest known welding process but requires transport, storage and handling of explosives.

Electron Beam Welding (EBW) - Produces narrow seam-type joint of the fusion variety by the heating effect of a beam of high energy electrons. The process is usually carried out in a vacuum chamber on earth, which can be dispensed with in space. A high-voltage power supply

TABLE V. POSSIBLE JOINING PROCESSES FOR USE IN SPACE

Process	Requires Special Power Supply	Requires Powered Tooling	Requires Atmosphere Other than Space Vacuum	Requires Tractor	Makes Autogenous Joint	Contains Fusion Zone	Contains Upset Region
HPRW	YES	YES	NO	NO	YES	NO	YES
Conventional RSW	YES	YES	NO	NO	YES	YES	NO
FW	YES	YES	NO	NO	YES	NO	YES
DW	YES	YES	NO	NO	YES	NO	YES
EW	NO	NO	NO	NO	YES	NO	YES
EBW	YES	NO	NO	YES	YES	YES	NO
LW	YES	NO	NO	YES	YES	YES	NO
GTAW	YES	NO	YES	YES	YES	YES	NO
PAW	YES	NO	YES	YES	YES	YES	NO
Brazing	NO	NO	NO	NO	NO	YES	NO
Adhesive Bonding	NO	NO	NO	NO	NO	NO	NO

must be provided, and there must be accurate relative motion between the electron gun and the joint. All mechanical tolerances must be exceptionally tight. There may be problems with outgassing of molten metal and with keeping the molten metal in position, but they will be less than with other fusion welding processes.

Laser Welding (LW) - Pulsed laser is capable only of spot or overlapping-spot seam welding. A continuous-wave gas laser can produce seam welds. Provision must be made for recirculation and cooling of the laser gas. This, plus the required length of the laser cavity, even if folded, and the bulk of the power supply, would make it difficult to provide relative motion between the laser beam and the work, but with clever joint design, serviceable laser welds routinely made in space may be possible. Concerns relative to control of the molten weld metal are the same as with other fusion welding processes.

Gas Tungsten-Arc Welding (GTAW) - The GTAW process is taken as being representative of several arc welding processes, since it is the one most likely to be considered for welding thin materials and is also perhaps the arc welding process that is most controllable and easiest to automate. Maintaining a stable welding arc under conditions in space, however, would be a difficult problem, and at the very least would require high flow rates of shielding gas. Control of the molten pool and its chemistry would be of concern also. If use of filler wire is attempted, a wire feeder must be supplied. There must be relative motion between the electrode and the work.

Plasma-Arc Welding (PAW) - Equipment for the PAW process is generally similar to that for the GTAW process. The differing operation of the torch, especially in the non-transferred mode, may give this process a better chance at overcoming arc stability problems. The other comments regarding GTAW apply also to PAW, however.

Brazing - For specific types of joints, those in which the joint design can provide for sufficient bond area to offset the (usually) lower mechanical strength of the brazing alloy relative to the workpiece surfaces. Required tolerances are fairly tight. Space vacuum may aid

in the brazing operation by causing the disappearance of surface films of oxides and adsorbed gases which must be removed by means of a flux in terrestrial brazing. The capillary forces which cause flow of the brazing alloy into the joint act regardless of gravitation, but the requirements for accuracy and uniformity of temperature throughout the joint remain and are practical limitations on the size of brazed joints. Exothermic brazing, a process somewhat analogous to thermit welding, in which heat is generated within the brazing alloy itself by a chemical reaction, has been proposed for joining materials in space. There must be no relative motion in a brazed joint until the brazing alloy has solidified, a process that will take longer in space than on earth due to the absence of convective heat transfer. The same comments made about brazing apply also for soldering, but the service temperatures of both brazed and soldered joints must of course be well below the melting point of the braze alloy or solder used.

Adhesive Bonding - The use of organic adhesives in space is attractive for certain applications, since it does not require heating to the high temperatures necessary for welding or brazing. Service life of joints may be limited by degradation of the adhesive, but can be of the order of several years. Curing times may be excessive in some cases, and shelf life of the adhesive may be a problem.

In summary, there are several possible joining techniques for use in space, all of which must be specially adapted and all of which present unique problems. Homopolar pulse resistance welding is a candidate process that has not been investigated heretofore for welding in space and is sufficiently different from any other joining method that its possible advantages should be explored.

Electromagnetic Launcher

The acceleration of macroparticles to hypervelocities by a plasma armature in an electromagnetic rail gun has been demonstrated by R. A. Marshall, et al., at the Australian National University*. It appears

*Reference: Rashleigh, S. C. and Marshall, R. A. "Electromagnetic acceleration of macroparticles to high velocities," J.Appl.Phys.49(4), April 1978

that further developments of such technology using HPG power supplies would be capable of efficiently accelerating significant payloads to escape velocity from the earth's surface. One approach to this interesting possibility is discussed in Appendix C.

Other Applications

The availability of compact, inexpensive pulsed power sources capable of extremely high peak output power suggests several other potentially attractive applications. The CPA which is being developed to power flashlamps for solid state lasers for the laser fusion program could also power high powered pulsed lasers from laser ranging. Although the present CEM prototype CPA is intended for solid state lasers, work is already underway on advanced CPA concepts for powering high efficiency lasers. There are undoubtedly other sensing schemes for planetary exploration (i.e. seismic) which could benefit from the availability of these pulsed power supplies.

Another potential application for pulsed power supplies involves burst transmission of accumulated data by advanced mission space probes. This may prove useful when and if the available average prime power supply is not capable of supplying the necessary transmitter power and may serve to relax the severe antenna pointing and tracking requirements for advanced missions.

SECTION III CONCLUSIONS

Although certain questions remain unanswered concerning the suitability of state-of-the-art bearings, seals and brushes for space applications of the HPG and CPA, the energy densities and peak power capabilities make these devices look attractive for space applications (Table VI).

TABLE VI
PRESENTLY ACHIEVABLE
ACCEPTANCE PARAMETERS
FOR HPG AND CPA

	<u>HPG</u>	<u>CPA</u>
MJ/m ³	30-40	0.5-1.0
kg/kJ	0.2-0.25	7-14
\$/J	0.005-0.01	0.068-0.68

The areas with greatest potential for improvement include reduction of brush wear at rotor speeds above 250 m/sec for the HPG and improvements in ground plane insulation shear strength, rotor banding performance and enhanced inductance variation for the CPA. With reasonable improvements in these areas, the above acceptance parameters may be improved to those in the table below.

TABLE VII
ADVANCED
ACCEPTANCE PARAMETERS
FOR HPG AND CPA

	<u>HPG</u>	<u>CPA</u>
MJ/m ³	~ 200	1.5-3.0
kg/kJ	~0.04	2.1-4.2

SECTION IV RECOMMENDATIONS

In order to better appreciate the potential advantages and liabilities of utilizing HPG and CPA for space applications, it is suggested that preliminary engineering point designs of systems for specific applications be undertaken for one or more applications. Unanswered questions such as uncompensated reaction torque should receive special attention during the proposed studies. In the case of the MPD thruster, it is suggested that a complete circuit model for the device be determined either experimentally or analytically.

The A-I-R HPG development program currently underway at CEM will answer many questions about the suitability of rolling element bearings for use in such devices. An analytical study of the suitability of magnetic bearings for use in pulsed rotating electrical machinery should indicate whether or not a magnetic bearing development effort would be warranted.

Finally, experimental investigation of the performance of sliding electrical contacts at speeds above 250 m/sec with an effort to reduce wear should be profitable. CEM expertise in this area is evidenced in the bibliography.

**SECTION V
NEW TECHNOLOGY**

No new technology was developed in the course of this program.

SECTION VI BIBLIOGRAPHY

SLOW DISCHARGE HOMOPOLAR GENERATORS

H.G. Rylander, et al, "Homopolar Motor-Generator Designs for Cheap Inertial Energy Storage." Technical Report ESL-9, Energy Systems Laboratories, College of Engineering, The University of Texas at Austin, January 1973.

R.E. Rowberg, et al, "Characteristics of a Homopolar Machine as a Power Supply for Large Pulsed Magnetic Fields for Fusion Experiments." Record of Technical Papers, 25th Annual Southwestern IEEE Conference & Exhibition, Houston, Texas, April 4-6, 1973, pp. 453-459.

H.G. Rylander, et al, "Homopolar Motor-Generator for Inexpensive Inertial Energy Storage." Texas Atomic Energy Research Foundation Project Progress Report No. 19 (November 1, 1972, to April 30, 1973), Bureau of Engineering Research, The University of Texas at Austin.

H.G. Rylander, et al, "Investigation of the Homopolar Motor-Generator as a Power Supply for Controlled Fusion Experiments." Presented at the Fifth Symposium on Engineering Problems of Fusion Research, Princeton, New Jersey, November 1973.

H.G. Rylander, et al, "Homopolar Motor-Generator for Inexpensive Inertial Energy Storage." Texas Atomic Energy Research Foundation Project Progress Report No. 20 (May 1, 1973, to October 31, 1973), Bureau of Engineering Research, The University of Texas at Austin.

H.G. Rylander and H.H. Woodson, "Homopolar Motor-Generator Inertial Energy Storage Systems." Presented at the DCTR Power Supply and Energy Storage Review Meeting, Germantown, Maryland, March 5-7, 1974.

H.G. Rylander, et al, "Homopolar Motor-Generator for Inexpensive Inertial Energy Storage." Texas Atomic Energy Research Foundation Project Progress Report No. 21 (November 1, 1973, to April 30, 1974), Bureau of Engineering Research, The University of Texas at Austin.

S.F. Mustafa, et al, "Electromagnetic Thrust Bearing for a Homopolar Machine - Theoretical Analysis." Technical Report ESL-23, Energy Systems Laboratories, College of Engineering, The University of Texas at Austin, May 1974.

Z. Islam, et al, "Electromagnetic Thrust Bearing for a Homopolar Machine - Experimental Implementation." Technical Report ESL-24, Energy Systems Laboratories, College of Engineering, The University of Texas at Austin, May 1974.

H.H. Woodson, et al, "Homopolar Motor-Generator for Inexpensive Inertial Energy Storage." Texas Atomic Energy Research Foundation Project Progress Report No. 22 (May 1, 1974, to October 31, 1974), Bureau of Engineering Research, The University of Texas at Austin, pp. 191-204.

W.F. Weldon, et al, "The Design, Fabrication, and Testing of a Five Megajoule Homopolar Motor Generator." Presented at the International Conference on Energy Storage, Compression and Switching, Torino, Italy, November 5-7, 1974.

M.D. Driga, et al, "A Topological Approach to Acyclic Machines." Internal Report, Energy Storage Group, The University of Texas at Austin, February 1975.

W.F. Weldon, et al, "Inexpensive Inertial Energy Storage Utilizing Homopolar Motor-Generators." Presented at the Energy System Session, Second Annual UMR-MEC Conference on Energy, University of Missouri-Rolla, October 7-9, 1975.

S.A. Nasar and H.H. Woodson, "Storage and Transfer of Energy for Pulsed Power Applications." Presented at the Sixth Symposium on Engineering Problems of Fusion Research, San Diego, California, November 18-21, 1975.

W.F. Weldon, et al, "The Design of Homopolar Motor-Generators for Pulsed Power Applications." Presented at the Sixth Symposium on Engineering Problems of Fusion Research, San Diego, California, November 18-21, 1975.

W.L. Bird, et al, "Preliminary Engineering Design of a Pulsed Homopolar Generator Power Supply " Presented at the IEEE International Pulsed Power Conference, Lubbock, Texas, November 9-11, 1976.

K.M. Tolk, et al, "Inertial Energy Storage Research at The University of Texas at Austin." Presented at the IEEE International Pulsed Power Conference, Lubbock, Texas, November 9-11, 1976.

H.H. Woodson, H.G. Rylander, and W.F. Weldon, "Pulsed Power from Inertial Storage with Homopolar Machines for Conversion." Presented at the IEEE International Pulsed Power Conference, Lubbock, Texas, November 9-11, 1976.

P. Wildi, S. Hutchins, and M.D. Driga, "Applying a Homopolar Power Supply to a Tokamak." Presented at the IEEE International Pulsed Power Conference, Lubbock, Texas, November 9-11, 1976.

W.C. Alexander, et al, "The Transient Temperature Field within a Disk-Type Homopolar Generator." Publication No. PN-30, Center for Electromechanics, The University of Texas at Austin, March 1977.

W.L. Bird, et al, "System Engineering and Design of a Pulsed Homopolar Generator Power Supply for the Texas Experimental Tokamak." Presented at the Seventh Symposium on Engineering Problems of Fusion Research, Knoxville, Tennessee, October 24-29, 1977.

W.F. Weldon, H.G. Rylander, and H.H. Woodson, "Homopolar Generator Development at The University of Texas." Presented at the Seminar on Energy Storage, Compression and Switching, The Australian National University, Canberra, Australia, and The University of Sydney, Sydney, Australia, November 15-21, 1977.

W.F. Weldon, H.G. Rylander, and H.H. Woodson, "The TEXT Energy Storage System." Presented at the Seminar on Energy Storage, Compression and Switching, The Australian National University, Canberra, Australia, and The University of Sydney, Sydney, Australia, November 15-21, 1977.

J.H. Gully, et al, "Rebuilding the Five Megajoule Homopolar Machine at The University of Texas." Digest of Technical Papers, 2nd IEEE International Pulsed Power Conference, Lubbock, Texas, June 12-14, 1979, pp. 325-329.

W.E. Drummond (Principal Investigator), "Homopolar Generators and Inductive Storage." Appendix B to Final Report (Fusion ? & D on Advanced Fuels, Homopolar Generators, Circuit Breakers and Tokamak Diagnostics), Electric Power Research Institute Research Project 96-2, Fusion Research Center, The University of Texas at Austin, September 1975, pp. 25-42.

K.M. Tolk, et al, "Design Considerations for a Homopolar Pulsed Power Supply for Shiva Upgrade." Final Report, Lawrence Livermore Laboratory Purchase Order No. 5407703, Center for Electromechanics, The University of Texas at Austin, April 1977.

R.C. Swanson (Editor), "Progress Report No. 1, Homopolar Motor-Generator Research for Inertial Energy Storage." Technical Report ESL-36, Energy Systems Laboratories, College of Engineering, The University of Texas at Austin, August 1975.

G.T. Santamaria, "Induction Motoring Systems for the TEXT Homopolar Generators: A Study of Design Alternatives." Master's Thesis, The University of Texas at Austin, December 1976.

S. Saibua, "Control of Homopolar Generator Output Pulse Current Waveshape." Doctoral Dissertation, The University of Texas at Austin, May 1978.

W.L. Bird, et al, "Pulsed Homopolar Power Supply for an Experimental Tokamak." Presented at the IEEE International Conference on Plasma Science, The University of Texas at Austin, May 24-26, 1976.

R.A. Marshall and W.F. Weldon, "Parameter Selection for Homopolar Generators Used as Pulsed Energy Stores." (Accepted for publication in Electric Machines and Electromechanics.)

FAST DISCHARGE HOMOPOLAR GENERATORS

M.D. Driga, et al, "Fast Discharge Acyclic Machines." Internal Report, Energy Storage Group, The University of Texas at Austin, April 1975.

W.F. Weldon, et al, "Inexpensive Inertial Energy Storage Utilizing Homopolar Motor-Generators." Presented at the Energy System Session, Second Annual UMR-MEC Conference on Energy, University of Missouri-Rolla, October 7-9, 1975.

H.G. Rylander, et al, "Role of Fast-Discharging Homopolar Machines in Fusion Devices." Presented at the American Nuclear Society Winter Meeting, San Francisco, California, November 16-21, 1975.

S.A. Nasar and H.H. Woodson, "Storage and Transfer of Energy for Pulsed Power Applications." Presented at the Sixth Symposium on Engineering Problems of Fusion Research, San Diego, California, November 18-21, 1975.

W.F. Weldon, et al, "The Design of Homopolar Motor-Generators for Pulsed Power Applications." Presented at the Sixth Symposium on Engineering Problems of Fusion Research, San Diego, California, November 18-21, 1975.

M. Brennan, et al, "Energy Storage and Transfer with Homopolar Machine for a Linear Theta-Pinch Hybrid Reactor." LA-UR-76-1203, Los Alamos Scientific Laboratory, April 1976.

H.G. Rylander, et al, "Pulsed Energy Storage in Fusion Devices." LA-UR-76-1837, Los Alamos Scientific Laboratory, August 1976.

J.H. Gully, et al, "One Millisecond Discharge Time Homopolar Machine (FDX)." Presented at the IEEE International Pulsed Power Conference, Lubbock, Texas, November 9-11, 1976.

H.F. Vogel (Los Alamos Scientific Laboratory) and M.D. Driga (The University of Texas at Austin), "Magnetics and Superconducting Coil Design of a 10-MJ, Fast-Discharging Homopolar Machine." Presented at the Sixth International Conference on Magnet Technology, Bratislava, Czechoslovakia, August 29-September 2, 1977.

W.F. Weldon, "Pulsed Homopolar Generator Research at The University of Texas at Austin." Proceedings of the First AFAPL Generators and Motors Seminar, Technical Report AFAPL-TR-79-2090, US Air Force Aero Propulsion Laboratory, Air Force Systems Command, Wright-Patterson Air Force Base, Ohio, August 1979, pp. 46-55.

J.H. Gully, et al, "Design, Fabrication and Testing of a Fast Discharge Homopolar Machine (FDX)." Presented at the Seventh Symposium on Engineering Problems of Fusion Research, Knoxville, Tennessee, October 24-29, 1977.

W.F. Weldon, H.G. Rylander, and H.H. Woodson, "FDX - a Fast Discharge Homopolar Generator." Presented at the Seminar on Energy Storage, Compression and Switching, The Australian National University, Canberra, Australia, and The University of Sydney, Sydney, Australia, November 15-21, 1977.

T.M. Bullion, et al, "Testing and Analysis of a Fast Discharge Homopolar Machine (FDX)." Digest of Technical Papers, 2nd IEEE International Pulsed Power Conference, Lubbock, Texas, June 12-14, 1979, pp. 333-342.

M.D. Driga, et al, "Fundamental Limitations and Topological Considerations for Fast Discharge Homopolar Machines." IEEE Transactions on Plasma Science, Vol. PS-3, No. 4, December 1975, pp. 209-215.

H.F. Vogel, et al, "Energy Storage and Transfer with Homopolar Machine for a Linear Theta-Pinch Hybrid Reactor." Report, LA-6174, Los Alamos Scientific Laboratory, April 1976.

J.H. Gully, et al, "The Design, Construction and Initial Testing of a Fast Discharge Homopolar Generator." Final Report, Electric Power Research Institute Research Project No. 469-3, Energy Storage Group, The University of Texas at Austin, December 1976.

K.I. Thomassen (Principal Investigator), "Conceptual Engineering Design of a One-GJ Fast Discharging Homopolar Machine for the Reference Theta-Pinch Fusion Reactor." Semi-Annual Report, EPRI ER-246, Research Project 469, Electric Power Research Institute, Palo Alto, California, August 1976.

M. Yunus, "Fast Discharge Drum Type Homopolar Machine." Master's Thesis, The University of Texas at Austin, December 1975.

Y. Hadaegh, "Design of a Disk Type Fast Discharge Homopolar Machine." Master's Thesis, The University of Texas at Austin, December 1975.

J.H. Gully, et al, "Engineering Design of a Fast Discharging Homopolar Demonstration Model." Presented at the IEEE International Conference on Plasma Science, The University of Texas at Austin, May 24-26, 1976.

J.H. Gully, et al, "Testing and Analysis of a Fast Discharge Homopolar Machine (FDX)." Presented at the IEEE International Conference on Plasma Science, Monterey, California, May 15-17, 1978.

COMPACT HOMOPOLAR GENERATORS

W.F. Weldon, H.G. Rylander, and H.H. Woodson (Principal Investigators), "Design, Fabrication and Testing of a Compact, Lightweight Pulsed Homopolar Generator Power Supply, Phase I." 1st Quarterly Technical Report, Naval Surface Weapons Center Contract No. N60921-80-C-A033, Center for Electromechanics, The University of Texas at Austin, January 1980.

W.F. Weldon, H.G. Rylander, and H.H. Woodson (Principal Investigators), "Design, Fabrication and Testing of a Compact, Lightweight Pulsed Homopolar Generator Power Supply, Phase I." Mid-Contract Technical Report, Naval Surface Weapons Center Contract No. N60921-80-C-A033, Center for Electromechanics, The University of Texas at Austin, February 1980.

W.F. Weldon, H.G. Rylander, and H.H. Woodson (Principal Investigators), "Design, Fabrication and Testing of a Compact, Lightweight Pulsed Homopolar Generator Power Supply, Phase I." 2nd Quarterly Technical Report, Naval Surface Weapons Center, Contract No. N60921-80-C-A033, Center for Electromechanics, The University of Texas at Austin, April 1980.

W.F. Weldon, H.G. Rylander, and H.H. Woodson (Principal Investigators), "Design, Fabrication and Testing of a Compact, Lightweight Pulsed Homopolar Generator Power Supply, Phase I." Final Report, Naval Surface Weapons Center Contract No. N60921-80-C-A033. (Aug 1980)

COMPENSATED PULSED ALTERNATORS

W.F. Weldon, H.G. Rylander, and H.H. Woodson, "Invention from Research." DISCOVERY: Research and Scholarship at The University of Texas at Austin, Vol. III, No. 2, December 1978, pp. 20-23.

W.F. Weldon, et al, "Compulsator - a High Power Compensated Pulsed Alternator." Second International Conference on Energy Storage, Compression, and Switching, Venice, Italy, December 5-8, 1978.

W.L. Bird, et al, "Applying a Compensated Pulsed Alternator to a Flashlamp Load for Nova - Part II." Digest of Technical Papers, 2nd IEEE International Pulsed Power Conference, Lubbock, Texas, June 12-14, 1979, pp. 463-466.

M. Brennan, et al, "The Mechanical Design of a Compensated Pulsed Alternator Prototype." Digest of Technical Papers, 2nd IEEE International Pulsed Power Conference, Lubbock, Texas, June 12-14, 1979, pp. 392-397.

J.H. Gully, et al, "Design of the Armature Windings of a Compensated Pulsed Alternator Engineering Prototype." Digest of Technical Papers, 2nd IEEE International Pulsed Power Conference, Lubbock, Texas, June 12-14, pp. 385-391.

M.A. Pichot, et al, "The Design, Assembly, and Testing of a Desk Model Compensated Pulsed Alternator." Digest of Technical Papers, 2nd IEEE International Pulsed Power Conference, Lubbock, Texas, June 12-14, 1979, pp. 398-401.

W.F. Weldon, et al, "Fundamental Limitations and Design Considerations for Compensated Pulsed Alternators." Digest of Technical Papers, 2nd IEEE International Pulsed Power Conference, Lubbock, Texas, June 12-14, 1979, pp. 76-82.

W.L. Bird, et al, "The Compensated Pulsed Alternator - Preliminary Test Results." Presented at the 8th Symposium on Engineering Problems of Fusion Research, San Francisco, California, November 13-16, 1979.

W.L. Bird, et al, "Pulsed Power Supplies for Laser Flashlamps." Final Report, Lawrence Livermore Laboratory Subcontract No. 1823209, Center for Electromechanics, The University of Texas at Austin, October 1978.

K.M. Tolk, W.L. Bird, and M.D. Driga, "A Study of the Engineering Limitations to Pulse Discharge Time for a Compensated Pulsed Alternator." Final Report, Los Alamos Scientific Laboratory Order No. N68-0899H-1, Center for Electromechanics, The University of Texas at Austin, May 1979.

K.M. Tolk, "The Design and Fabrication of a Second-Generation Compensated Pulsed Alternator." Final Report, Naval Surface Weapons Center Contract No. N60921-78-C-A249, Conceptual Design Phase, Center for Electromechanics, The University of Texas at Austin, January 1980.

W.L. Bird and H.H. Woodson, "Detailed Design, Fabrication and Testing of an Engineering Prototype Compensated Pulsed Alternator." Final Report, Lawrence Livermore Laboratory Purchase Order No. 3325309, Center for Electromechanics, The University of Texas at Austin, March 1980.

W.F. Weldon, et al, "A Pulsed Alternator for Laser Flash Lamps." Presented at the IEEE International Conference on Plasma Science, Monterey, California, May 15-17, 1978.

W.F. Weldon, et al, "Compensated Pulsed Alternator." Brochure, Lawrence Livermore Laboratory, Livermore, California, July 1978.

J.A. Parekh, "Space Harmonic Analysis of Magnetic Fields in a Compensated Pulsed Alternator." Master's Thesis, The University of Texas at Austin, May 1980.

SLIDING ELECTRICAL CONTACTS

M. Brennan, et al, "Test Data on Electrical Contacts at High Surface Velocities and High Current Densities for Homopolar Generators." Presented at the Seventh Symposium on Engineering Problems of Fusion Research, Knoxville, Tennessee, October 24-29, 1977.

M. Brennan, et al, "The Testing of Sliding Electrical Contacts for Homopolar Generators." IEEE Transactions on Components, Hybrids, and Manufacturing Technology, March 1979, pp. 111-115.

M. Brennan, et al, "Design, Construction, Evaluation, and Test Results of a High Speed Controlled Atmosphere Brush Test System." Final Report, Electric Power Research Institute Research Project No. 469-3, Energy Storage Group, The University of Texas at Austin, December 1976.

R.A. Marshall, "Preliminary Results Obtained with 400kA Brush Tester." Report, Texas Atomic Energy Research Foundation Research Project, Center for Electromechanics, The University of Texas at Austin, December 1979.

D.J. Ortloff, "The Design of a Brush Test Machine and the Verification of the Machine Design and Brush Design under Test Conditions of High Current Densities and High Relative Surface Velocities." Master's Thesis, The University of Texas at Austin, January 1975.

J.M. Casstevens, "Measurement of the Friction and Wear Characteristics of Copper-Graphite Sliding Electrical Contact Materials at Very High Speeds and Current Densities." Master's Thesis, The University of Texas at Austin, August 1976.

J.M. Weldon, "Design, Construction, and Evaluation of a High Speed Controlled Atmosphere Brush Test System." Master's Thesis, The University of Texas at Austin, August 1976.

R.C. Swanson, "The Optimal Control of a Homopolar Motor-Generator Using Electrical Brush Mechanical Load Variation." Doctoral Dissertation, The University of Texas at Austin, December 1976.

C.H. Ramage, "An Investigation of the Tribological Properties of Graphite Fiber-Metal Matrix Composites." Doctoral Dissertation, The University of Texas at Austin, December 1977.

M.J. Bharucha, "Testing and Evaluation of Brushes Used for the Fast Discharge Homopolar Generator through the Use of the Controlled Atmosphere Brush-Testing Facility." Master's Thesis, The University of Texas at Austin, December 1978.

M. Brennan, "The Experimental Investigation of the Effects of Contact Area and Large Currents on Sliding Electrical Contacts." Master's Thesis, The University of Texas at Austin, May 1979.

J.M. Weldon, et al, "Design of a High Speed Controlled Atmosphere Test System for Sliding Electrical Contacts Conducting Large Power Pulses." Presented at the IEEE International Conference on Plasma Science, The University of Texas at Austin, May 24-26, 1976.

R.A. Marshall, "High Current and High Current Density Pulse Tests of Brushes and Collectors for Homopolar Energy Stores." (To be presented at the 26th Holm Conference on Electrical Contacts, Chicago, Illinois, September 29-October 1, 1980.)

WELDING WITH THE HOMOPOLAR GENERATOR

G.B. Grant, et al, "Resistance Welding Using Homopolar Generators as Power Supplies." Texas Atomic Energy Research Foundation Project Progress Report No. 27 (November 1, 1976, to April 30, 1977), Fusion Research Center, The University of Texas at Austin.

J.M. Weldon (Astec Industries, Inc.) and W.F. Weldon (The University of Texas at Austin), "The Homopolar Generator as a Pulsed Industrial Power Supply." Presented at the Conference on Industrial Energy Conservation Technology, Houston, Texas, April 22-25, 1979.

W.F. Weldon and R.E. Keith (The University of Texas at Austin), and J.M. Weldon (Astec Industries, Inc.), "Billet Heating with the Homopolar Generator." Presented at the Second Annual Conference on Industrial Energy Conservation Technology, Houston, Texas, April 13-16, 1980.

G.B. Grant, et al, "Homopolar Pulse Resistance Welding, a New Welding Process." Welding Journal, Vol. 58, No. 5, May 1979, pp. 24-36.

G.B. Grant, et al, "Resistance Welding of Two Inch Schedule 40 Steel Pipe with a Homopolar Generator." Final Report, Astec Industries Research Project, Center for Electromechanics, The University of Texas at Austin, June 1978.

R.E. Keith, et al, "Feasibility Study of Pipe Welding Using a Homopolar Generator." Final Report, NP-1285, Research Project 1122-1, Electric Power Research Institute, Palo Alto, California, December 1979.

G.B. Grant, et al, "Feasibility Study of Pipe Welding Using a Homopolar Generator." First Annual Report, Electric Power Research Institute Research Project No. RP1122-1, Center for Electromechanics, The University of Texas at Austin, 1977.

H.G. Rylander, "Resistance Welding with Homopolar Generators." Progress Report, National Science Foundation Grant No. DAR77-23874, Center for Electromechanics, The University of Texas at Austin, November 1978.

H.G. Rylander, "Resistance Welding with Homopolar Generators." Final Report, National Science Foundation Grant No. DAR77-23874, Center for Electromechanics, The University of Texas at Austin. (To be published.)

ELECTROMAGNETIC PROPULSION

J.P. Barber (International Applied Physics), R.A. Marshall (The University of Texas at Austin), and S. Rashleigh (Max-Planck Institute), "Magnetic Propulsion for a Hypervelocity Launcher." Presented at the Second International Conference on Megagauss Magnetic Field Generation and Related Topics, Washington, D.C., May 29-June 1, 1979.

R.A. Marshall, "Railgun Overview." Presented at the Department of Energy Impact Fusion Workshop, Los Alamos Scientific Laboratory, Los Alamos, New Mexico, July 10-13, 1979.

R.A. Marshall and W.F. Weldon, "Comparison of Linear Induction, Synchronous and Homopolar Generators for Accelerating 25 and 700 Gram Projectiles to Velocities of One and Four Kilometers per Second." Final Report, Naval Surface Weapons Center Contract No. N60921-78-C-A249, Modification P00003, Center for Electromechanics, The University of Texas at Austin, January 1980.

R.A. Marshall and W.F. Weldon, "Analysis of Performance of Rail Gun Accelerators Powered by Distributed Energy Stores." Presented at the 14th Pulse Power Modulator Symposium, Orlando, Florida, June 3-5, 1980.

APPENDICES

APPENDIX A. Homopolar Generator Rotor Stresses

APPENDIX B. Homopolar Resistance Welding Process

APPENDIX C. Analysis of Electromagnetic Launchers

APPENDIX A

HOMOPOLAR GENERATOR ROTOR STRESSES

Right Circular Cylindrical Rotors

The maximum stress due to spin for a flat circular disk with no central hole is given by

$$s = \frac{3 + \nu}{8} \rho (V_0)^2 \quad (A-1)$$

where s is the stress, ν is Poisson's ratio for the material, ρ is the density of the material, and V_0 is the surface speed. This rotor, having no central hole, has no provision for the attachment of a shaft. A hub must therefore be included near the center of this rotor for the attachment of a shaft. The stress concentration factor for the attachment of the shaft will be taken to be 1.5, which is a reasonable value for a careful design. The stress equation becomes

$$s = \frac{1.5(3 + \nu)}{8} \rho (V_0)^2 \quad (A-2)$$

The addition of a small hole in the center of the rotor for the insertion of a shaft introduces an additional stress concentration factor of approximately 2.0. The original factor of 1.5 will be retained to insure adequate pressure between the rotor and shaft at operating speed. Thus, the stress in a rotor which has been shrunk on a small shaft may be approximated by

$$s = \frac{1.5(3 + \nu)}{4} \rho (V_0)^2 \quad (A-3)$$

Modified Constant Stress Disks

The ideal constant stress disk has an infinite outer radius and zero thickness at the periphery. Obviously, this is not practical for the rotor of a homopolar machine. When this type of disk is truncated to a finite radius, it is capable of supporting a radial load at the outer periphery. This radial load could be a properly designed rim for brush contact.

For these initial calculations, a rim of rectangular cross-section was considered. The radial stress between the disk and rim was treated as a uniform pressure on the inside of the rim, balancing the force transmitted to the disk. (If more accurate results are required, a finite element stress solution of this rotor could be made with special attention to this transition region.) Using this assumption, the displacement of the inside of the rim ($r = r_i$) can be shown to be

$$U_r = \frac{r_i}{E} - \frac{(1-\nu)}{\gamma-1} \frac{(1+\nu)}{\gamma} s \frac{t_0 e^{-\xi}}{t_{rim}} + \frac{\xi s}{2} [(3+\nu)\gamma - (1-\nu)] \quad (A-4)$$

where

E = modulus of elasticity for the material

$\gamma = \left(\frac{\text{outer radius of rim}}{\text{inner radius of rim}} \right)^2$

s = working stress in the material

t_0 = disk thickness at center

t_{rim} = width of rim

ξ = a dimensionless parameter which identifies the "degree of taper" present in the disk

ν = Poisson's ratio for the material

Similarly, the corresponding displacement of the disk is given by

$$U_r = \frac{r}{E} s (1 - \nu) \quad (A-5)$$

Setting the two deflections equal and rearranging gives

$$\frac{t_0}{t_{rim}} = - \frac{[1 - \frac{\xi}{2} (\frac{3+\nu}{1-\nu} \gamma - 1)] (\gamma - 1)}{e^{-\xi} (1 + \frac{1+\nu}{1-\nu} \gamma)} \quad (A-6)$$

Evaluating this equation with

$$\xi = 2.5$$

$$\nu = 0.3$$

$$\gamma = 1.2$$

gives

$$\frac{t_o}{t_{rim}} = 3.64 \quad (A-7)$$

Recalling the definition of the parameter γ , the rim radial thickness is seen to be approximately 10% of the rotor radius. The rim width is approximately 27% of the disk's central thickness. This rotor appears to be feasible.

Recalling the definition of ξ and solving for stress gives

$$s = \frac{\rho(V_o)^2}{2\xi} \quad (A-8)$$

The stress concentration factor for the attachment of a shaft capable of supporting the rotor and conducting the current will again be taken to be 1.5. The stress equation then becomes (with $\xi = 2.5$)

$$s = 0.3 \rho(V_o)^2 \quad (A-9)$$

The NRL Rotor Design

In the course of designing the inertial-inductive energy storage system for the LINUS program at the Naval Research Laboratory, the NRL personnel developed another, similar, modified constant stress design

using finite element techniques.* This rotor is made of beryllium-copper and is reported to have a maximum stress of 586 MPa (85,000 psi) at a surface speed of 540 m/sec.

The generalized spin stress for a rotating elastic body can be approximated by the equation

$$s = K\rho(V_o)^2 . \quad (A-10)$$

Taking the density of the material to be 8200 kg/m³ the value of the constant K for the NRL rotor can be found to be 0.245. The stress for this type rotor design with other similar materials can therefore be approximated by

$$s = 0.245 \rho(V_o)^2 . \quad (A-11)$$

It is interesting to note that the stress in this design is slightly lower than that of the other constant stress type rotor described above. This is probably due to the inclusion of the shaft attachment in the finite element analysis. The stress concentration due to this attachment could therefore be minimized during the design.

Summary of Rotor Stress Considerations

The following table gives the speed at which the spin stress becomes the limiting factor. For each material two stress levels are considered. The first is 80% of the material's published yield strength. The other is 80% of the material's endurance limit (100 million cycles).

It should be noted that several simplifying assumptions were made in the generation of this table. These assumptions are thought to be conservative, but a complete stress and life analysis should be done before designing a rotor to operate at the given speeds.

*Robson, A.E., et. al., "A Multi-Megajoule Inertial-Inductive Energy Storage System" International Conference on Energy Storage, Compression, and Switching, Torino, Italy, Nov. 5-7, 1974.

TABLE A-I
SPIN STRESS LIMITS ON ROTOR SURFACE SPEEDS

Rotor Material	Density kg/m ³	Stress MPa (ksi)	Limiting Speed m/sec			
			Flat Disk	Flat Disk Shrunken on Small Shaft	Modified Constant Stress Disk	NRL Design
Aluminum 6061-T6	2700	221 (32.0)	360	255	522	578
Aluminum 7075-T6	2800	77.2 (11.2)	213	151	309	342
		403 (58.4)	478	338	693	766
BeCu	8200	127 (18.4)	268	190	389	430
		828 (120.0)	402	284	589	642
Ti 6-4	4430	232 (33.6)	213	151	307	340
		828 (120.0)	550	389	789	873
Steel AISI 4340	7800	336 (48.7)	350	248	503	556
		1100 (160.0)	477	338	686	758
		552 (80.0)	338	239	486	537

In the limit, these values would result in the following changes to the acceptance parameters for the HPG.

TABLE A-II
ACCEPTANCE PARAMETERS
FOR ADVANCED HOMOPOLAR GENERATORS

	Present Rotors	Advanced Ferromagnetic Rotors	Advanced Non-magnetic (Titanium rotors)
MJ/m ³	30 - 40	~200	~145
kg/kJ	0.2 - 0.25	~0.04	~0.003
\$/Joule	0.005 - 0.01	?	?

It should be kept in mind while comparing these figures that the non-magnetic rotors will require greatly increased excitation.

APPENDIX B .

THE HOMOPOLAR PULSE RESISTANCE
WELDING PROCESS

HOMOPOLAR PULSE RESISTANCE WELDING,
A NEW WELDING PROCESS
based on the unique electrical characteristics of pulsed
homopolar generators

by

G. B. Grant, W. M. Featherston, R. E. Keith

W. F. Weldon, H. G. Rylander, H. H. Woodson

Center for Electromechanics
The University of Texas at Austin
Austin, Texas 78712

American Welding Society
60th Annual Meeting
Detroit, Michigan
April 2-6, 1979

HOMOPOLAR PULSE RESISTANCE WELDING,

A NEW WELDING PROCESS,

based on the unique electrical characteristics of
pulsed homopolar generators

by

G. B. Grant, W. M. Featherston, R. E. Keith,

W. F. Weldon, H. G. Rylander, H. H. Woodson

Center for Electromechanics

The University of Texas at Austin

Austin, Texas 78712

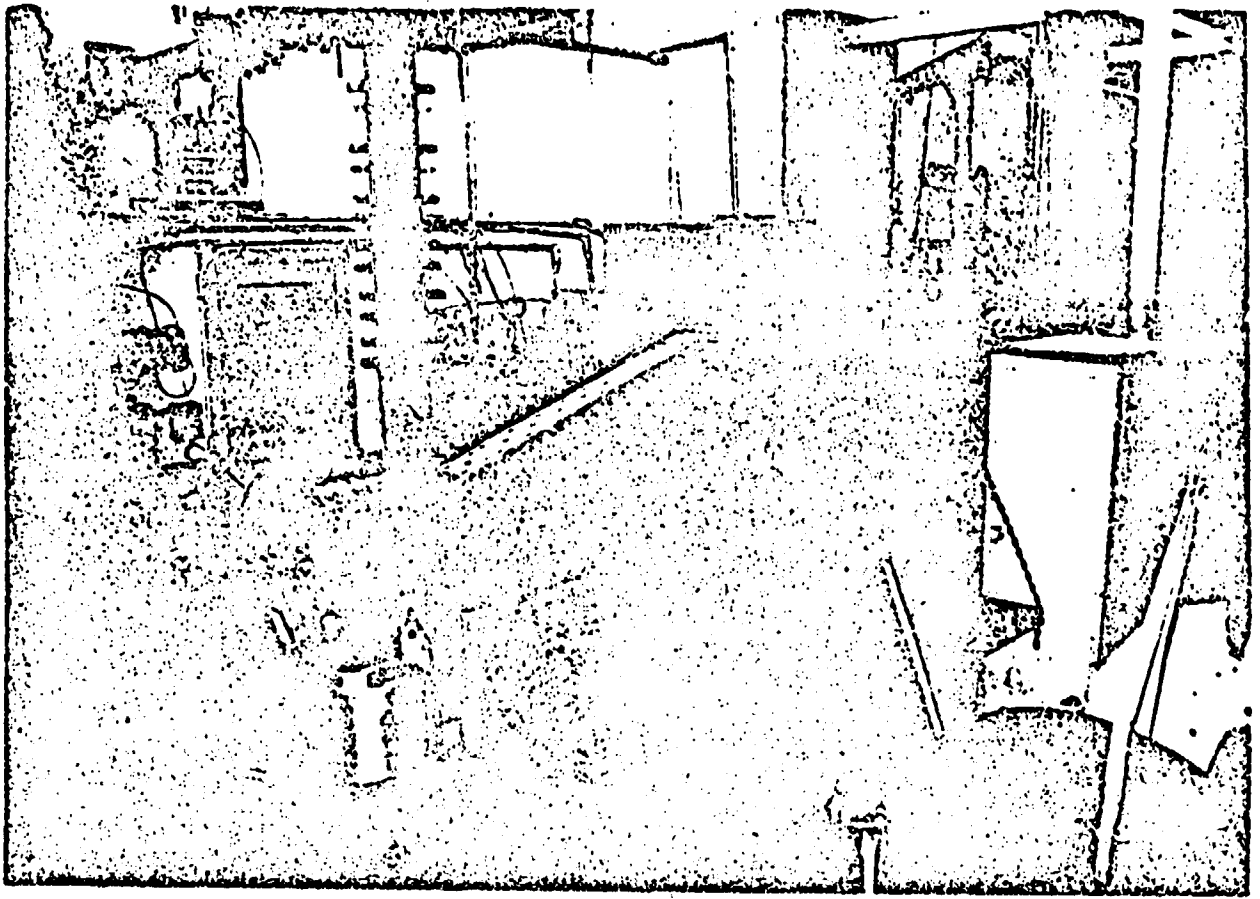
ABSTRACT

A new welding process based on the unique electrical characteristics of pulsed homopolar generators is being developed at The University of Texas Center for Electromechanics (UT-CEM). The process is a stored energy resistance welding process with several unique characteristics. It has the capability to weld very large (1-100 in.²) metal sections in very short times (1-30 s) and can be adapted to both shop and field welding applications. The process also offers the potential for in-process weld quality control for a variety of applications.

Welds done to date using the present UT-CEM 5 megajoule machine include bars, pipes and other shapes up to 4.4 in.² in cross-section with

actual welding times of from 0.5 to 1.0 seconds at currents in excess of 300 kA and at generated power levels in excess of 6000 kW. The input power required by the welding equipment during these welds was about 250 kW. Projects presently underway will explore process characteristics on welds of up to 7 in.² cross-section of various metals of industrial interest. Future projects include the construction of a 50 MJ machine for welding experiments on much larger metal sections, approaching 100 in.², to be welded on the same time scale.

The paper presents the basic characteristics of the HPRW process, briefly describes the design, construction and capabilities of pulsed homopolar generators and describes the results of welding experiments to date.



ORIGINAL PAGE IS
OF POOR QUALITY

Figure 1: Homopolar Pulse Resistance Welding (HPRW) equipment for
4-in. schedule 80 Type 304 stainless steel pipe

INTRODUCTION

The technology of pulsed homopolar generators, a product of government-funded research into the area of controlled thermonuclear fusion, may be of immediate benefit to the metal joining industry as a power source for resistance welding.

The University of Texas Center for Electromechanics (UT-CEM) has been involved since 1972 in programs intended to address the need for large pulsed power supplies for use in experiments leading to controlled thermonuclear fusion power generating plants.¹ Since that time, UT-CEM has been involved both in design studies and in construction and testing of a number of pulsed power machines intended to meet a broad spectrum of performance requirements in terms of quantity of energy stored and energy delivery rates.^{2,3,4,5}

One of these machines, the 5 MJ homopolar generator, was designed and built in 1974 to explore further the electrical characteristics of this type machine when used in a pulsed mode. The machine exceeded its design goals by a considerable margin, and it has become apparent that machines of this kind offer promise as pulsed power sources in a variety of industrial, military, and research applications.

One promising application is the welding of large metal sections. UT-CEM has developed the Homopolar Pulse Resistance Welding (HPRW) process over the past two years, using the 5 MJ homopolar machine as the power source. Welding activities began as unfunded experiments used to demonstrate the capabilities of the homopolar generator technology. Now underway are several major projects devoted to exploring the characteristics and capabilities of the process for specific metal joining applications.

The objectives of this paper are to describe the basic characteristics of the HPRW process, the design, construction and capabilities of pulsed homopolar generators, and the results of welding experiments to date.

THE HPRW PROCESS

The HPRW process is a resistance welding process in which the faying surfaces in solid contact are heated by interface resistance to electric current. In this respect it is similar to upset butt welding. However, we feel that several of the process characteristics and capabilities are sufficiently unique to warrant calling it a new welding process. These are discussed below.

Figure 2 shows a schematic equivalent electrical circuit for the process. The pulsed homopolar generator can be modeled electrically as a large variable capacitor. The mode of operation used in the HPRW process is one in which the generator is "charged" by motoring-up its rotor slowly, either by means of an external motoring system or by closing switch S_1 and applying a voltage across the terminals of the machine, causing it to "self motor." The 5 MJ homopolar machine is both a motor and a generator. When the generator is charged to slightly over the desired energy level (determined by the rotor speed), switch S_1 is opened, and the generator rotor begins coasting. When the speed has decreased to the appropriate point, the pneumatically actuated brushes are lowered onto the rotor and a fraction of a second later the discharge switch S_2 is closed. At this time, the discharge path is completed and the rotational kinetic energy of the homopolar machine is converted quickly to electrical energy in the form of a very high current, relatively low voltage dc pulse. Note that at the time the pulse is delivered there is no connection between the homopolar generator and the electric lines. This is an important point of difference from conventional resistance welding processes, which are often subject to high power demand charges because of the sudden loads they impose on the utility power lines.

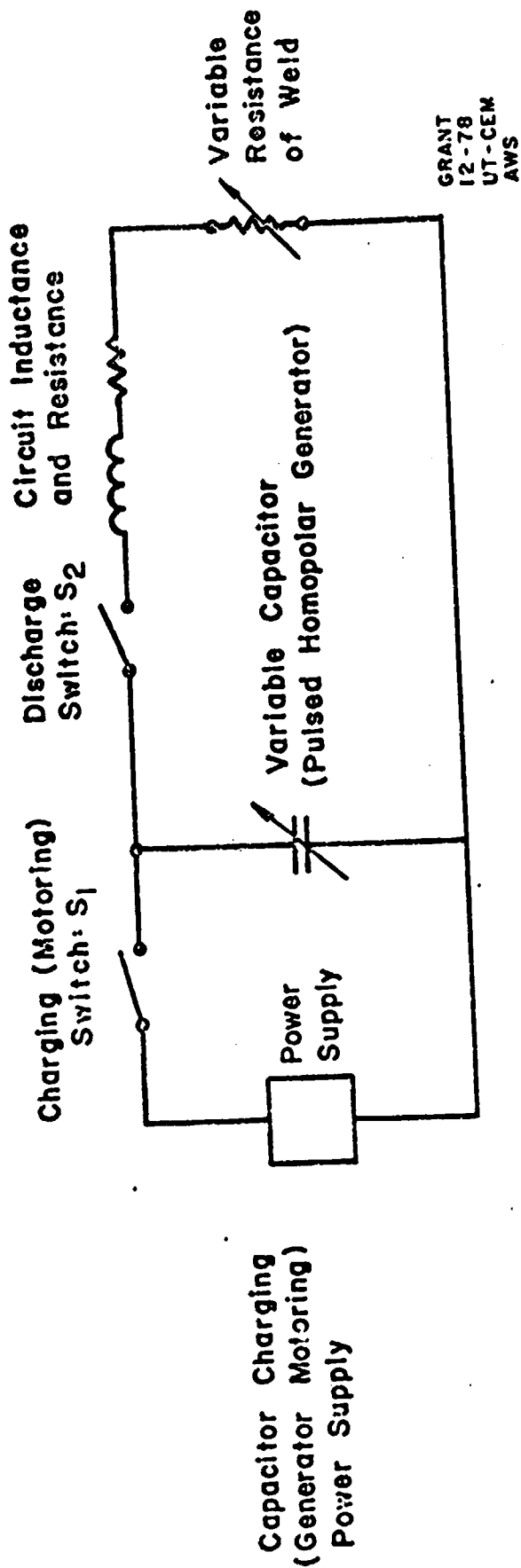


Figure 2: Equivalent electrical circuit for the HPRW process

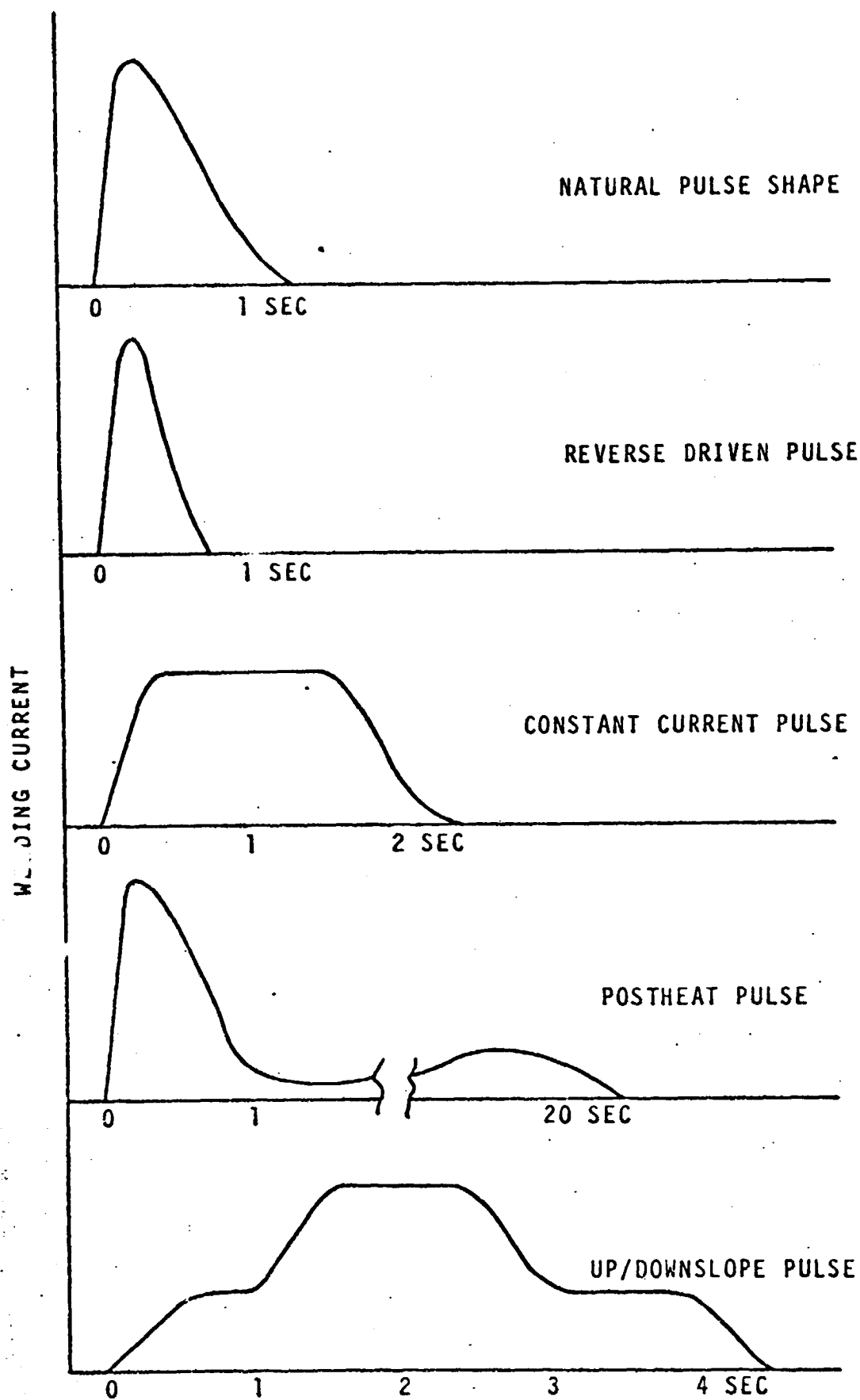


Figure 3: Some current waveforms possible from the pulsed homopolar



Figure 4: Functional illustration of a typical HPRW fixture

The generator capacitance is controllable by preprogramming a varying field excitation level in the machine during the weld pulse. The generator capacitance can be thought of as a measure of the rate at which energy can be removed from the generator. By varying the generator capacitance, the energy delivery rate of the machine can be controlled. Thus a wide variety of welding current waveforms can be generated into the discharge circuit. Some of the many waveforms possible are illustrated in Figure 3. It is possible first to produce the weld and then to provide a degree of heat-treatment by controlling the weld metal cooling rate, all during the same current pulse. As is the case in conventional spot welding, welds may cool so fast that quench cracks occur in such materials as ferritic steels. This problem can be eliminated by controlling the cooling rate in the fashion described above.

The process requires use of a welding fixture, the functions of which are to clamp and hold the workpiece, provide the means, via copper electrodes, to transfer the welding current to the work piece during weld heating, and then to forge the pieces together after heating. Except for heavier current leads, fixtures are similar to conventional upset butt welding fixtures. A functional illustration of a typical welding fixture is shown in Figure 4.

After the welding current pulse has been delivered, the generator has usually been fully discharged, and its rotor is at standstill. In a production environment the generator would again be charged by accelerating its rotor with a clutch-connected prime mover while the completed workpiece is being removed from its welding fixture and a new one installed. Thus little or no time is lost waiting for the system to become ready to deliver the next weld pulse, and the electrical load on the utility is essentially

constant. The attainable cycle time is dependent only on how fast the work-piece can be changed and how large a prime mover is used to motor-up the machine rotor. It follows that for very large, low production welds, the machine charging (or rotor accelerating) time could be relatively long, requiring only a small power input, while the system could still produce the megawatt-level output pulses required for the weld. The resulting savings on installed electrical capacity, buswork, and electrical demand costs compared to a large transformer-type flash welding system, for example, could be substantial.

HPRW PROCESS FEATURES

Probably the most significant process feature is the speed at which the weld can be created. For example, in using the HPRW process to weld four-inch schedule 80 type 304 stainless steel pipe (4.4 in.^2), the weld occurs in less than 0.5 s, with a total weld pulse time of less than 3 s.

Of course conventional resistance welders, both spot and upset butt, can also produce welds in a few tenths of a second, but we are not aware of a process of this speed which can weld sections as large with the relatively low (less than 250 kW) input power required. Even more important are the scaling characteristics of the technology which make it appear possible to weld much larger cross-sections (up to at least 100 in.²) on the same time scale, with comparable input power requirements.

Another process feature is one shared with conventional resistance welding processes but not readily available with arc-welding processes. Since the process can be automated, the power across and energy deposited in the weld zone can be preprogrammed and monitored in real time. This offers the possibility of having an accept/reject criterion based on comparison of the monitored parameter values with waveforms of previous destructively tested welds. Also, feedback control may eventually be possible which could further assure high weld quality. Thus, the process offers to large-section welding the possibility of weld quality control/monitoring techniques similar to those now available and being used in conventional spot welding.

Finally, the variable capacitance feature of the pulsed homopolar generator offers the possibility of controlling heating and cooling rates as required to produce the desired properties in the weld zone. It may eventually be possible with improved generator field control systems and weld process models to completely preprogram temperature vs. time waveforms for a given weld. This would allow sophisticated heat treating to be accomplished after the weld is accomplished but during the same welding pulse.

The process offers major potential advantages when compared to both conventional arc-welding processes and resistance/flash welding processes in some applications.

The significant potential advantages the HPRW process has when compared to the arc welding processes include:

- *it is much faster (weld time measured in seconds);
- *it is less labor intensive (the process is easily automated)
- *it may make welds more easily inspectable (the weld zone is very narrow)
- *it uses no filler metal, flux, or protective gas atmosphere
(cost of consumables should be less)
- *it leaves no cast metal in the weld zone (all molten metal is pushed out of the weld zone during forging)
- *it may eliminate metallurgical problems in some applications (weld metallurgy is much simpler; process heating and cooling rates are easily controllable)
- *it should result in an improved residual stress pattern, since heating and cooling are peripherally symmetrical
- *pre- and post-weld heat treating are possible at the time of welding
- *it may make possible reliable in-process weld quality control
- *it minimizes noxious or unsafe fumes present when arc welding some alloys
- *it may be possible to join a wider variety of dissimilar metals
- *it offers to the welding of large metal cross-sections many of the resistance welding process features available previously only in the production of smaller parts

The significant potential advantages the HPRW process has when compared to conventional resistance and flash welding systems include:

- *its energy storage capability makes power requirements for very large welds relatively small (megawatt outputs from kilowatt inputs)

- *the process equipment can be made semi-portable for on-site field welding (a relatively small diesel generator would supply all the power required for megawatt-level welds)

Of course the process does have its limitations. The major of these (relative to arc welding) are:

- *the process is capital equipment intensive (a relatively large initial investment in equipment would be required for most applications)

- *the equipment is relatively large and heavy compared to an arc welding supply

- *the process requires special fixturing for clamping and forging the work

- *the process may prove to be cost-effective only in applications in which there is a relatively high production volume to defray the fixture costs

- *periodic maintenance of the sliding electrical contacts (brushes) is required

- *the process equipment is in an early stage of commercial development

PULSED HOMOPOLAR GENERATORS

Homopolar generators have been known, studied and used for both continuous and pulsed duty ever since Michael Faraday built the first one in 1831. They have never achieved widespread use because they are inherently high current, low voltage machines and are thus not suited for transmitting energy over long distances.⁶ For some applications, however, including resistance welding and other forms of resistance heating, the electrical characteristics of these machines are ideal.

In homopolar machines, a voltage is generated across a conductor that moves through a unidirectional magnetic field. The essential difference from a conventional generator is that the current travels through the rotor itself and makes only one transit across the magnetic field. There are no rotor windings and there is no commutator. There are two basic machine configurations suitable for welding; a disk rotating in an axial magnetic field with radially separated sliding contacts as illustrated in Figure 5A, or a drum rotating in a radial magnetic field with axially separated sliding contacts as illustrated in Figure 5B. Each configuration has its own advantages. Other machine topologies have been analyzed in detail elsewhere.⁷

Homopolar machines have been used previously as welding power supplies. Westinghouse built a homopolar generator resistance welding supply for pipe seam welding in the mid 1930's⁸ and Progressive Welder Company built a small homopolar flash/spot welder in the late 1940's.⁹ Both of these machines were used in a continuous duty mode (from the brush heating/wear viewpoint) and had relatively complex rotor geometries. The Progressive Welder machine also used a separate flywheel. Neither of these

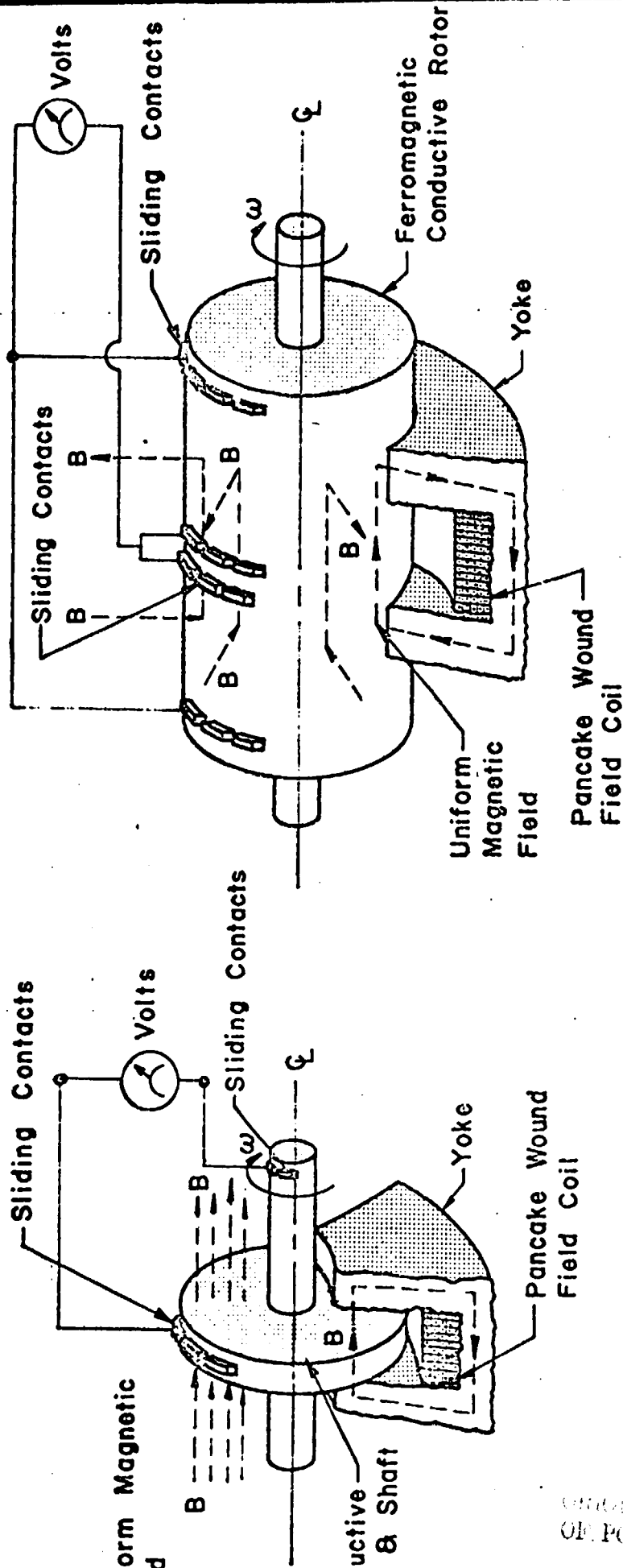


Figure 5: Functional illustration of disk and drum configurations of homopolar generators: A--disk type (left); B--drum type (right)

machines received widespread acceptance as welding supplies. The homopolar machines designed and developed at UT-CEM differ greatly from both of these machines in design, construction, and mode of operation, particularly with respect to their rotors, and brushes.

Since in a homopolar machine the brushes must slide on the rotor at a large radius and must carry full power, frictional brush losses and heating are significant and contribute to brush wear. Two developments help overcome this basic machine limitation. The first is the use of the generator as a stored energy machine in a pulsed duty mode. Remotely controllable brush actuation mechanisms which lower the brushes when necessary during a discharge, but raise them during external motoring, minimize machine frictional losses and brush wear. Second, the development of very high metal-content composite brushes has further increased the wear life of brushes operating at high current densities for pulsed power machines of this kind.¹⁰

The simple solid disk or drum rotor configurations offer at least two significant advantages over some of the complex geometries used in the past. First, with no slots, wedges or laminations, the rotor consists only of a right circular cylinder of steel, so the manufacturing cost is inherently low. Second, and just as important, when using the homopolar machine in a pulsed duty, stored energy mode in which the machine rotor serves also as the energy storage flywheel, the deceleration forces resulting during a discharge are body forces acting directly on all rotor mass elements in which the energy is inertially stored. Thus the torques and stresses are distributed and are relatively low. This means that the energy can be safely transferred very quickly at very high power levels. This is not the case when using an external flywheel, because

the entire deceleration torque must be transmitted through a connecting shaft, and this limits the energy transfer rate due to allowable shaft stress levels.

As has been mentioned earlier, a pulsed homopolar generator models electrically as a large variable capacitor. The governing equation for its capacitance is

$$C = \frac{2 E}{V^2} \quad (1)$$

where C = machine capacitance (F)

E = energy stored (J)

V = voltage generated (V).

For homopolar machines of the configurations shown in Figures 5A and 5B, the voltage generated between the sets of sliding contacts on the rotor rotating in the cylindrically symmetric magnetic field is

$$V = \frac{\omega \phi}{2\pi} \quad (2)$$

where ϕ = total flux cut by the rotor between the sliding contacts

(Wb)

ω = rotor rotational speed (rad/s)

and the energy stored in the rotor is

$$E = \frac{J\omega^2}{2} \quad (3)$$

where J is the rotor mass moment of inertia (kg-m^2).

The final fundamental design equation gives the electromagnetic torque acting on the rotor during a discharge, and is

$$T = \frac{\phi i}{2\pi} \quad (4)$$

where: T = electromagnetic torque (N-m)

i = rotor current (A).

Once a particular machine has been designed, it is possible to reduce the above equations to a more useful form. For a given field coil, when operating below saturation in the yoke, the magnetic flux ϕ can be shown to be directly proportional to the applied field current i_f . For a given machine, the above equations (1), (2), and (3) can be reduced to:

$$C = \frac{K_1}{i_f^2} \quad (5)$$

$$V = K_2 \omega i_f \quad (6)$$

$$E = K_3 \omega^2 \quad (7)$$

where i_f is the applied field current (A) and K_1 , K_2 , K_3 are machine constants. These simple relationships show that terminal voltage varies directly with rotor speed and field current, stored energy varies as the square of rotor speed, and capacitance varies inversely as the square of field current.

THE 5 MJ HOMOPOLAR GENERATOR

A schematic of the 5 MJ disk-type homopolar generator developed at UT-CEM is shown in Figure 6. A listing of its mechanical and electrical parameters is given in Table 1.

The machine constants for the 5 MJ generator are:

$$K_1 = 429 \times 10^6 \quad (F - A^2)$$

$$K_2 = 2.62 \times 10^{-4} \quad \left(\frac{V-s}{A}\right)$$

$$K_3 = 14.66 \quad (J - s^2)$$

Thus, the capacitance, voltage, and energy storage characteristics for the 5 MJ machine can be easily determined from the independently controlled machine parameters of field current and rotor speed. The essential concept to remember regarding machine capacitance is that by controlling the field current during a weld, the capacitance and thus the energy delivery rate from the machine, can be controlled. Figure 7 shows the open circuit voltage and energy stored vs rotor speed and field current for the 5 MJ generator. Using Figure 7 the desired values of voltage and stored energy for a particular experiment can be quickly found.

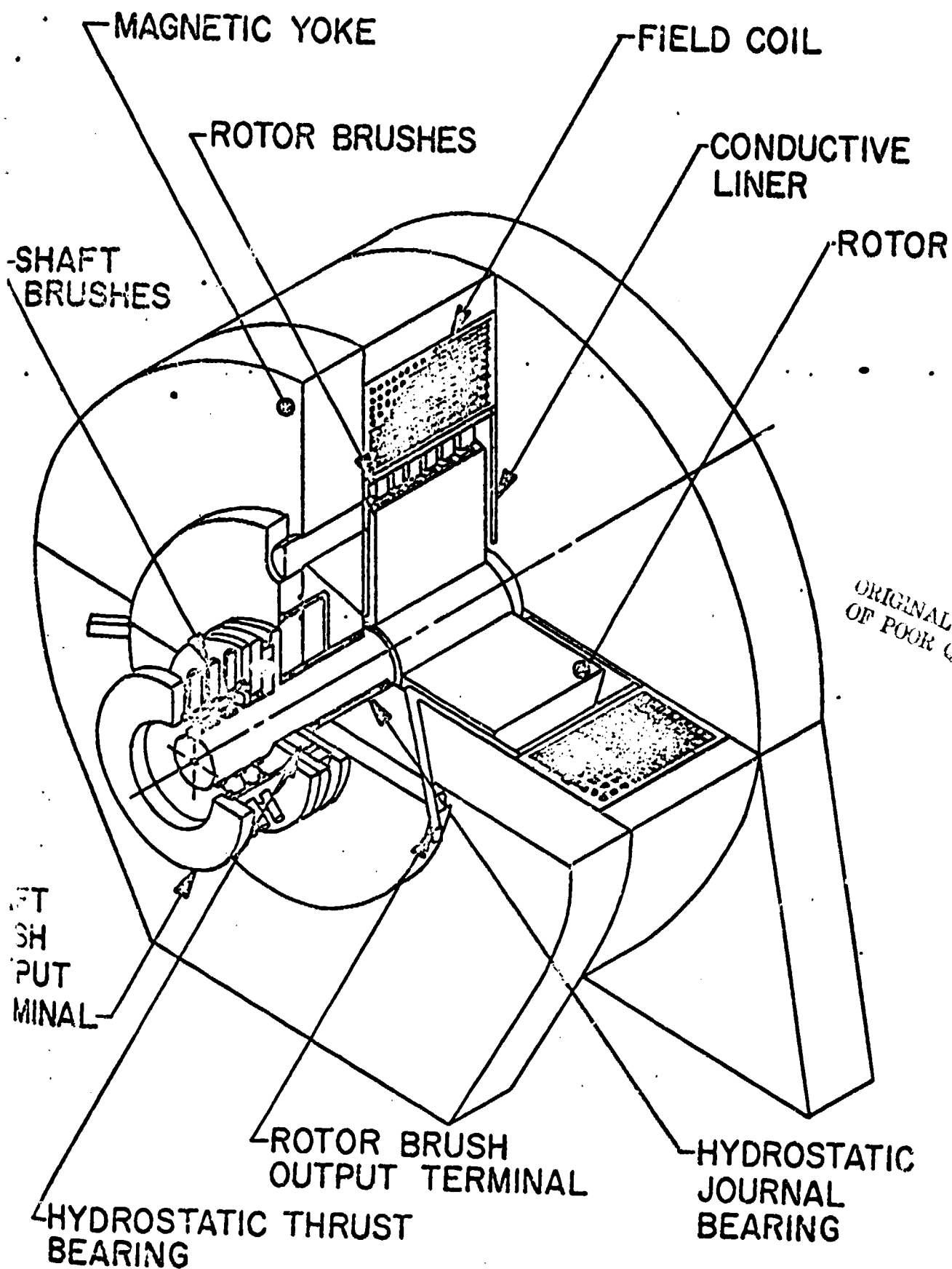


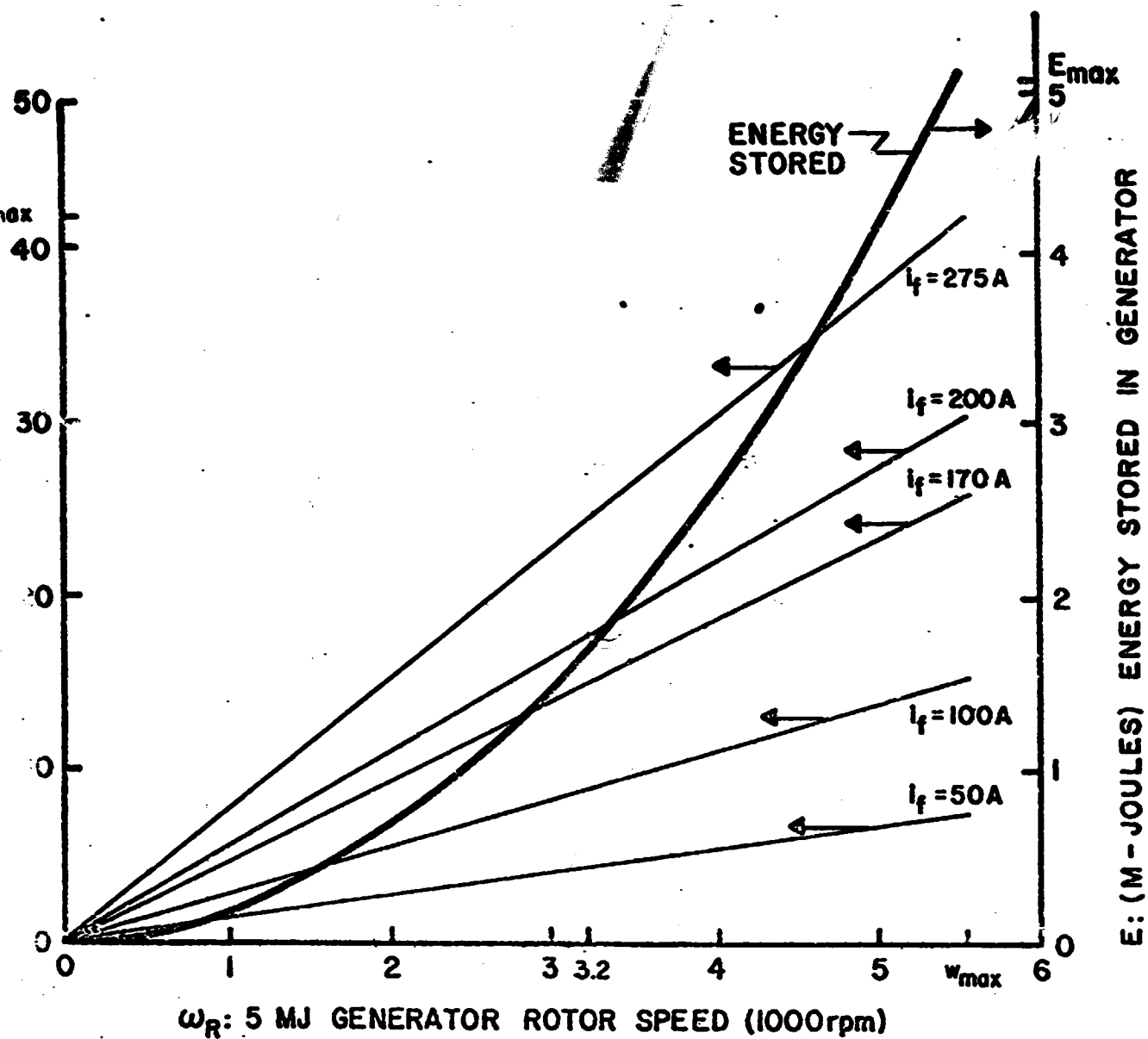
Figure 6: Schematic drawing of 5-MW disk-type pulsed homopolar generator

TABLE 1: MECHANICAL AND ELECTRICAL PARAMETERS OF

5 MJ HOMOPOLAR GENERATOR

Generator Weight (w/o Auxiliaries)	- 7700 kg (17,000 lb)
Major Dimensions (length x width x height) (w/o Auxiliaries)	- 1.37 m x 0.91 m x 1.52m
Rotor Diameter	$D_R = 0.61 \text{ m (2 ft)}$
Rotor Inertia	$I_R = 29.71 \text{ kg-m}^2$ (21.9 lb-ft-s^2)
Maximum Rated Speed	$\omega_{MAX} = 584 \text{ s}^{-1}$ (5580 rpm)
Maximum Energy Storage	$E_{MAX} = 5 \times 10^6 \text{ J}$ $(3.74 \times 10^6 \text{ ft-lb})$
Maximum Terminal Voltage (open circuit)	$V_{MAX} = 42 \text{ V}$
Maximum Discharge Current	$i_{MAX} = 560,000 \text{ A}$
Equivalent Minimum Capacitance	$L_{MIN} = 5670 \text{ F}$
Peak Power Output (tested to date)	$P_{max} > 10 \text{ MW}$
Maximum Power Consumption (input)	$P_{motor} < 250 \text{ kW}$

C-2



GRANT
UT-CEM
AWS
12-78

ORIGINAL PAGE IS
OF POOR QUALITY

Figure 7: Stored energy and terminal voltage vs rotor speed and field current for 5-MJ homopolar generator

FUTURE HOMOPOLAR MACHINES

For resistance welding and other low voltage, high current, high energy applications it appears that the drum-type configuration shown in Figure 5B will be superior from performance and economic viewpoints.¹¹ The scaling relations for these machines are also reasonably straightforward¹² and the welding experiments done to date indicate that we are presently operating on the low end of the cross-sectional area welding capabilities of the technology. Table 2 gives an indication of the machine scaling characteristics and potential welding capabilities. The welding time will remain short and the required input power small even for the larger machines.

TABLE 2: HOMOPOLAR GENERATOR SCALING CHARACTERISTICS

Energy Stored,	Machine Type	Peak Current,	Welding Capability, Steel	Approximate Weight (w/o Auxiliaries),	
MJ		A	in. ² (cm ²)	lb	(kg)
5	Disk	560,000 (a)	7 (45)(b)	17,000	(7,700)
5	Drum	500,000	10 (65)	10,000	(4,500)
10	Drum	1,000,000	20 (129)	14,000	(6,350)
20	Drum	2,000,000	40 (258)	23,000	(10,400)
30	Drum	3,000,000	60 (387)	32,000	(14,500)
40	Drum	4,000,000	80 (516)	41,000	(18,600)
50	Drum	5,000,000	100 (645)	48,000	(21,800)

(a) Tested to date

(b) Projected from 4.4 in.² welds



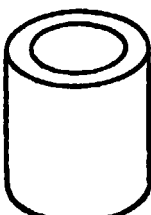

All other values calculated

WELDING EXPERIMENTS

Table 3 presents a summary of the welds performed to date using the HPRW process equipment. Many of our early welding experiments were performed with discretionary funds, and only very simple and inexpensive fixtures were built to provide the clamping and forging forces. Also, the current-feeding electrodes were very simple. In fact, the initial experiments in the welding of 1-in. bars, 4-in. pipe, track-shoe grouser bars, and railroad rail used compressed Belleville washers clamped between platens to provide the forging force and displacement. Thus, control over initial contact force and forging force for these welds was very limited. As a result, considerable flashing occurred at the weld interface. This flashing made the appearance of these early welds unappealing (but no worse than conventional flash welded pieces), but did demonstrate that the 5 MJ machine had more than sufficient energy storage and output power to accomplish the welds in fractions of a second.




The first funded project was to investigate the technical feasibility of making girth welds in 2-in. schedule 40 ASTM A 106B boiler pipe. The second funded project was directed at demonstrating technical feasibility of welding 4-in. schedule 80 Type 304 stainless steel boiling water reactor (BWR) pipe and investigating the metallurgical characteristics of the welds, particularly regarding heat-affected zone sensitization. BWR piping is one of the most critical of welding applications in terms of required weld metallurgy, mechanical properties, inspection and regulatory requirements.

A third funded welding project is now in its early stages. This project is concerned with establishment of welding requirements and quality

Shape	Description-Material	Metal Area, in. ² (cm ²)	Peak Weld Current, A	1b	Peak Forging Force, (N)	Weld Tensile Strength, 1b / in. ² (MPa)	Number Of Welds To Date
	1" Dia. bar-1018 steel	0.79 (5.1)	36,000	15,300	(68,100)(a)	85,000 (586)	30
	1" Dia. bar-304 stain-less	"	25,000	"	"	-	4
	1" Dia. bar-Titanium	"	25,000	"	"	-	1
	2" Sch. 40 Pipe-A 106B steel	1.08 (7.0)	64,000	17,500	(71,800)	60,000 (414)	60
	4" Sch 80-304SS pipe	4.41(28.4)	315,000	103,000	(958,200)	83,000 (573)	35
	4" Sch 40-mild steel	3.17(20.4)	175,000	14,000	(62,300)(a)	-	10
	1.5" Dia. Track-shoe pin-1045 Mn mod. steel	1.57(10.1)	74,000	25,750	(114,500)	-	14

(a) = Calculated force (from Belleville washers)

TABLE 3. WELDS MADE TO DATE WITH THE NPKW PROCESS (CONT'D.)

Shape	Description-Material	Metal Area, in. ² (cm ²)	Peak Weld Current, A	1b	Peak Forging Force, (N)	Weld Tensile Strength, lb /in. ² (MPa)	Number Of Welds To Date
	Track-shoe grouser bar high carbon steel	3.8 (24.5)	190,000	14,000	(62,300)(a)	-	2
	Railroad rail-steel	5.4 (34.8)	162,000	14,000	(62,300)(a)	-	1
	Spot weld-1-in. steel	-	130,000	20,000	(89,000)	-	2

(a) = Calculated force (from Belleville washers)

criteria for various shapes in a variety of materials. Table 4 lists the materials that will be welded and studied during Phase I of this project. During Phases II and III, tubes, angles, I-beams, vails, and possibly other structural shapes will be welded in order to study the effect of work piece shape on current distribution and weld quality. Some dissimilar metal combinations will also be included in the experimental program. For use on this project, welding fixture of advanced design is being built which will handle all of these shapes in cross-sections of up to 7 in.² if they will fit inside a 3 in. diameter circle. Following completion of this project, information will be available which will allow the HPRW process to be more easily applied to a large number of metal joining applications.

TWO-INCH SCHEDULE 40 STEEL PIPE

A special welding fixture was built to hold and forge the 2-in. pipe samples during the welding cycle. This fixture can be switched between two preset upset force levels by means of a hydraulic actuation system. The lower force is used during the initial heating of the weld. The higher forging force is usually applied about 0.15 seconds after the start of the weld cycle. This fixture also controls the field level of the 5 MJ generator in order to obtain the desired welding current waveform.

Over 60 specimens of the 2-in. pipe have been welded and studied. It was established early in the project that the HPRW process could produce satisfactory welds as determined by ASME QW-160 bend tests, tensile tests and microstructure analysis.

TABLE 4: TENTATIVE LIST OF MATERIALS TO BE WELDED

Steels

- 1018
1040
1080
4140
4340

Aluminums

- 6061
2024

Stainless Steels

- 316
416
430
17-4PH

Titanium

- 6Al-4V

Other Alloys

- Inconel X
S7 Tool Steel

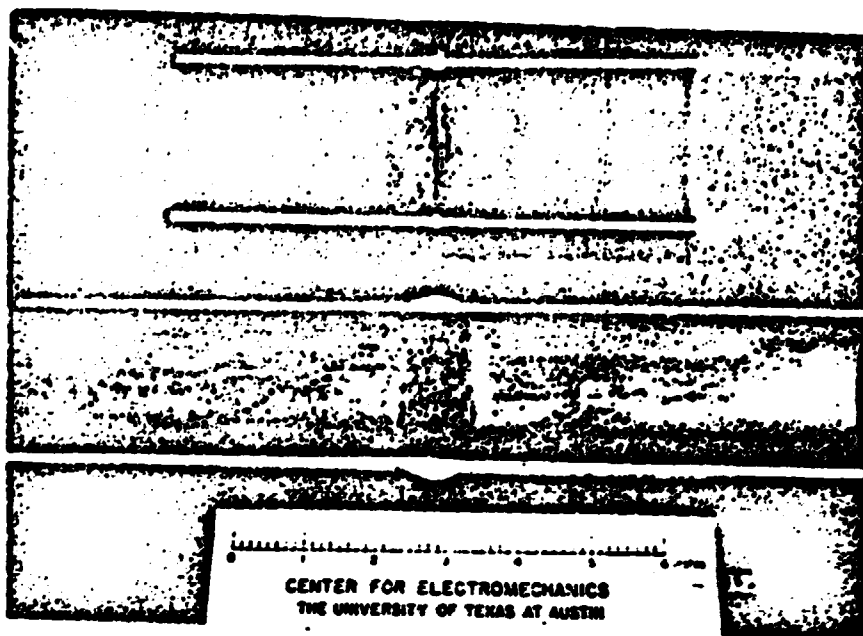
Once the weld quality had been verified, the remainder of the project was devoted to improving the appearance, alignment, and inner diameter weld contour, and to analyzing the various welding parameter records in order to establish a possible in-process weld quality criterion. A photograph comparing an SMA welded pipe and a HPR welded pipe is presented as Figure 8.

Figure 9 shows the appearance of an HPR weld cross section in 2-in. ASTM A 106B steel pipe. This weld was made under conditions that resulted in some melting and inward expulsion of metal.

It became evident early in the experimental program that some shaping of the weld current pulse was necessary for this weld configuration. Weld 11011 was made using a programmed reduction in the generator field current 0.35 s after initiation of the weld current pulse. This had the effect of decreasing the total energy, slowing the energy delivery rate during the latter portion of the weld cycle, and decreasing the cooling rate in the heat-affected zone (HAZ).

Figure 10 shows the weld line and base metal microstructures of Weld 11011. Although there was considerable coarsening of the structure in the vicinity of the bond line in this particular heat of steel, repeated 180° root bend tests on this and other similarly programmed welds were uniformly successful. The weld line itself, which runs horizontally across the approximate center of Figure 10A, is not clearly distinguishable.

A microhardness traverse of Weld 11011 is shown in Figure 11. The traverse confirms the metallographic observation that there is no martensitic region in the HAZ. There appears to be a very narrow softened region about 0.175 in. from the weld line. A similar region appeared on the traverse of at least one other weld, so we are inclined



ORIGINAL PAGE IS
OF POOR QUALITY

Fig. 8 - Comparison between arc- and HPR-welded 2-in. schedule 40 steel pipe

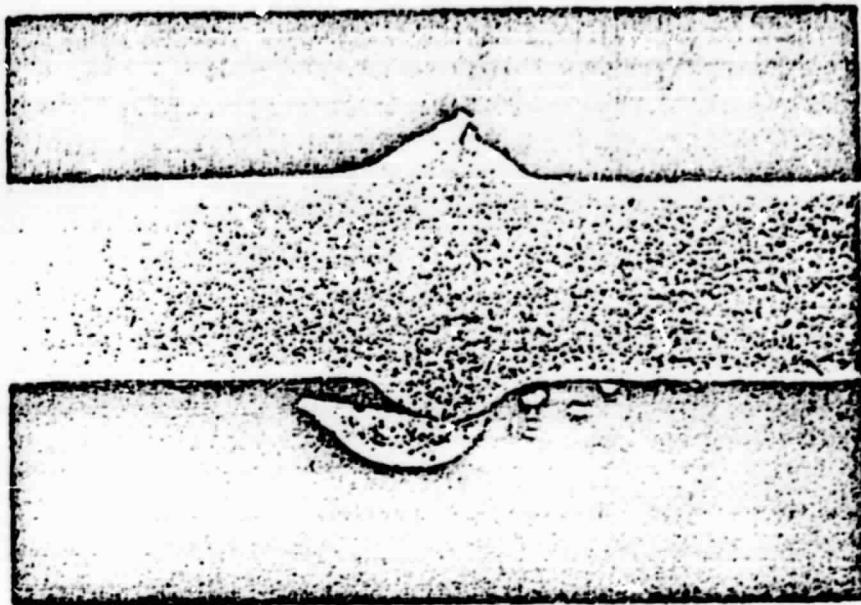


Fig. 9 - Cross-section of 2-in. ASTM A106B steel pipe weld. Flash is on inner diameter. X6.25

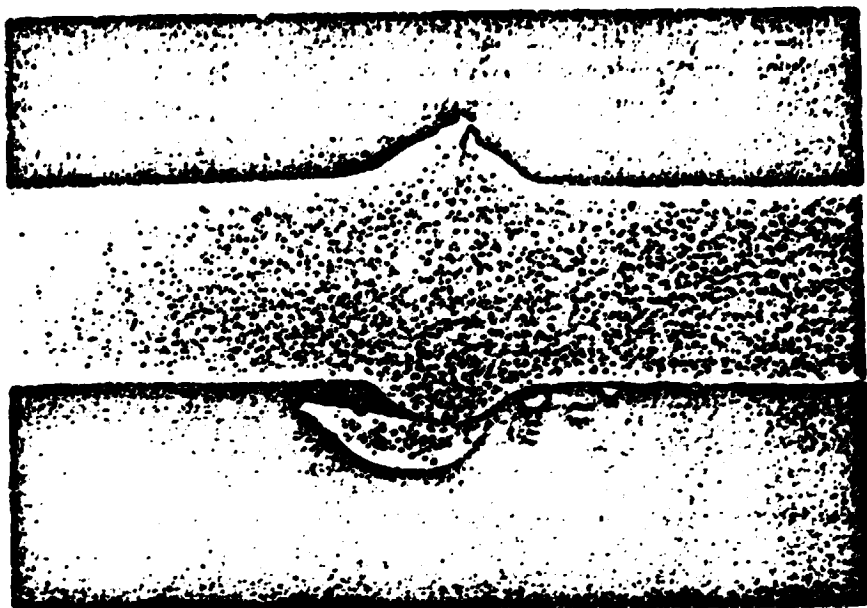
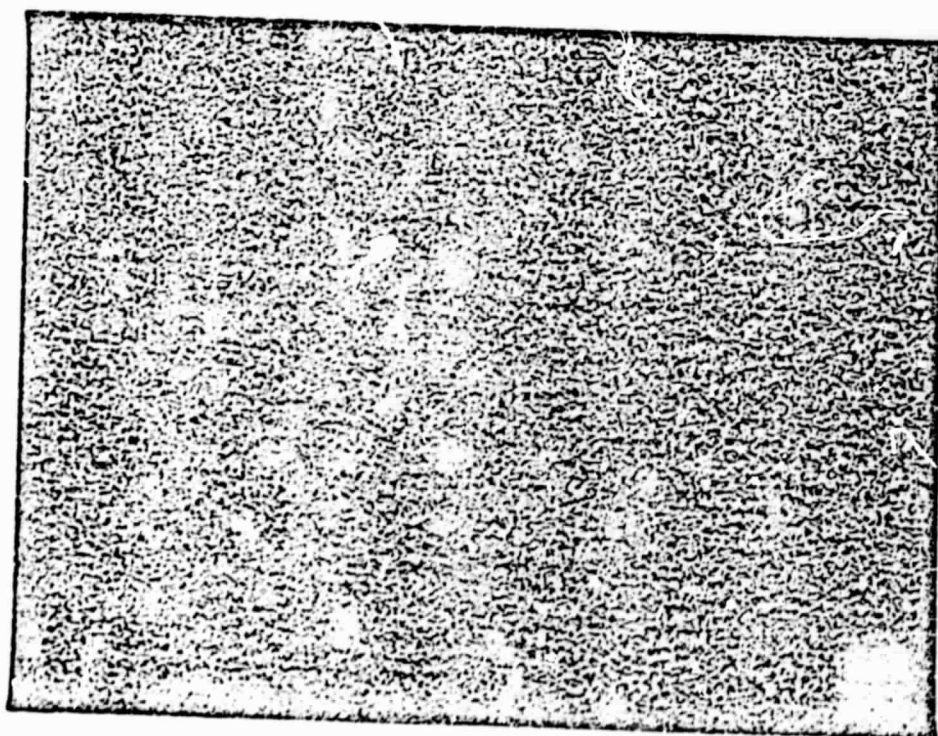


Fig. 9 - Cross-section of 2-in. ASTM A106B steel pipe weld. Flash is on inner diameter. X6.25



ORIGINAL PAGE
OF POOR QUALITY

Fig. 10 - Microstructures of weld in 2-in. steel pipe. Nital etch. X100.
A -- weld line (runs horizontally); B -- base metal

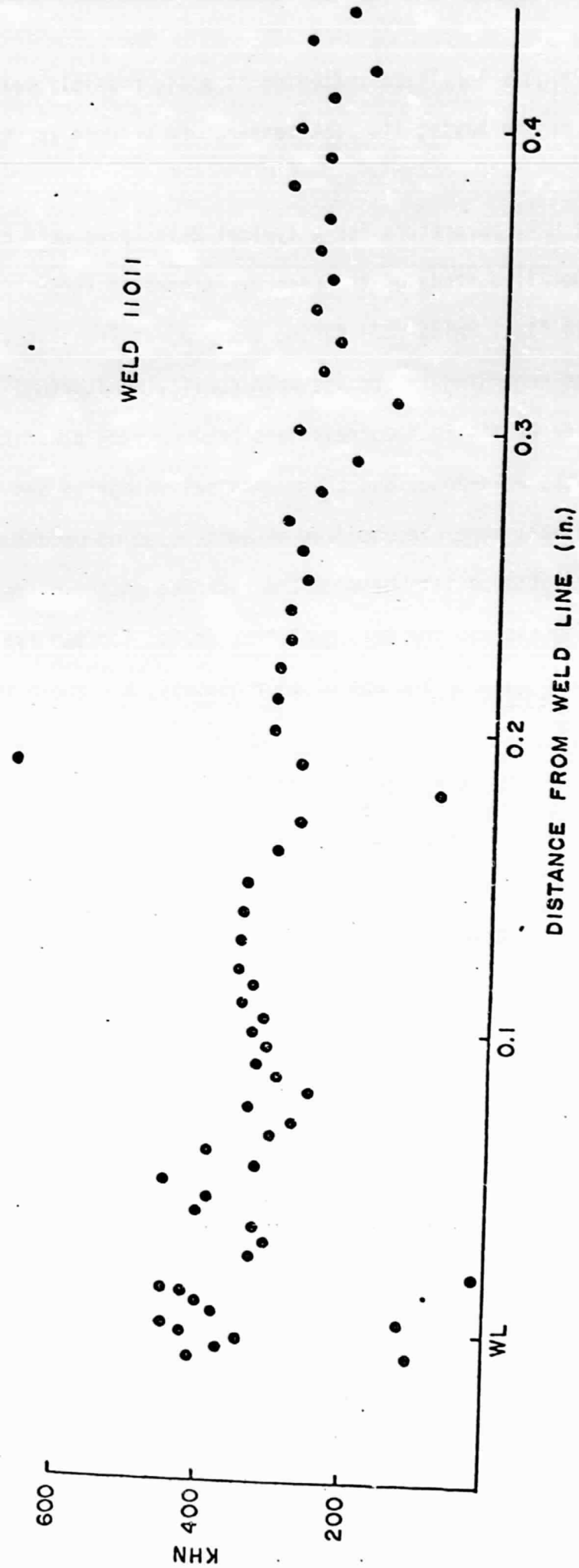


Figure 11: Microhardness traverse of the weld shown in Figures 9 and 10.
Knoop, 65 g load

to believe that the highly localized softening is real, possibly being the stress-relieved region having its peak temperature between about 800 and 1300°F.

The significant HPRW parameters for a typical 2-in. pipe weld are given in Table 5. Detailed study of the recorder traces of these parameters for the 14 final welds made during the project led to several tentative conclusions regarding in-process weld quality monitoring. First, there appear to be distinct correlations between peak power level, energy deposited in the weld-zone, and the mechanical integrity and strength of the weld, all other independent parameters being unchanged. Also, a similar correlation exists between the recorded shapes of voltage, current, and power signals and the weld quality. Traces for two typical pipe welds, one of good quality and one of poor quality, are shown in Figure 12.

Although further analysis and testing are required, these results suggest the possibility of developing an in-process weld quality criterion which could supplement, or in some cases eliminate, the need for conventional postweld nondestructive testing.

FOUR-INCH SCHEDULE 80 STAINLESS PIPE

With present welding techniques, there are problems of intergranular stress corrosion cracking (IGSCC) in the welds of some stainless steel BWR piping carrying high-purity O₂ saturated water.¹³ The IGSCC problems are attributed primarily to sensitization of the weld heat-affected zone during arc welding and to the residual stress pattern in the vicinity of the weld.¹⁴ The characteristics of the HPRW process offer the possibility of eliminating or reducing significantly the sensitization

TABLE 5: TYPICAL HPRW PROCESS PARAMETERS FOR
2-INCH SCHEDULE 40 A 106B STEEL PIPE

Peak welding current	I_W - 64.0	(kA)
Time to end of "weld and forge" cycle	- 0.75	(s)
Time to end of post weld heat treat	- 23.0	(s)
Peak voltage across weld	$(V_W)_{MAX}$ - 4.8 @ 0.15	(V @ s)
Peak generator power	$(P_g)_{MAX}$ - 760.0 @ 0.06	(kW @ s)
Peak power into weld zone	$(P_W)_{MAX}$ - 270.0 @ 0.15	(kW @ s)
Open circuit terminal voltage	V_{to} - 15.0	(V)
Terminal voltage at t_o^+ (-0.001 sec)	V_t - 11.6	(V)
Rotor speed @ discharge	ω_D - 3.0×10^3	(rpm)
Total energy stored (in generator)	E - 1.5×10^6	(J)
Total energy delivered to weld zone	E_W - 0.2×10^6	(J)
Motoring time	- 180	(s)
Motoring power	- 250	(kW)

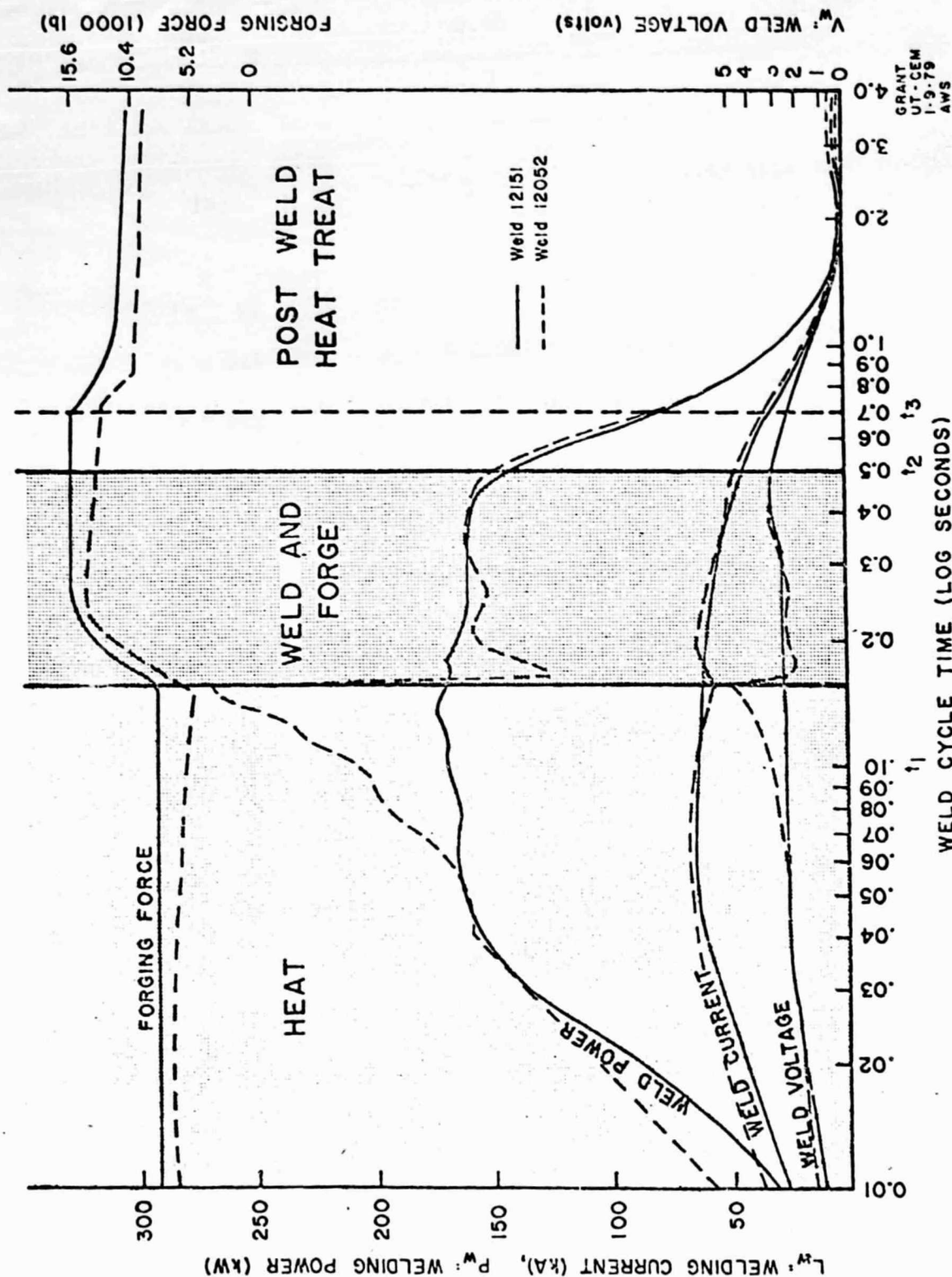


Figure 12: Weld voltage, current, power, and forging force for two typical welds in 2-in. steel pipe. Weld 12151 was unacceptable; weld 12052 had acceptable mechanical properties

and residual stress problems in these welds. Sensitization due to carbide precipitation is a time dependent process,¹⁵ and the HPR welds occur in less than one second. Also, because the faying surfaces of HPR welds are heated uniformly and simultaneously, the residual stress pattern in the weld zone is expected to be improved compared to the pattern resulting from a concentrated, moving heat source, such as on arc. This stress pattern will be the subject of further investigation.

Over 35 welds have been produced to date. The significant process parameter values are given in Table 6.

Figure 13 shows the outside and inside appearance and wall contour of welds in 4-in. stainless steel pipe. The exterior view is of Weld 25, while the interior view is of Weld 14B. A small portion of the exterior of Weld 14B is visible at the bottom of Figure 13B, however, and can be seen to be similar in appearance to Weld 25. The inner contour consists of a small, smooth bead having a slight crevice. Although the contour would probably not present an objectionable obstacle to flow, we are concerned about possible corrosion in the crevice and are attempting to improve the inner contour. There is also a small crevice in the outer contour, but this is of less concern than the inside crevice, since it will normally be accessible for removal.

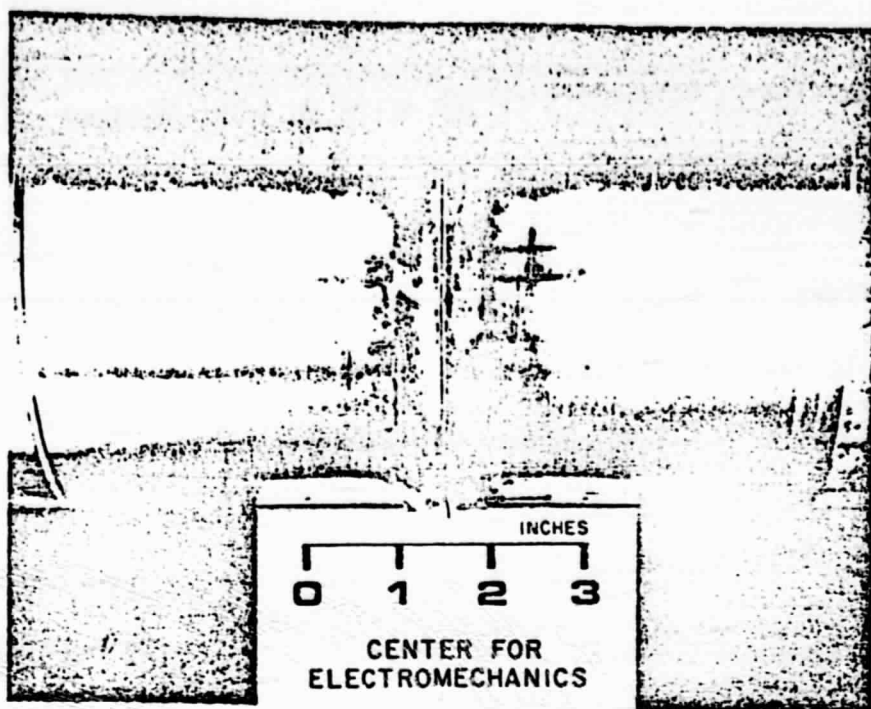
The results of transverse tensile tests of welds in 4-in. stainless steel pipe are presented in Table 7, and the specimens themselves after testing are shown in Figure 14.

Figure 15 shows the contours of Weld 14B perhaps more clearly than Figure 13. This weld contains a narrow fusion zone, which clearly defines the weld line. The shallowness of the outside crevice is apparent.

TABLE 6: TYPICAL HPRW PROCESS PARAMETER FOR 4-INCH SCHEDULE

80 TYPE 304 STAINLESS STEEL PIPE

Peak welding current	I_W	~ 315	(kA)
Total weld cycle time	t_W	~ 3.0	(s)
Peak power into weld zone	P_W	~ 2000	(kW)
Peak generator power output	P_G	~ 6300	(kW)
Peak voltage across weld	V_W	~ 6.4	(V)
Terminal voltage @ t_o^+	V_{t^+}	~ 21.0	(V)
Open circuit terminal voltage	V_t	~ 33.0	(V)
Rotor speed @ discharge	ω_R	~ 4400	(rpm)
Total energy stored (in generator)	E_R	~ 3.2×10^6	(J)
Total energy delivered to weld	E_W	~ 0.6×10^6	(J)
Motoring time	t_m	~ 240	(s)
Motoring power	P_m	~ 250	(kW)



ORIGINAL PAGE
OF POOR QUALITY

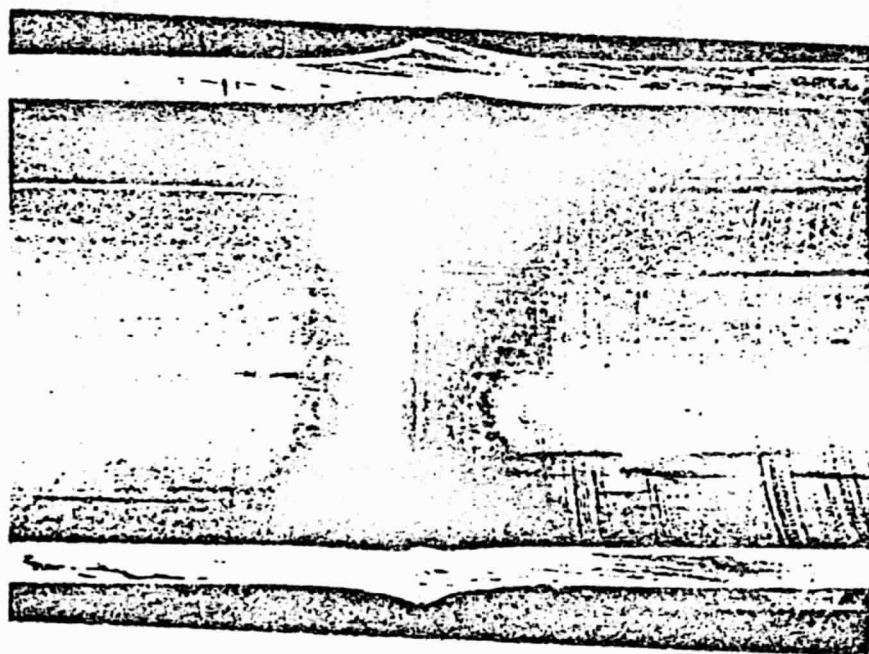
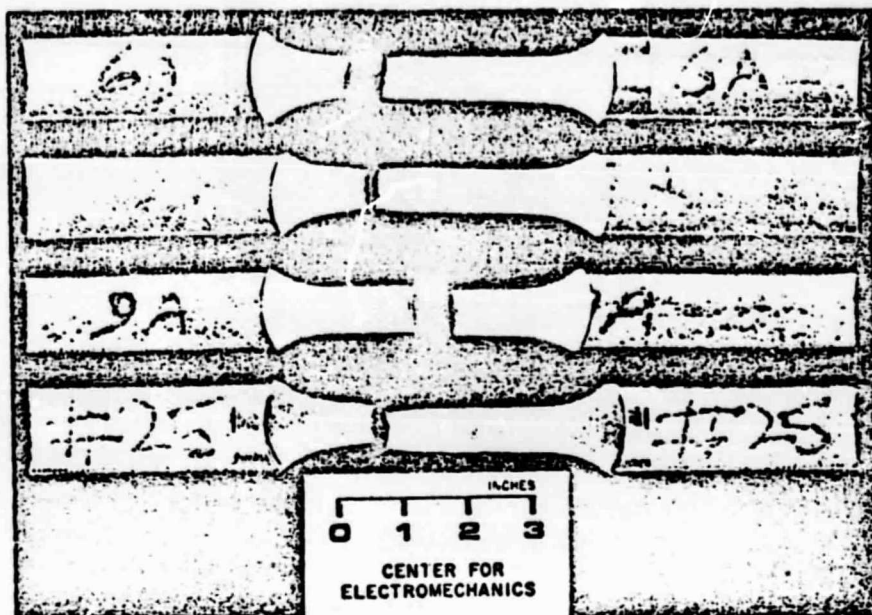


Fig. 13 - Welds in 4-in. schedule 80 Type 304 stainless steel pipe.
A -- exterior of Weld 25; B -- cross-section and interiors of Weld 14B

TABLE 7: TRANSVERSE TENSILE PROPERTIES OF HPR WELDS IN 4-IN. SCHEDULE
80 TYPE 304 STAINLESS STEEL PIPE

Weld No.	0.2% Offset Yield Stress, lb/in. ² (MPa)		Ultimate Tensile Stress, lb/in. ² (MPa)		Elongation in • 2 in., %	Fracture Location
6A	45,160	(311)	77,400	(534)	30.5	Base metal
8A	46,100	(318)	76,600	(529)	38.5	Base metal
9A	52,900	(365)	73,200	(505)	14.5	Weld line
25	44,000	(303)	83,300	(575)	38.0	Base metal



ORIGINAL PAGE IS
OF POOR QUALITY

Fig. 14 - Transverse tensile specimens of 4-in. stainless steel pipe welds after testing

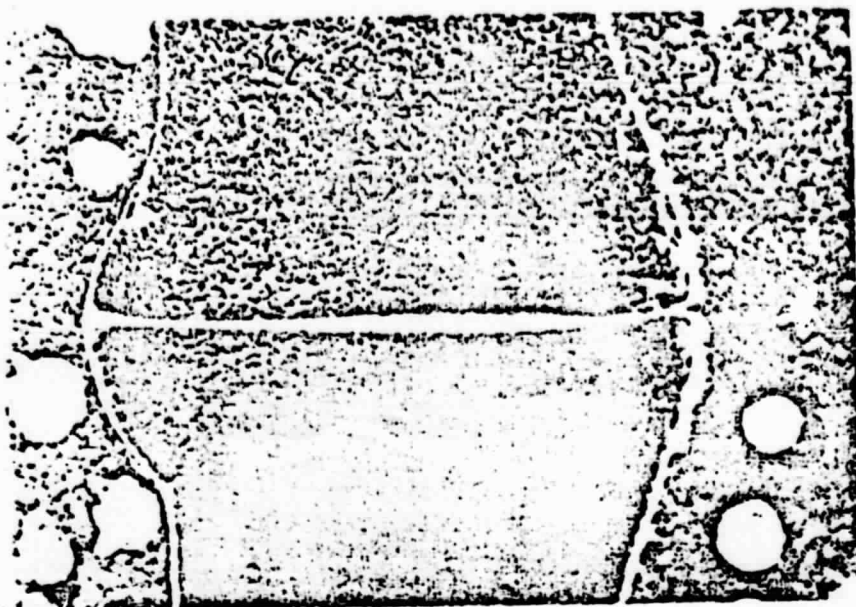


Fig. 15 - Cross-section of 4-in. stainless steel pipe weld 14B. Inner diameter is on the left

Figure 16 shows the microstructure of the weld line region in a weld that is typical of welds presently being produced. Because the joint design for this weld did not favor transverse flow of metal, oxide films present on the faying surfaces were not swept out of the weld interface, but remained in place and merely spheroidized. This is similar to the way the surface films would have behaved in a diffusion weld. There was no metallographic evidence of melting in Weld 25. In fact, Figure 16B, which is typical of the microstructure all along the weld line, clearly shows diffusional grain growth across the weld interface. Presence of the oxide particles had no adverse effect on the tensile properties of the weldment (Table 7 and Figure 14). Welds can also be produced having a variety of microstructures with partial or complete melting at the interface. We expect to report fully on this subject in a future publication.

A microhardness travers of Weld 25 is shown in Figure 17. As would be expected in Type 304 stainless steel, there was no hardening in the heat-affected zone -- merely a slight softening associated with relief of fabrication stresses.

Figure 18 shows the microstructure of the weld line and one heat-affected zone of Weld 25 electrolytically etched with oxalic acid according to ASTM A 262 Procedure A, the screening method for revealing grain boundary sensitization. If sensitization has occurred in any portion of the heat-affected zone during welding, the carbide-containing grain boundaries are severely attacked by the etch, clearly revealing the sensitized region. There is no visible sensitization in Weld 25, nor did we expect to find any in this or any other HPR weld. Sensitization is a diffusion-controlled process that takes place at intermediate temperatures during heating and cooling. A typical 4-in. schedule 80 BWR pipe weld, if made using

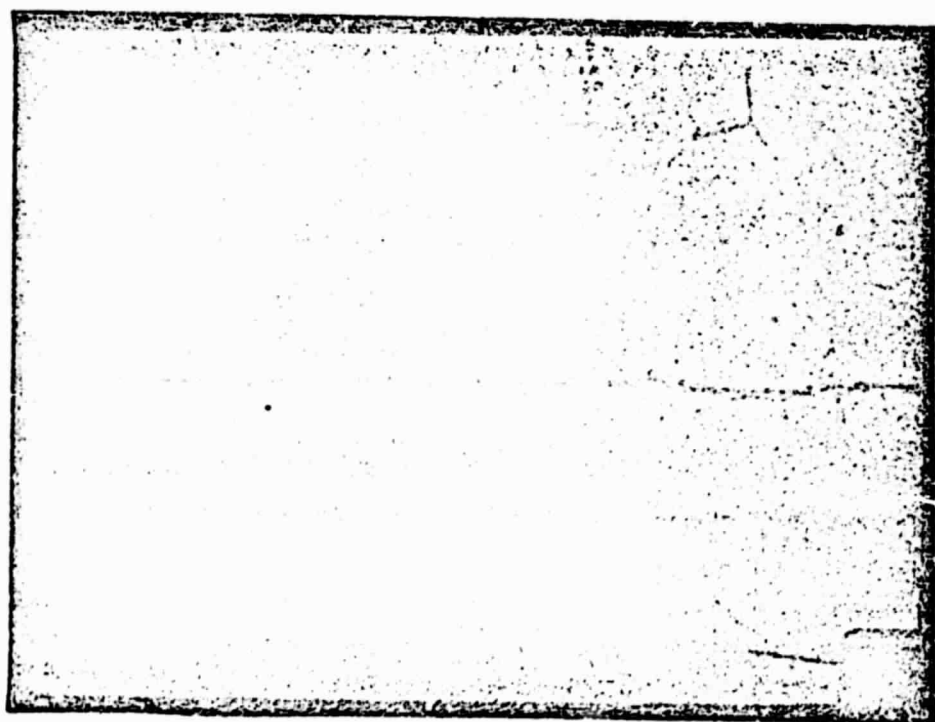
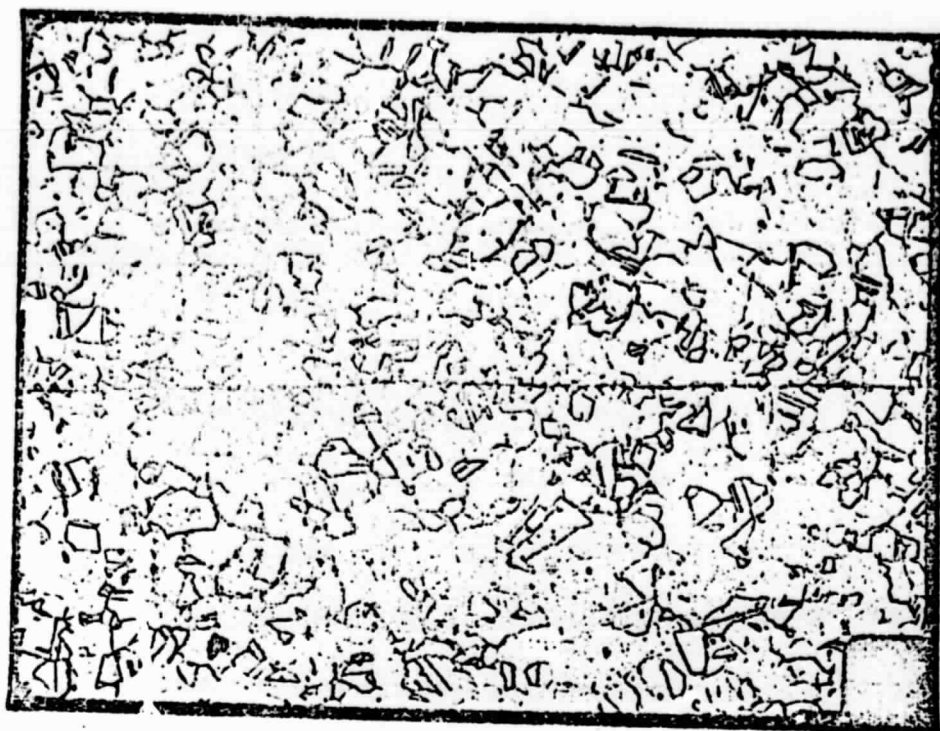


Fig. 16 - Microstructure of 4-in. stainless steel pipe weld 25.
 $10\text{HNO}_3:10\text{CH}_3\text{COOH}:1\text{HCl}$ etch: A -- weld line. X100;
 B -- same region. X800

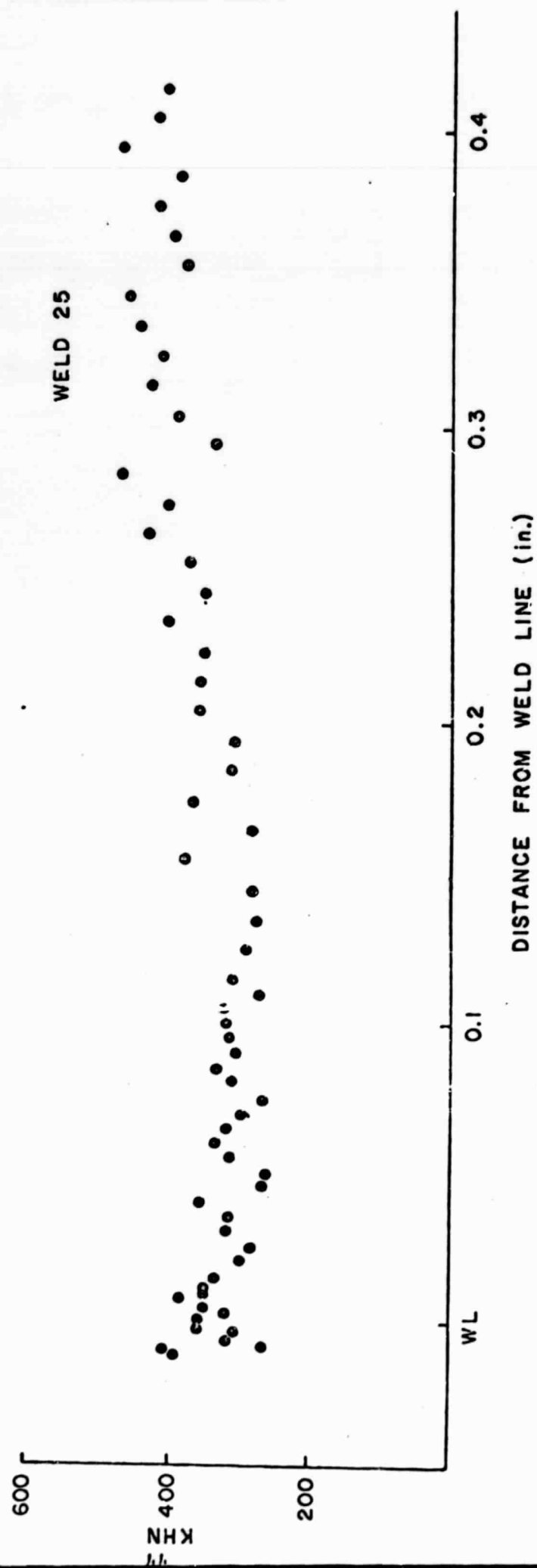


Figure 17: Microhardness traverse of 4-in. pipe weld 25. Knoop, 60 g load

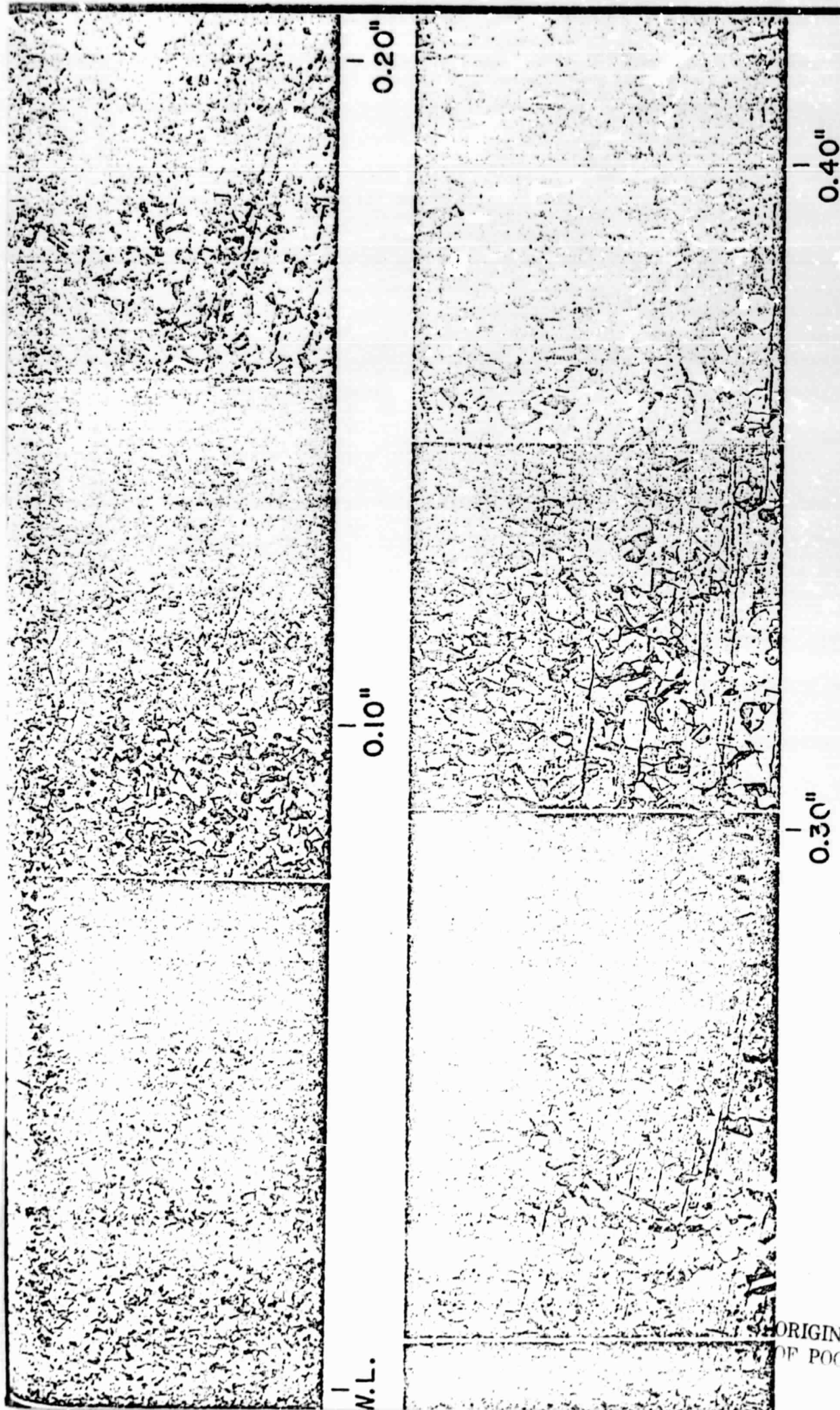


Fig. 18 - Montage showing microstructure of 4-in. Type 304 stainless steel weld 25, for detection of sensitization. (COOH)₂ etch, ASTM A262, Procedure A. X50

arc welding, will require about seven passes, and the HAZ will be within the sensitization temperature range for at least several minutes. An HPR weld, on the other hand, is accomplished within seconds during a single temperature excursion, and the HAZ is within the sensitization region for a significantly shorter time than in an arc weld. There is good reason to believe that sensitization, and therefore susceptibility to intergranular stress corrosion cracking, if it occurs at all, will not be a serious problem in HPR welds made in Type 304 stainless steel.

OTHER WELDS

Presently funded projects will explore the welding characteristics for various materials and metal shapes of up to 7 in.² cross-section. Since the existing 5 MJ disk-type machine appears to be capable of welding only 7 to 10 in.² of steel, plans are presently underway to design and build a 50 MJ drum-type generator in the near future. This 50 MJ machine will give us the capability to weld metal sections approaching 100 in.² and we hope it will be a major contribution to the welding research capability of the free world.

SUMMARY AND CONCLUSIONS

A new welding process based on the unique electrical characteristics of pulsed homopolar generators is being developed. Homopolar Pulse Resistance Welding (HPRW) is a stored energy resistance welding process having the capability of welding very large metal sections (up to 100 in.²) in very short times (≤ 1 second). It appears that this process will greatly expand the economically feasible range of weldment size for resistance welding. We believe that HPR welding will become a serious competitor for flash, electron beam, diffusion, and arc welding in some applications. Representatives from several industries, including automotive, pipeline, pipe fabrication, construction, and heavy equipment manufacturing, are already beginning to consider the HPRW process as a supplement or possible alternative to the presently available welding methods. Among HPRW applications visualized but not yet being actively pursued are welding in space and under water.

Several process features make HPRW attractive. The process can be adapted to both shop and field welding. The weld current pulse can be shaped to control weld heating and cooling rates and to accomplish postweld heat treatment. Electrical power requirements are inherently modest. The process also offers the potential for in-process weld quality control.

Welds made to date using the present 5 MJ machine include bars, pipes and other shapes up to 4.4 in.² in cross-section with actual welding times of from 0.5 to 1.0 seconds at generated power levels in excess of 6000 kW. The power required by the welding equipment during these welds was only about 250 kW. Projects presently underway will

explore process characteristics on welds in various metals in sections up to 7 in.². Future projects include the possible construction of a 50 MJ machine for welding experiments on metal sections approaching 100 in.².

We believe continued development of the HPRW process will occur and will parallel the commercial development of the pulsed homopolar generator and other equipment which serve as the basis for the process. In addition, development of this equipment will lead to its use in other industrial processes such as billet heating, localized heating and forming, resistance brazing, and other applications requiring or capable of using a large resistance heating power source.

ACKNOWLEDGEMENTS

Funding for the construction and development of the 5 MJ homopolar generator was provided by the U. S. Department of Energy and the Texas Atomic Energy Research Foundation. Funding for the welding projects discussed was provided by Astec Industries, Inc., the Electric Power Research Institute (Contract no. RP1122-1) and the National Science Foundation (Grant No. DAR77-23874). The EPRI project manager is Dr. Karl Stahlkopf and the NSF project manager is Dr. Richard Schoen.

The authors would also like to acknowledge the valuable contributions made by R. C. Zowarka, K. M. Tolk, K. R. McFerren, E. J. Bloomer, S. E. Donnell, J. L. Kepner, and the other CEM employees who have participated in the completion of the work herein described.

REFERENCES

1. Tolk, K. M., Driga, M. D., Becker, E. B., Weldon, W. F., Bird, W. L., Rylander, H. G., and Woodson, H. H., "Inertial Energy Storage Research at The University of Texas at Austin," Transactions IEEE International Pulsed Power Conference, Lubbock, Texas, November 9-11, 1976.
2. Weldon, W. F., Driga, M. D., Woodson, H. H., and Rylander, H. G., "The Design, Fabrication, and Testing of a Five Megajoule Homopolar Motor-Generator," International Conference on Energy Storage, Compression, and Switching, Torino, Italy, November 5-7, 1974.
3. Bird, W. L., Grant, G. B., Weldon, W. F., Rylander, H. G., and Woodson, H. H., "System Engineering and Design of a Pulsed Homopolar Generator Power Supply for the Texas Experimental Tokamak," Seventh Symposium on Engineering Problems of Fusion Research, Knoxville, Tennessee, October 24-29, 1977.
4. Gully, J. H., Driga, M. D., Grant, G. B., Rylander, H. G., Tolk, K. M., Weldon, W. F., and Woodson, H. H., "Design, Fabrication and Testing of a Fast Discharge Homopolar Machine (FDX)," Seventh Symposium on Engineering Problems of Fusion Research, Knoxville, Tennessee, October 24-29, 1977.
5. Robinson, C. A., "Power Generation Key to Beam Weapons," Aviation Week & Space Technology, November 6, 1978, 50 to 57.

6. Woodson, H. H., Rylander, H. G., and Weldon, W. F., "Pulsed Power from Inertial Storage with Homopolar Machines for Conversion," IEEE International Pulsed Power Conference, Lubbock, Texas, November 9-11, 1976.

7. Driga, M. D., Nasa, S. A., Rylander, H. G., Weldon, W. F., and Woodson, H. H., "Fundamental Limitations and Topological Considerations for Fast Discharge Homopolar Machines," IEEE International Conference on Plasma Science, Ann Arbor, Michigan, May 14-16, 1975.

8. Meyer, E. H., "The Unipolar Generator," The Westinghouse Engineer, March, 1956, 59 to 61.

9. Crawford, T. J., "The Homopolar Generator for Resistance Welding," The Welding Journal, March, 1950, 211 to 215.

10. Brennan, M., Eliezer, Z., Weldon, W. F., Rylander, H. G., and Woodson, H. H., "The Testing of Sliding Electrical Contacts for Homopolar Generators," Proceedings Twenty-Fourth Annual Holm Conference on Electrical Contacts, Chicago, Illinois, November 11, 1978.

11. Weldon, W. F., Driga, M. D., Rylander, H. G., and Woodson, H. H., "The Design of Homopolar Motor-Generators for Pulsed Power Applications," Sixth Symposium on Engineering Problems in Fusion Research, San Diego, California, November 18-21, 1975.

12. Driga, M. D., Nasar, S. A., Rylander, H. G., Weldon, W. F., and Woodson, H. H., "A Topological Approach to Acyclic Machines," Internal

Report, 1975, Center for Electromechanics (then Energy Storage Group),
The University of Texas at Austin, Austin, Texas.

13. Hanneman, R. E., "Concepts for Stress Corrosion Cracking in Steel .
Pipe Weldments," ASM Materials and Processing Congress, Philadelphia,
Pennsylvania, November 7-9, 1978.

14. Giannuzzi, A. J., editor, "Studies on AISI Type-304 Stainless
Steel Piping Weldments for Use in BWR Applications - Final Report,"
Nuclear Energy Engineering Division, General Electric Company, San Jose,
California.

15. Del Vecchio, E. J., editor, Resistance Welding Manual, 3rd
Edition, Volume I, Resistance Welder Manufacturers' Association,
Philadelphia, Pennsylvania, 1956, p. 168.

APPENDIX C

ANALYSIS OF ELECTROMAGNETIC LAUNCHERS

ANALYSIS OF PERFORMANCE OF RAIL GUN ACCELERATORS
POWERED BY DISTRIBUTED ENERGY STORES

R.A. Marshall and W.F. Weldon



Presented at the
14th Pulse Power Modulator Symposium
Orlando, Florida
June 3-5, 1980

Publication No. PN-63
Center for Electromechanics
The University of Texas at Austin
Taylor Hall 167
Austin, Texas 78712
512-471-4496

ANALYSIS OF PERFORMANCE OF RAILGUN ACCELERATORS
POWERED BY DISTRIBUTED ENERGY STORES

Richard A. Marshall and William F. Weldon

Center for Electromechanics
Taylor Hall 167
The University of Texas at Austin
Austin, Texas 78712
(512)471-4496

ORIGINAL PAGE IS
OF POOR QUALITY

Summary

It has been established that centimeter sized projectiles weighing several grams can be accelerated by electrical forces to velocities in excess of five kilometers per second in a classical railgun. The technologies required to do this are adequately understood, at least in the case where a single energy store is connected to the breech end of the gun.

There are two disadvantages to using a single energy store. It is generally desirable to keep gun current as nearly constant as possible and this is difficult to achieve with a single store without making the store excessively large. Rail resistance also becomes a dominating factor as higher velocities are reached because higher velocities require greater gun lengths and correspondingly larger gun resistances.

One way to by-pass these limitations is to distribute energy stores along the length of the gun. Not only does this reduce the average rail resistance by reducing the length of rail that carries current at anytime, but it permits inductive energy to be usefully transferred down the gun rather than allowing it to dissipate resistively in the rails.

This paper shows how the performance of such a gun may be simulated, by computing the instantaneous rate of change of current in each energy store and by using these values to obtain projectile acceleration. Two specific rail gun systems are examined, the first being a "scientific railgun" designed to propel a three gram projectile to a speed of 20 kilometers per second, and the second being a "space-launch railgun" to accelerate one metric ton to 7.5 kilometers per second.

Introduction

The basic concept of the parallel-rail railgun accelerator has been known for a long time. The accelerating force is obtained by the interaction of the current in the driven armature with the magnetic field produced by the current in the rails, the armature and rails being connected in series. The recent work done in Canberra has shown that an electric arc can successfully be used as a railgun armature.¹ The other important contribution made was the realization that current control was essential to success, and that the use of an inductor was one way to achieve such control.² Projectiles with a mass of three grams were accelerated to velocities of up to 5.9 km/s in the Canberra railgun.

There are other ways of achieving current control in railguns. A program at present being conducted by a LLL-LASL group involves the use of explosive flux compression generators.³ This very flexible generation scheme makes it possible to generate currents which vary in time in a wide variety of ways.

The use of a single current generator connected to the breech of a railgun has two disadvantages. As gun rails become longer to obtain higher performance, then a larger proportion of the input energy is lost resistively in the rails.⁴ The other is that the inductive energy remaining in the gun at projectile exit represents a considerable inefficiency. A way of circumventing both of these problems is to distribute energy stores along the length of the gun.^{5,6,7,8} It should be noted that the use of many power supplies along an accelerator is not new. It is commonly employed in atomic particle accelerators, and has been proposed for use in travelling magnetic wave macroparticle accelerators.⁹ It has also been used in the MIT Massdriver.¹⁰ The aim in all these cases is to deliver energy to a projectile in small increments many times.

In this paper we present a method by which the distributed inductive energy store railgun can be analysed, and apply this analysis to two railgun systems.

Analysis

The schematic representation of a railgun with inductive energy stores distributed along its length is shown in Fig. 1. Stores have inductance L and resistance R and are spaced at intervals ℓ along the rails. Each is delivering current I_n into the railgun at a voltage of E_n . The projectile has moved a distance x into gun section number 1. It has a mass of m and a velocity of x . The railgun has an inductance and resistance of L' and R' per unit length.

The current flowing in each gun section is the sum of the currents being delivered by each energy store up to and including the one in that gun section. Current is prevented from flowing backwards in the inductors. The arc armature driving the projectile is assumed to have a volt drop MV (so called because this is the voltage that is measured from rail to rail at the gun's muzzle.)

In order to compute the performance of the rail gun, it is first necessary to find the rates of change of the inductor currents, I_n . The first step in doing this is to write the equations for the power supply circuits (LH side below Fig. 1) and for the railgun sections (RH side below Fig. 1). These are then solved for I_n which are obtained from the matrix equation (1). //

The simulation is now performed in the following manner. At any instant, x and \dot{x} are known as are all I_n . When an appropriate value for MV is chosen then all the terms in [A] and [C] are known. Thus [B] is found, enabling new values of current to be calculated for the next step of the simulation. New values of \dot{x} and x are also found from the calculated value of \dot{x}

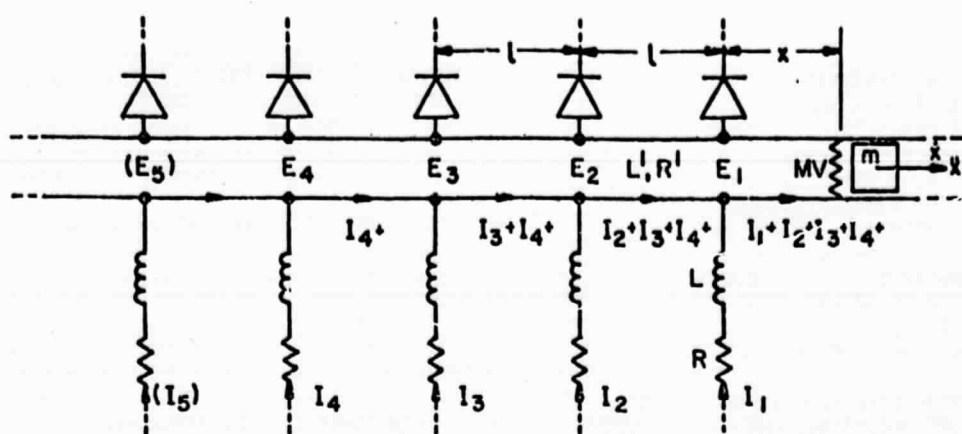


Fig. 1. Circuit diagram showing parameters and variables used in the analysis.

$$\begin{aligned}
 -E &= L\dot{I}_1 + RI_1 & E_1 &= L'x(\dot{I}_1 + \dot{I}_2 + \dot{I}_3 + \dot{I}_4) + (L'x + R'x)(I_1 + I_2 + I_3 + I_4) + MV \\
 -E_2 &= L\dot{I}_2 + RI_2 & E_2 - E_1 &= L'\ell(\dot{I}_2 + \dot{I}_3 + \dot{I}_4) + R'\ell(I_2 + I_3 + I_4) \\
 -E_3 &= L\dot{I}_3 + RI_3 & E_3 - E_2 &= L'\ell(\dot{I}_3 + \dot{I}_4) + R'\ell(I_3 + I_4) \\
 -E_4 &= L\dot{I}_4 + RI_4 & E_4 - E_3 &= L'\ell(\dot{I}_4) + R'\ell(I_4) \\
 & & & \dots
 \end{aligned}$$

Eliminating the voltages E_n gives

$$\begin{aligned}
 L(\dot{I}_1) + L'x(\dot{I}_1 + \dot{I}_2 + \dot{I}_3 + \dot{I}_4) &= R(-I_1) - (L'x + R'x)(I_1 + I_2 + I_3 + I_4) - MV \\
 L(-\dot{I}_1 + \dot{I}_2) + L'\ell(\dot{I}_2 + \dot{I}_3 + \dot{I}_4) &= R(I_1 - I_2) - R'\ell(I_2 + I_3 + I_4) \\
 L(-\dot{I}_2 + \dot{I}_3) + L'\ell(\dot{I}_3 + \dot{I}_4) &= R(I_2 - I_3) - R'\ell(I_3 + I_4) \\
 L(-\dot{I}_3 + \dot{I}_4) + L'\ell(\dot{I}_4) &= R(I_3 - I_4) - R'\ell(I_4) \\
 & \dots
 \end{aligned}$$

giving

$$\begin{bmatrix} (L+L'x) & L'x & L'x & L'x & \dots \\ -L & (L+L'\ell) & L'\ell & L'\ell & \dots \\ 0 & -L & (L+L'\ell) & L'\ell & \dots \\ 0 & 0 & -L & (L+L'\ell) & \dots \\ \dots & \dots & \dots & \dots & \dots \end{bmatrix} \begin{bmatrix} \dot{I}_1 \\ \dot{I}_2 \\ \dot{I}_3 \\ \dot{I}_4 \\ \dots \end{bmatrix} = \begin{bmatrix} R(-I_1) - (L'x + R'x)(I_1 + I_2 + I_3 + I_4) - MV \\ R(I_1 - I_2) - R'\ell(I_2 + I_3 + I_4) \\ R(I_2 - I_3) - R'\ell(I_3 + I_4) \\ R(I_3 - I_4) - R'\ell(I_4) \\ \dots \end{bmatrix}$$

Defining the matrix equation as

$$[A][B] = [C]$$

then values of the rates of change of the currents, \dot{I}_n , are obtained from the equation $[B] = [A^{-1}][C]$.

(1)

which is given by $\ddot{x} = L'(\Sigma I_n)^2/(2m)$.

At each step the value of x is tested and when it gets greater than ℓ , it is replaced by $(x-\ell)$ and at the same time all the currents are shifted one sun stage, i.e., I_2 is replaced by I_1 , I_3 by I_2 , I_4 by I_3 , etc. and I_1 is set equal to the assumed initial value of current from the next energy store. The appropriate dimensions of the matrices are also in-

creased by one because there is now one more power circuit-in use.

At each step also, the magnitude of the current in the rearmost energy store is checked and when it goes negative, that store is "removed" by reducing the dimensions of the matrices by one.

The "Scientific Railgun"

As an example of the method, a simulation has been made of a railgun for accelerating a three gram projectile to 20 km/s. The first point to note about the design of the system is that constant average acceleration of the projectile is both desirable and possible. Since energy equals force times distance, this means that the energy stores should be uniformly distributed. Aiming at an average current of around 375 kA (1) and assuming a gun inductance (L') of 0.6 $\mu\text{H/m}$ give a force on the projectile of 42 kN ($=0.5 L'^2$), giving an acceleration to the projectile of 14 Mm/s^2 . Thus, the length of gun required to reach 20 km/s is 14 m.

The kinetic energy of the projectile at exit is 600 kJ. If the gun were to be 100% efficient, and each store held 10 kJ of energy, then these would have to be spaced 0.23 meters apart. For the simula-

tion spacing of 5 stores per meter was assumed.

The arc armature volt drop (MV) is assumed to be 160 V, the value that was observed in the Canberra railgun. The rail resistance (R') is taken as 0.002 Ω/m , being the resistance of copper rails 1.5 mm thick by 13 mm high. The inductor resistance is taken as 0.001 Ω .

The inductor current, when fully charged, has been taken as 125 kA and with the 10 kJ inductor energy gives a calculated inductance of 1.28 μH .

The resulting simulation is shown in Fig. 2. It has been assumed that the projectile is injected into the gun breech with a velocity of 1,000 m/s. The overall efficiency indicated is 70%, 598 kJ kinetic energy being obtained for the expenditure of 850 kJ (10 kJ from each of 85 energy stores). The stage efficiencies rise down the gun, starting from around 20% in the first few stages and rising to 84% in the last stage.

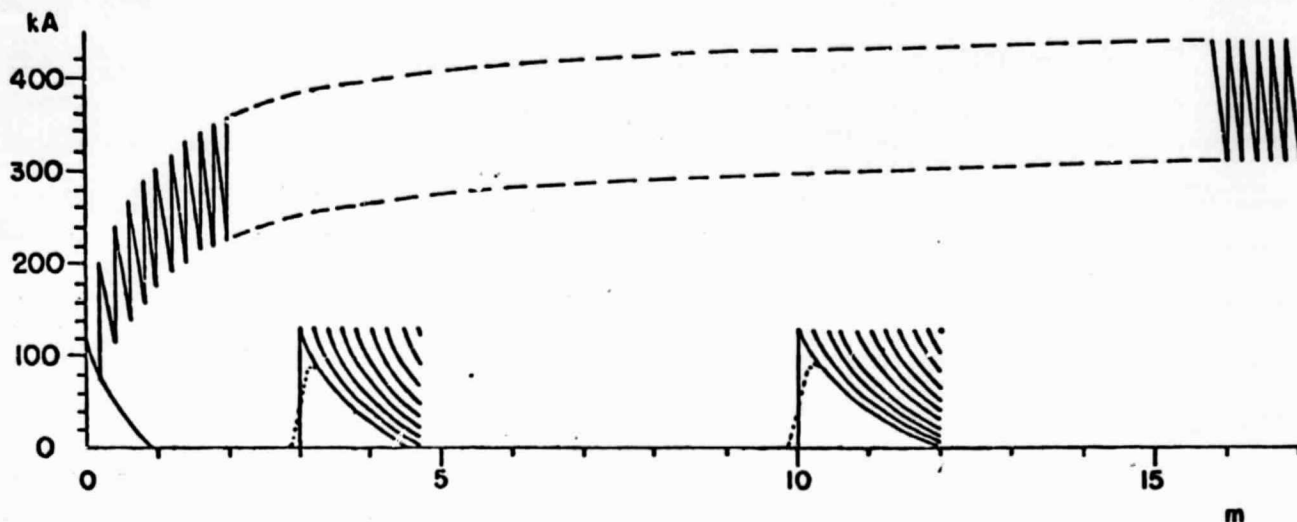


Fig. 2. Simulation of the "scientific railgun" showing current (kA) as a function of projectile travel (m) down the gun. The upper curve shows the total current. The lower curves (only partially drawn) show the currents in individual energy stores. The three gram projectile reaches a velocity of 20 km/s in the 17 m of gun length.

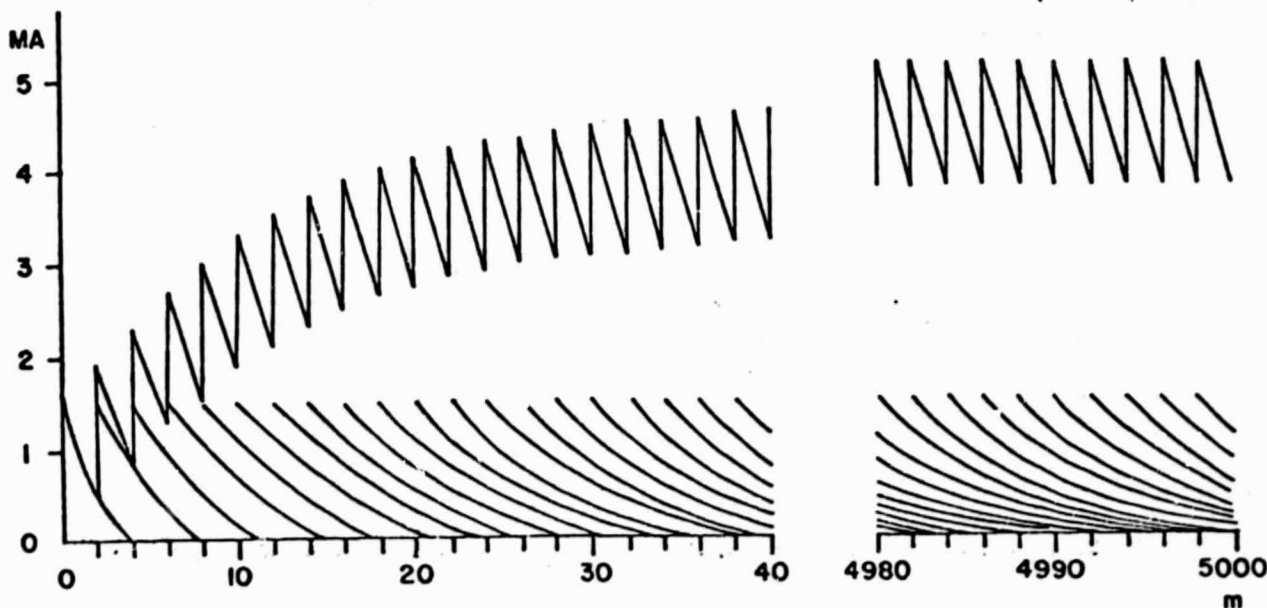


Fig. 3. Simulation of the "space-launch railgun" showing current (MA) as a function of projectile travel (m) down the gun. The curves are discontinuous, the length from 40 m to 4,980 m being omitted. The upper curve is the total current; the lower curves show the currents in individual energy stores. The one tonne projectile reaches a velocity of 7,500 m/s in the 5,000 m gun length.

The "Space-Launch Railgun"

A simulation has also been made of the acceleration of a relatively large mass, 1000 kg, to earth orbit velocity of 7,500 m/s. An acceleration of 500 gravities is assumed which gives a required gun length of 5,700 m. The kinetic energy of the projectile at gun exit is 28.1 GJ which means that about 5 MJ of energy must be delivered to the projectile each meter of travel down the gun barrel. It is assumed that 12 MJ inductors are distributed along the gun at a spacing of 2 m. The total average current required to give the assumed acceleration is 4 MA.

The peak inductor currents are taken as 1.5 MA, requiring an inductance of 10.7 μH .

In the absence of any better information, the arc armature volt drop is again taken as 160 V. Rails of one meter high by three centimeters thick are assumed giving a gun resistance of 2 $\mu\Omega/\text{m}$. The coil inductance has the same value as about 20 m of gun, the resistance of which is 40 $\mu\Omega$. Thus, a reasonable value to take for inductor resistance is 20 $\mu\Omega$.

The results of the simulation are shown in Fig. 3. The projectile reaches its desired velocity in a gun length of 5000 m, i.e., with the expenditure of 30 GJ, being 2500 energy stores of 12 GJ each. Thus, the overall efficiency is 93.8%. Again, the stage efficiency starts low (~20%) but rises rapidly as speed increases to reach a value of 98% at the exit end of the gun.

Switching

Accelerators of the type described above can only be made to work if the current from each energy store is switched into the gun at exactly the right moment. Synchronism with projectile position is crucial. There are many ways that the arrival of the projectile at any point along the gun can be detected. One obvious way is to interrupt a light beam. There are two other ways in which projectile passage can be used to provide very strong signals. The first is to use the arrival of the high pressure plasma of the armature. A small part of this could be allowed to pass through a vent from the gun base to trigger a switch. Radiation from the arc might be used for the same purpose. The second possibility is to use the magnetic field produced by the driving current to do the triggering. This field rises very fast as the armature passes, and can be used to give a strong, noise immune, signal accurately synchronized with the armature position.⁵ This signal could be used directly to activate a switch as indicated in Fig. 4.

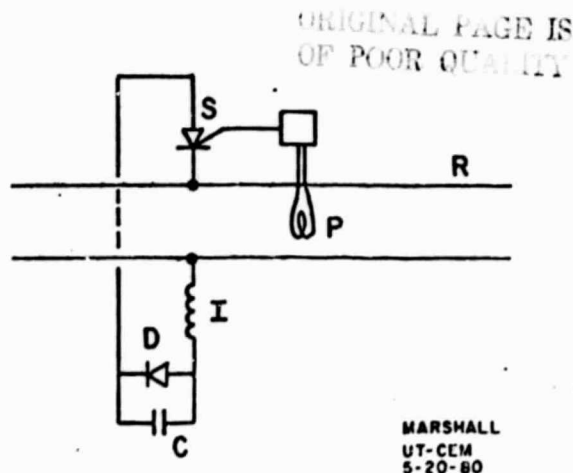


Fig. 4. Schematic of an energy store circuit, showing railgun R, inductor I, capacitor C, diode D, switch S, and pick-up loop P.

When the switch (it can be an SCR) is activated, the energy in the capacitor transfers quickly to the inductor. When the transfer is completed, the diode then effectively removes the capacitor from the circuit. The switch S must also behave like a diode to prevent current from flowing in reverse through the inductor after the latter is discharged.

In the case of the space-launch railgun, the currents are sufficiently high that the use of solid state switches may be expensive. A possible low cost solution may be to have the gun's driving field do the switching directly as shown in Fig. 5.

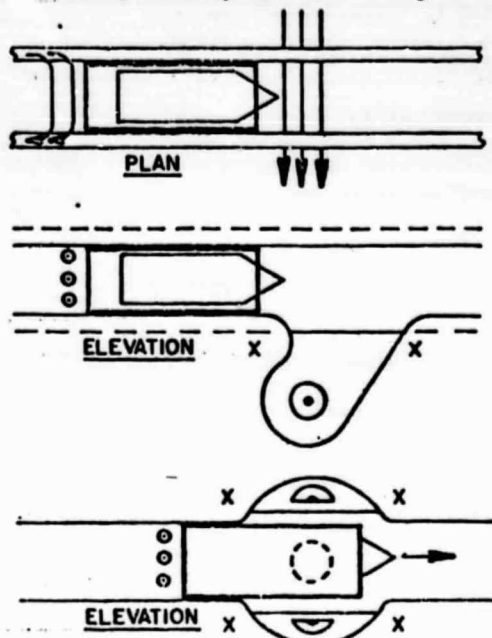


Fig. 5. Direct switching of current into a rail gun using the gun's driving field.

It may be possible to establish an arc, carrying the current from the energy store, between the rails (or electrodes embedded therein) in front of the moving projectile, the arc being stabilized by suitable placement of the current supply leads, xx. As the projectile passes, the arc responds to the driving field and moves in behind the projectile to form part of the armature current. It may be possible to trap the arc as shown in the lower elevation. The projectile would then divide the arc, to have it join the armature behind the projectile after it has passed.¹²

Discussion

The simulations assume that the energy stores consist of precharged inductors which are switched in instantaneously. The method can be expanded to include such effects as the current rise in the inductor which will be roughly as shown by dotted lines in Fig. 2. Note that a parameter not used is the capacitor voltage. In a real system choice of this would be made to provide appropriate rates of rise of inductor currents. Increasing capacitor voltage will probably be desirable with distance down the gun.

Decreasing skin depth in the rails down the gun has not been included, and the assumption of 160 V for the arc drop in the space-launch railgun may not be correct.

No attempt has been made to optimize the two systems studied. If desired, the efficiency of the scientific railgun will improve by using smaller energy stores closer together. The indicated efficiency of the space-launch railgun is surprisingly good. However, the overall efficiency in a real system will be reduced somewhat because the efficiency

of transfer of energy from homopolar generators (which will be required as primary stores) to inductors is lower than the transfer from electrostatic capacitors to inductors. The railgun space-launcher would seem to be a good candidate for firing H. Kolm's telegraph pole atmosphere penetrators.¹³

Conclusion

The outlines presented of the two inductively driven railgun systems show how the simple parallel-rail railgun macroparticle accelerator may be used to impart high velocities to "micro-macro" particles (gram-sized) and to "macro-macro" particles (tonne-sized) with good efficiency.

Acknowledgments

This work was conducted with the support of the Texas Atomic Energy Research Foundation.

References

1. Rashleigh, S.C. & Marshall, R.A., "Electromagnetic acceleration of macroparticles to high velocities," *J. Appl. Phys.* 49(4) April 1978.
2. Barber, J.P., "The Acceleration of Macroparticles and a Hypervelocity Macroparticle Accelerator," Ph.D. Thesis, Australian National University, Canberra 1972.
3. Hawke, R.S., Scudder, J.K. of LLL, and Fowler, C.M., Peterson, D.R. of LASL, The LLL-LASL flux compressor railgun program.
4. Hawke, R.S., Scudder, J.K., "Magnetic Propulsion Railguns: their Design and Capabilities," presented at the Second International Conference on Megagauss Magnetic Field Generation and Related Topics, Washington, D.C. (1979).
5. Marshall, R.A., "Railgun Overview," presented at the DOE Impact Fusion Workshop held at LASL, July 1979.
6. Muller, R.A., et al., "Impact Fusion with a Segmented Rail Gun," *ibid.*
7. Hawke, R.S., "Railgun Accelerators for Launching 0.1-g Payloads at Velocities Greater than 150 km/s," *ibid.*
8. Tidman, Derek A. and Goldstein, Shyke A., "Mass Accelerator for Producing Hypervelocity Projectiles using a Series of Imploding Annular Discharges," *ibid.*
9. Winterberg, F., *Plasma Physics* 8, 541 (1966).
10. Kolm, H.H., "Basic Coaxial Mass Driver Reference Design," *Proc. Princeton Conference on Space Manufacturing*, May 1977.
11. Marshall, R.A., "A Method of Numerically Simulating the Performance of Railguns Powered by Distributed Energy Stores," presented at the DARPA/ARRADCOM Review, Washington, D.C., 9 April 1980.
12. Weldon, W.F. & Marshall, R.A., "Work in Progress at U.T., C.E.M." presented at the DARPA/ARRADCOM Review, Washington, D.C., 19 Sept. 1979.
13. Kolm, H., et al., "Electromagnetic Propulsion Alternatives," presented at the Princeton Symposium on Space Manufacturing, 1979.